Institut für Nutzpflanzenwissenschaften und Ressourcenschutz - Phytomedizin

Infection and spread of *Peronospora sparsa* on *Rosa* sp. (Berk.) - a microscopic and a thermographic approach

Inaugural-Dissertation

zur Erlangung des Grades

Doktor der Agrarwissenschaften

(Dr. agr.)

der Landwirtschaftlichen Fakultät

der Rheinischen Friedrich-Wilhelms-Universität Bonn

von

Sandra Gómez Caro

aus

Bogotá, Colombia

Referent: Prof. Dr. H.-W. Dehne

Korreferent: Prof. Dr. J. Léon

Tag der mündlichen Prüfung: 18.12.2013

Erscheinungsjahr: 2014

INFECTION AND SPREAD OF *Peronospora sparsa* IN *Rosa* sp. (Berk.)- A MICROSCOPIC AND THERMOGRAPHIC APPROACH

Downy mildew caused by *Peronospora sparsa* is one of the most destructive disease of roses, observed to produce asymptomatic infections and therefore difficult to control. The present research took different approaches to study the development and spread of *P. sparsa* in rose plants. On one hand, microscopical and histological observations of the infection process were conducted; on the other hand, IR thermography was evaluated as a non-invasive method for detecting the infection. These analyses were performed with isolates collected during epidemics of the disease in Colombian rose crops, the obtained samples being characterized by their latent period, incidence of sporulation and production of sporangia and oospores. The isolates proved to be alike with respect to the evaluated biological parameters. Hence, their aggressiveness can be said to be similar regardless of the location or cultivar of origin.

P. sparsa generated germ tubes and invaded the leaves not only in a direct mode making use of appressoria, but through the stomata on the abaxial surface as well. As to the vertical spread of the pathogen in the leaves, infection of epidermal cells on the opposite layer to the inoculated surface occurred 96 hours after inoculation (hai). Horizontally, the whole leaf lamina was colonized 120 hai. Mesophyll, epidermal and bundle sheath cells were penetrated by filiform haustoria. Although the capacity of *P. sparsa* to sporulate through the upper cuticle was observed, sporangia were more densely produced on the abaxial leaf surface. Oospores formed mainly in the spongy parenchyma after abaxial inoculation. Following adaxial inoculation, they were also produced under the upper cuticle, where hyphae spread extensively on the horizontal plane. These observations were associated with the strong damage observed in heavily infected leaves. Leaf age affected the speed and distance of pathogen spread, as well as the amount of sporangia and oospores produced. The highest values and the fastest spread of the pathogen occurred in young leaves as contrasted to more mature ones. Hyphae grew in parallel to leaf veins, along the cortical tissue of petioles and in the stem cortex. Progression of *P. sparsa* growth by hyphae was rarely observed in xylem and phloem. These results confirm that the intercellular space is highly important for long distance colonization by the pathogen. Leaf petioles were necessary for infection spread along the leaf and into the stems. The presence of oospores in leaflets and petioles showed the trajectory of the pathogen, while their density indicated the favorability of leaf tissues to *P. sparsa* development. The ability of the pathogen for systemic invasion of plant tissue from localized sites of infection was demonstrated. Leaf tissue colonization was observed to occur acro- and basipetally.

Thermography allowed the detection of downy mildew one or two days earlier than by visual inspection of the plants. Infection by *P. sparsa* resulted in a progressive leaf temperature increase, associated in turn to stomatal closure. Temperature declined at the late stages of the disease due to dense colonization and tissue damage, which favored leaf transpiration and water loss. Thermal imaging confirmed the spread of *P. sparsa* from localized infection sites to asymptomatic colonized areas. Changes in leaf temperature during pathogenesis also allowed differentiation of the rose cultivars by their susceptibility. Thus, thermal imaging comes to be an ideal tool for studying *P. sparsa* - *Rosa* sp. interaction. Moreover, the potential of IR thermography for the detection of downy mildew in presymptomatic stages was demonstrated.

Infektion und Ausbreitung von *Peronospora sparsa* an *Rosa* sp. (Berk.) – eine mikroskopische und thermographische Befallsbewertung

Der Falsche Mehltau, *Peronospora sparsa*, ist einer der wirtschaftlich am meisten schädigenden Krankheitserreger an Rosen, vor allem in vielen Ländern mit der Produktion von Schnittrosen. Das Pathogen befällt Rosen symptomlos und ist daher schwer zu detektieren und zu kontrollieren. In den vorliegenden Untersuchungen wurden verschiedene Ansätze zur Differenzierung der Entwicklung und der Ausbreitung von *P. sparsa* an Rosen durchgeführt. Zum einen wurden mikroskopische und histologische Beobachtungen des Infektionsprozesses durchgeführt; zum anderen wurde IR-Thermographie als nicht invasive Methode genutzt, um Infektionen nachzuweisen. Diese Analysen wurden mit verschiedenen Isolaten des Pathogens durchgeführt, die nach epidemischem Auftreten in kolumbianischen Schnittrosenkulturen gesammelt worden waren. Die Isolate wurden charakterisiert hinsichtlich ihrer Latenzperioden, des Sporulationsverhaltens und der Bildung von Sporangien und Oosporen. Sie erwiesen sich als sehr ähnlich hinsichtlich der biologischen Parameter. Daher konnte deren Aggressivität als ähnlich eingestuft werden, unabhängig vom Fundort und der jeweiligen Sorte.

P. sparsa bildete Keimschläuche und drang in die Blätter nicht nur durch direkte Infektion unter Bildung von Appressorien ein, sondern auch durch die Spaltöffnungen der abaxialen Blattoberfläche. Es konnte eine vertikale Ausbreitung des Pathogens in den Blättern beobachtet werden, wobei die Besiedelung der Epidermiszellen auf der der Inokulation gegenüber liegenden Blattseite 96 Stunden nach der Inokulation nachgewiesen werden konnte. In horizontaler Ebene wurde das gesamte Blatt nach etwa 120 Stunden besiedelt. Das Mesophyll, Epidermiszellen und Blattgefäßzellen wurden durch filiforme Haustorien penetriert. Obwohl die Fähigkeit von *P. sparsa* zur Sporulation auch auf der oberen Kutikula der Blätter zu beobachten war, wurden Sporangien deutlich häufiger auf der unteren Blattoberfläche gebildet. Oosporen wurden nach Inokulation der unteren Blattseiten vor allem im Schwammparenchym gefunden. Nach Inokulation der Blattoberseiten, wurden Oosporen auch unter der oberen Kutikula gebildet, wo unter diesen Bedingungen eine extensive Ausbreitung von Hyphen in horizontaler Ebene gefunden wurde. Diese Beobachtungen gingen mit einer starken Blattschädigung der intensiv befallenen Blätter einher. Das Blattalter beeinflusste die Schnelligkeit und Intensität der Ausbreitung im Blatt aber auch die Menge der gebildeten Sporangien und Oosporen. Die höchste Ausbreitungsintensität und die schnellste Ausbreitung des Pathogens wurden in jungen Blättern nachgewiesen, in reiferen Blättern war dies deutlich geringer der Fall. Hyphen wuchsen parallel zu den Blattadern, entlang dem Gefäßgewebe der Blattstiele und in der Stammrinde. Die Ausbreitung von *P. sparsa* wurde nur sehr selten im Xylem und Phloem gefunden. Diese Ergebnisse bestätigen, dass der Interzellularraum für die Langstreckenausbreitung des Pathogens sehr bedeutend ist. Die Blattstiele waren für die Infektion und Ausbreitung in Blättern und Stielen notwendig. Das Vorkommen von Oosporen in den Blattflächen und Blattstielen reflektierte die Entwicklungswege des Pathogens, während die Besiedelungsdichte die Eignung von Blattgewebes für den Befall durch *P. sparsa* verdeutlichte. Bemerkenswert war die Fähigkeit des Pathogens zur systemischen Ausbreitung. Die Besiedelung von Blattgewebe wurde sowohl in acro- als auch basipetaler Richtung beobachtet.

Die Thermographie erlaubte den Nachweis von Falschem Mehltau ein oder zwei Tage vor dem Auftreten sichtbarer Symptome. Die Infektion von *P. sparsa* führte zu einem progressiven Anstieg der Blatttemperaturen hervorgerufen durch das Schließen der Spaltöffnungen, was in späteren Stadien der Erkrankung sich wiederum verringerte, was zu erhöhter Blatttranspiration und Wasserverlust führte. Auch die thermograpische Visualisierung bestätigte die Ausbreitung von *P. sparsa* von lokalen Infektionsorten zu symtomlos besiedelten Blattzonen. Im Verlauf der Pathogenese erlaubten Veränderungen der Blatttemperaturen eine Differenzierung der Anfälligkeit von Rosensorten. Die IR-Thermographie erwies sich als eine ideale Möglichkeit zur Untersuchung von *P. sparsa* – Rosen Interaktionen. Das Potential dieses nicht-invasiven Verfahrens zur Erkennung und Differenzierung von Falschen Mehltauinfektionen in frühen symptomlosen Stadien konnte belegt werden.

Abbreviations

AUDPC	Area under disease progress curve
cv.	Cultivar
°C	Celsius
dai	Day(s) after inoculation
hai	Hour(s) after inoculation
HRH	High relative humidity
IR	Infrared
K	Kelvin
LRH	Low relative humidity
mm	Millimeter
ml	Milliliter
MTD	Maximum temperature difference
µl	Microliter
Ps	*Peronospora sparsa*
RH	Relative humidity
RGB	Red green blue
rpm	Rotation per minute
SI	Sporulation index
TEM	Transmission electron microscopy
T°max	Maximum temperature
T°min	Minimum temperature
T°avg	Average temperature
ΔT	Delta temperature

1. GENERAL INTRODUCTION

The beauty, fragrance and multiple uses of roses as cut flowers or landscape plants have made this an appreciated crop since ancient times. From an economical standpoint, roses are the most important plants in ornamental horticulture (Hummer and Janick, 2009). Together with the genera *Fragaria*, *Rubus*, *Potentilla* and *Geum*, *Rosa* belongs to the subfamily Rosideae within the family Rosaceae. The genus *Rosa* comprises about 180 species (Debener and Linde, 2009), most of which are woody perennial shrubbs with a basic chromosome number of seven and ploidy levels ranging from 2x to 8x (Cairns, 2003; Wissemann, 2006; Debener and Linde, 2009). *Rosa* spp. are found throughout the colder and temperate regions of the Northern hemisphere, form the Arctic to the subtropics (Hummer and Janick, 2009).

Concerning the cultivated roses, in 1999 the American Rose Society, who are responsible for establishing the classification system of these flowers, classified them in three major classes: (i) species often referred to as “wild roses”, listed according to their Latin names; (ii) old garden roses, which comprise 21 groups; and (iii) modern roses, with 13 groups (Cairns, 2003; Wellan, 2009). This scheme of classification reflected not only the botanical but also the commercial development of roses (Cairns, 2003). Some well-known groups are *Hybrid perpetual* roses, *Hybrid tea* roses, *Polyantha* roses, *Tea* roses, *China Bengal* roses, *Noisette* roses, *Multiflora* roses and *Wichuriana* roses (Horst, 1983). *Hybrid tea* roses (*Rosa* x *hybrida*) are the most popular class of modern roses. Corresponding to garden and (predominantly) glasshouse roses, this group is currently highly appreciated due to its fragrance, shapely blooms, amount of petals, long straight stems and recurrent flourishing habit (Horst, 1983; Wellan, 2009). Dominated by *Rosa dilecta*, this group includes crosses between hybrid perpetuals and all other rose groups (Horst, 1983). The first Hybrid tea cultivar was La France, created in 1867. This and all the rose classes obtained after it are classified as modern roses, while those created before are known as old garden roses (Wellan, 2009). Modern cultivars are mostly interspecific hybrids usually deriving from *R. canina*, *R. chinensis*, *R. foetida*, *R. gallica*, *R. gigantea*, *R. moschata*, *R. multiflora*, *R. phoenicea*, *R. rugosa* and *R. wichuraiana* (Hummer and Janick, 2009).

There is evidence that roses were first cultivated 4,000 to 5,000 years ago in northern Africa. Since then, speciation has produced many hybrids and hybrid groups (Horst, 1983). Cultivated roses are grown all around the world in almost all climates in three major horticultural groups: garden roses, pot roses, and cut-roses (Debener and Linde, 2009).

The cut flower industry is becoming globalized with production moving to South and Central America and Africa (Hummer and Janick, 2009). Nowadays, an important cut-rose production takes place at higher altitudes in the tropics (De Vries, 2003; Chaanin, 2003). Environmental conditions like day/night temperature, intense irradiation and the availability of cheaper labor force make countries like Kenya, Zimbabwe and Ecuador quite suitable for rose production all year round (Yan, 2005).

Blom and Tsujita (2003) mentioned that under cover cut-rose production worldwide occupied approximately 8,500 ha, with an annual yield of around 15-18 billion stems. The greatest production areas are located in Colombia, Ecuador and Kenya. The Netherlands, Italy, France and Japan may be considered as intermediate producers. In 2012, the Colombian production of cut roses represented $350 million USD corresponding to about 50,000 tons, which were produced under cover in 2,600 ha and mainly sold in the American market (Gonzales and Sarmiento, 2013). The Netherlands was ranked as the main rose supplier for the European Union, followed by Colombia, Spain, Kenya, Israel and Turkey (Sudhagar and Phil, 2013). Concerning the prices, as a general rule it can be said that the taller the stems, the higher the price, stem length usually varying from 30 to 100 cm (Blom and Tsujita, 2003). In the case of potted miniatures, the introduction of new cultivars in the 1980´s resulted in a significant renovation and increase of the pot rose market, whose world production was estimated in 60-80 million by 2003 (Pemberton et al., 2003).

Both pot plants and cut roses, either planted outdoors or in glasshouses are susceptible to many phytopathogens. Among the most serious foliar diseases, it is worth mentioning downy mildew, powdery mildew, black spot and rust. Other important diseases include Botrytis blight, caused by *Botrytis cinerea*, which affects roses during storage or transportation and may also be the causal agent of cane canker. For its part, *Coniothyrium fuckelii* is responsible for common canker, which colonizes wounded rose stems (Horst, 1983). In the current chapter, basic information about the main foliar fungal diseases is presented and aspects related to downy mildew are discussed in more detail.

Caused by the obligate biotroph *Podosphaera pannosa* (syn. *Sphaerotheca pannosa*), powdery mildew may be the most widely distributed disease among glasshouse, garden and field-grown roses. Severe damage affects the visual value of the flowers and, therefore, their commercial price (Horst, 1983; Linde and Shishkoff, 2003). Its early symptom consists in slightly blistered red areas on the upper leaf surface. Apparently, conidia do not germinate on moisture free surfaces, warm temperatures and ≥70% RH

during the day are suitable for conidia maturation and release. Fungal growth may develop on young stems, pedicels and petals (Horst, 1983). On the other hand, rust is mainly a foliar disease, although stems and blooms may be attacked as well (Shattock, 2003). *Phragmidium mucronatum* and *P. tuberculatum* are the two most common species in cultivated roses, provided that other five species of *Phragmidium* have also been reported in roses (Horts, 1983). Irregular purple to yellow brown spots dispersed on the upper leaf surface are typical symptoms. These lesions coincide with orange-yellow pustules on the lower side of the leaf and dense production of uredinospores, which later turn black due to the formation of teliospores (Shattock, 2003). The most important disease in garden roses is black spot, which is caused by *Diplocarpum rosae* and which is only occasionally observed in greenhouse roses (Gullino and Garibaldi, 1996). Typical disease symptoms are 2 to 12 mm diameter black spots on the upper leaf surface with yellow tissue surrounding the lesions, followed by chlorosis that extends and then causes leaflet drop (Drewes-Alvarez, 2003; Horts, 1983). Petioles, stipules, peduncles and sepals may present discrete black spots. In the yellowing area of the infected tissue, the metabolic activity of the pathogen is intense (Drewes-Alvarez, 2003).

Downy mildew is caused by the oomycete *Peronospora sparsa*. Oomycetes are a diverse group of eukaryotic organisms widely distributed in very diverse environments. Some oomycete morphological features like an ornamented flagellum during motile stages demonstrate their phylogenetic affinity with diatoms and brown algae of the Kingdom Straminipila (Dick, 2002). Most oomycete species are parasites of plants (Thines and Kamoun, 2010). Evolution processes occurred in different lineages of the Oomycota have resulted in obligate biotrophic pathogens such as the causal agents of white blister rusts and downy mildews, which are considered to have evolved from an apparently saprophytic ancestor (Thines and Kamoun, 2010). All species of downy mildew are obligate parasites with limited host range and low tissue damage of the infected plants (Ingram, 1981).

Oomycetes produce infection structures like appressoria, hyphae and haustoria, but features like cellulose as the main component of the cell wall, coenocytic hyphae and, in some cases, the production of motile spores make them different from true fungi (Slusarenko and Schlaich, 2003). As they have developed the ability to infect plants independently of true fungi, they might have different mechanisms for interacting with plants (Kamoun et al., 1999). In contrast to filamentous fungi, oomycetes contain low or no membrane sterols (Osbourn, 1996).

P. sparsa infecting rose plants was first reported in England in 1862. In 1880, it was reported in Midwester (United States) and by 1900's it was observed in Europe and the Soviet Union (Horst, 1983). The disease may be found where roses are cultivated (Xu and Pettitt, 2003). Most rose cultivars are susceptible to it, but severity is variable (Schulz and Debener, 2010). Leaves, stems, peduncles, calices and sepals can be infected, showing typically purplish to brown lesions (Horst, 1983). The most prominent symptoms are those associated with leaves and stems (Alfieri, 1968). Flowers and flower buds are malformed even under the influence of a light infection. The drop of severely infected leaves is quite common (Horst, 1983). Typical morphological characteristics of *P. sparsa* are 300-465 µm long sporangiophores that branch 3-4 times and produce ellipsoidal to nearly spherical, 18-24 x 16-20 µm, pale yellow sporangia bearing a short stalk sometimes present in detached sporangia. Oospores are 22-30 µm diameter, with a hyaline outer wall c. 2 µm thick (Francis, 1981). A branching intercellular coenocytic mycelium makes them an extensive absorbing surface that penetrates plant cells through filiform haustoria (Fraymouth, 1956). Erected sporangiophores are produced on the lower leaf surface through leaf stomata (Xu and Pettitt, 2003).

The disease is frequently observed in greenhouses. It constitutes a severe problem in plant containers and nurseries (Horst, 1983; Xu and Pettitt, 2003). It may cause very strong losses under plastic tunnels, but in heated commercial greenhouses the disease may not be severe (Gullino and Garibaldi, 1996). Though it is a destructive disease, especially in commercial rose crops in the tropics, information about crop losses is limited. Downy mildew is one of the most important diseases affecting greenhouse roses in Colombia (Restrepo and Lee, 2007). Suárez (1999) reported losses due to the disease coming close to US$ 3,000 per hectare at the Bogota Plateau. In Colombia several greenhouse models have been developed to minimize the impact of *P. sparsa*, but the disease still reaches high levels for over half of the growers (Restrepo, 2004). In Wasco, CA, where they produce more than 50% of the bare-root roses of the United States, there have been sporadic but continuing problems with rose downy mildew since early 1990s. Severe defoliation of infected plants reduces plant vigor while rootstock cuttings may fail to root and the canes cannot reach the diameter required for the market. In addition, there is the possibility of exporting the pathogen due to its presence within propagation materials (Aegerter et al., 2002).

The incidence of the disease increases with prolonged leaf wetness periods. Germination of *P. sparsa* sporangia has been observed to be high from 2-18°C and to decline under and over these values. No germination has been observed at 26°C (Xu and Pettitt, 2003).

In leaf discs of tummelberry plants (*Rubus* sp.) infected by *P. sparsa* (syn. *P. rubi*) the incidence of the disease occurred from 2 to 28 °C and the highest values were observed at 15 °C (Breese et al., 1994). Spores are produced in great numbers on the undersurface of infected leaves in short periods of time (about three days) and for as long as one month under favorable conditions (Alfieri, 1968). In drier conditions they are often sparse and thus easily unnoticed (Wheeler, 1981). Sporulation may take place in infected rose leaves before symptoms appear (Xu and Pettitt, 2003). Disease development is favored by 90-100% humidity and relatively low temperatures. Therefore, rose downy mildew occurs mainly in glasshouses, rather than outdoors (Wheeler, 1981). The role of oospores in disease transmission is not clear to date. They have been found in leaves, stems and flowers, but their occurrence seems to be sporadic (Fraymouth, 1956; Xu and Pettitt, 2004). The number of oospores has been found to vary across infected leaves and infected plants, with oogonia forming in necrotic lesions, but rarely in the green areas of affected leaves (Xu and Pettitt, 2003). These authors found oogonia to be formed one week after infection in the mesophyll of detached leaves. The transmission as dormant mycelium in cuttings and plants has also been reported (Alfieri, 1968; Francis, 1981). In addition, the pathogen may overwinter in infected stems in the form of dormant hyphae (Francis, 1981). In a more recent study, DNA of *P. sparsa* was detected not only in the cortex of stems and root tissues of symptomatic plants, but also in the cortex of crown tissues of asymptomatic mother plants used as a source of propagation material (Aegerter et al., 2002). By microscopy techniques, these authors confirmed the presence of profuse hyphae and oospores within the stem cortex of infected canes and the occurrence of perennating infections of *P. sparsa*.

In greenhouses for the commercial production of cut roses, epidemics usually begin in localized areas of the crop. This event, together with the pattern of appearance of the disease symptoms in plants suggests a particular association between *P. sparsa* and the plant tissue. Xu and Pettitt (2003) have mentioned that *P. sparsa* does not spread from leaves to stems according to their histological observations that showed the mycelium locally restricted. In effect, they failed to observe it invading even minor vascular tissues and did not find it in petiolar vascular tissue. Therefore, they concluded that the invasion of the stems through petioles was quite unlikely. In a recent study, Gomez and Filgueira (2012) reported the capacity of *P. sparsa* to move through the xylem vessels in micro-propagated rose plants. These contrasting results show that the development of *P. sparsa* has not been completely elucidated. Downy mildews, which are obligate biotrophs, are difficult to handle because their growth depends on living plant tissue. This explains the limited knowledge of some of these organisms (Coates and Beynon, 2012).

The pathogen requires moisture and is difficult to control with fungicides (Karlik and Tjosvold, 2003). Different studies have shown the response of *P. sparsa* to environmental factors and the strong effect of favorable environmental conditions on the development of the disease (Aegerter et al., 2003; Restrepo and Lee, 2007). Roses grown under less than 85% relative humidity were not infected. These factors indicate the importance of maintaining low relative humidity levels by using heat if necessary, and of avoiding sudden temperature drops during the night, as they greatly increase relative humidity (Horst, 1983). Good ventilation and air circulation are also important. Some control of the disease can be achieved in glasshouse by temporarily raising the temperature to 27°C and ventilating to reduce humidity (Wheeler, 1981). Indeed, the feasible environmental conditions that may limit the development of rose downy mildew in greenhouses seem to be those provided by hot air heating systems and motile ventilation in the roof (Restrepo and Lee, 2007). The reduction or elimination of water leaks and wet benches are strongly suggested (Alfieri, 1968; Horst, 1983).

Oospore formation seems to be variable and there are evidences that *P. sparsa* perennates as dormant mycelium in stems. Control measures should include the removal and destruction of cuttings and symptomatic leaves along with infected fallen leaves and stems or parts of the plant that probably carry structures of *P. sparsa* (Alfieri, 1968; Wheeler, 1981; Horst, 1983). Downy mildew is currently controlled with foliar fungicides that are applied preventively (Aegerter et al., 2003). Protectant sprays with fungicides and oomyceticides are recommended when environmental conditions are ideal for the infection (Horst, 1983). Chemicals like chlorothalonil, dithiocarbamates and mancozeb provide good protection. Fosetyl-aluminum and phenylamide fungicides (e.g. metalaxyl and oxadyxil) are used to control and reduce the severity of the disease. Nonetheless, resistance to phenylamides has been seen in different oomycetes (Schwinn, 1981; Gisi, 2003; Xu and Pettitt, 2003). Foliar treatment is the most common type of fungicide application when it comes to downy mildew control. Several spray applications per crop cycle are necessary due to the development of progressive epidemics (Gisi, 2003). Rose growers apply fungicides or oomyceticides routinely because losses are potentially devastating (Aegerter et al., 2003). In 1996, 16.7% of the sales value of the global fungicides market corresponded to products for downy mildew control. Concerning plant crops, 4% of the downy mildew fungicides market was related to downy mildews of ornamental crops (Gisi, 2003). In commercial crops, due to the permanent nature of young apical growth in the plants, the elevated market prices of roses produced by susceptible cultivars, and the limited possibility of including heating systems in current production schemes, the disease is difficult to handle.

In a number of plant-oomycete interactions, hypersensitive response (HR) is the major defense reaction in resistant and in some partially resistant plants. In susceptible plants, HR is ineffective and numerous escaping hyphae remain after the plant's response (Kamoun et al., 1999). Breeding for disease resistance has not been the most important task of modern rose breeders. Flower color, tolerance to cold, lack of prickles, shoot yield and recurrent flowering have been the main features of interest. Recently, the screening of 183 wild rose accessions with downy mildew isolates resulted in the identification of 19 resistant accessions. Histochemical evaluations revealed HR as the main resistance response (Schulz and Debener, 2010). Since downy mildew resistance genes have been already identified in wild rose species and their introgression into modern cultivars is possible, resistance to rose downy mildew may be attainable in the future.

Most rose growers regularly and systematically monitor and inspect plants or particular areas of the crop to detect the disease and determine the adequate control method and corresponded timing when necessary. In some downy mildews, the lack of visible symptoms during early stages of infection and until asexual sporulation difficults field assessment (Clark and Spencer-Phillips, 2004). In addition, the commercial production of potted or cut roses allows little damage of the harvested crop (Karlik and Tjosvold, 2003). Thus, crop protection is critical and the financial risk associated with losses due to uncontrolled pest populations is certainly high (Bout et al., 2010). Integrated pest management (IPM) implies a multifaceted approach and stresses the importance of early pest detection (Karlik and Tjosvold, 2003). Indeed, IPM monitoring strategies provide tools for managing this risk, but conventional methods are usually highly time-consuming (Bout et al., 2010). Towards a sustainable IPM in roses, especially in labor-intensive plantations where crop protection is critical and often involves the use of chemical methods, non-invasive techniques to detect plant diseases may play an important role.

The capture of data from an object using sensors that are not in direct contact with it is defined as remote sensing. Remote sensing technologies may be an alternative to visual disease assessment and provide new quantitative information concerning disease risk (Nutter et al., 2010). Sensors vary according to the measuring range in the electromagnetic spectrum and the assessment scale. They also vary depending on whether they are imaging or non-imaging, passive or active sensors. Just as well, they may be equipped or not with an own source of radiation (Mahlein et al., 2012). Thermography, reflectance and fluorescence measurements are currently the most promising techniques for the detection and monitoring of plant diseases (Chaerle and Van der Straeten, 2000).

Chlorophyll fluorescence imaging allows the study of spatio-temporal changes in photosynthetic processes, which are monitored with high precision within plant tissues prior to the occurrence of visible symptoms (Lenk et al., 2007). The captured images are used to characterize plant health condition and show the distribution and variation of the disease over the sample (Lenk et al., 2007). The system possesses high resolution but it is not easy to apply to outdoor plant canopies because of the need of an extra illumination system (Chaerle et. al., 2007).

Hyperspectral imaging (HIS) is a relatively young technology and its application to plant pathology is particularly recent. Nonetheless, it has been suggested as a novel, powerful and useful tool in this area as it generates a lot of information on the spectral characteristics of the leaf surface, which can be used to detect diseases symptoms (Bock et al. 2010). HIS provides information from multiple narrow wavelength zones and their combination can be indicative of specific stresses (Chaerle et. al., 2007). The information provided by a hyperspectral image is based on the spatial X- and Y axes and a spectral Z-axis that allows a more detailed interpretation of the signals obtained from the object (Mahlein et al., 2012). Diseases may cause modifications in reflectance resulting from changes in the biophysical and biochemical characteristics of plant tissue (West et al. 2010). Hence, contrasting disease symptoms may be detected through correspondingly different wavebands (Mahlein et al., 2010). In fact, some studies have shown the potential of HSI for disease identification. Nevertheless, the imagery that these sensors generate is large and complex. Therefore, as a plant disease assessment tool, this technique is still under development (Bock et al., 2010).

Thermal imaging converts the invisible radiation pattern of an object into visible images (Vadivambal and Jayas, 2011). Thermography allows the visualization of differences in surface temperature by detecting emitted infrared radiation (8–14 μm long-wave). Then, a software package transforms this radiation data into thermal images in which temperature levels are indicated by a false-color gradient (Chaerle and Van der Straeten, 2000). Originally developed for military purposes, infrared thermal imaging was later applied to fields such as agriculture, civil engineering and human and animal medicine. Through thermal imaging, highly accurate temperature measurements are possible. Most thermal imaging cameras scan at a rate of 30 times per second within a temperature range from -20°C to 1,500°C (Vadivambal and Jayas, 2011).

The intensity of the radiation emitted by an object is a function of its surface temperature. Therefore, the higher the temperature, the greater the intensity of the infrared radiation

emitted by the object under study (Vadivambal and Jayas, 2011). Changes in leaf temperature in plants mainly result from transpiration alterations responding to particular stresses (Chaerle and Van der Straeten, 2000). Thermography is based on the principle that leaves cool down as water is lost through the stomata; while they heat up when stomata close (Grant et al., 2006). Alterations in the water status of a plant caused by unfavorable conditions promote changes in leaf transpiration, in turn resulting from the active regulation of stomatal aperture. The patterns of leaf cooling can be monitored instantly and remotely by thermographic imaging (Chaerle and Van der Straeten, 2000).

Imaging techniques possess high spatial resolution and, thus, the capability of displaying patterns and gradients (Chaerle and Van der Straeten, 2000). Therefore, thermography allows spatial and temporal transpiration heterogeneities caused by plant diseases to be imaged and monitored both pre symptomatically and along disease development (Mahlein et al., 2012). The major advantage of infrared thermal imaging is the non-invasive and non-contact nature of the technique when it comes to determining the temperature of the object over a short period of time (Vadivambal and Jayas, 2011). The technique is particularly suitable to outdoor measurements even at large spatial scales (Chaerle et al., 2007), but it is highly sensitive to environmental conditions during measurement and the visualized thermal response does not allow plant disease identification (Mahlein et al., 2012). Plant evaluation by thermal imaging has broad uses in agriculture, covering different areas such as crop water stress assessment, seed viability evaluation and estimation of soil water status (Vadivambal and Jayas, 2011).

The application of thermography has been demonstrated for the detection of early plant responses in various pathosystems such *as Pseudoperonospora cubensis* (Lindenthal et al., 2005; Oerke et al., 2006), *Cercospora beticola* in sugar beet (Chaerle et al., 2004), cucumber downy mildew caused by *Plasmopara viticola* in grapevine (Stoll et al., 2008), *Venturia inaequalis* in apple leaves (Oerke et al., 2011) and *Fusarium oxysporum* f. sp. *cucumerinum* in cucumber (Wang et al., 2012). Likewise, Chaerle et al. (2004) imaged the hypersensitive response and cell death induced by tobacco mosaic virus (TMV). Under field conditions, thermography has been used to detect *Fusarium* head blight in ears of winter wheat with the possibility to evaluate the severity of the disease across plots (Oerke and Steiner, 2010). This methodology may be useful in programs aimed at the reduction of health risks resulting from the mycotoxins produced by *Fusarium* spp. (Mahlein et al., 2012).

A comprehensive understanding of the development of *P. sparsa* at the histological level in rose tissue is needed, not only to implement suitable and timely disease control strategies, but also as part of the knowledge required for the adequate understanding of the outcomes provided by tools used for the early detection of the disease. In the direction of development of a more efficient integrated control program for rose downy mildew, this research makes an approach to the development of *P. sparsa* in rose tissue and introduces the use of a non-invasive method in the study of rose downy mildew infection. The current investigation was based on the premises that, (i) like other downy mildews, *P. sparsa* spreads through plant tissues in a process regulated by host maturity and that (ii) leaf tissue responses induced by the pathogen after infection can be sensed during early stages by thermal imaging.

In this context, the aims of this research were to:

i. evaluate biological characteristics of different isolates of *P. sparsa*,
ii. study the development of *P. sparsa* at the histological level in rose tissues,
iii. assess the development of *P. sparsa* from localized infection sites in order to elucidate its ability to form systemic infections in the plant,
iv. estimate the potential of infrared thermography as a non-invasive method to detect early infection of downy mildew in roses, and
v. characterize the thermal response of rose leaves when infected by *P. sparsa*.

2. BIOLOGICAL CHARACTERIZATION OF *Peronospora sparsa* ISOLATES FROM COLOMBIAN ROSE CROPS

2.1 Introduction

Extensively used for decorative purposes and praised for their beauty and fragrance, roses hold a privileged position over all other flowers (Ahmad et al., 2011). Cut-roses can be downgraded due to short or injured stems or poor flower or foliage condition (Scott and Healy, 1991). Since bud size and stem length determine rose prices (Blom and Tsujita, 2003), any damage on leaves, flower buds or stems may affect quality standards and directly take a toll on the commercial price. Downy mildew is a severe disease that affects the quality of cut roses. *Peronospora sparsa* (Oomycete, Peronosporaceae) infects young leaves and stems at the shoot apex, peduncles, calyxes, sepals and petals. Infected plant material normally presents purplish to black spots, chlorosis and drop of diseased leaves (Horst, 1983; Wheeler, 1981). However, flowers can be retarded or malformed by infections showing no visible damage on the leaves (Stahl, 1973).

Roses are among the leading cut flowers in global floriculture trade. Colombia is the second major rose producing country of the world after The Netherlands (Evans, 2009; Bonarriva, 2003). Most Colombian crops are located in the Bogota Plateau, where the entire production takes place in plastic greenhouses and the average cropping cycle length is about five years, from planting to renovation (Parrado et al., 2011). The disease has affected Colombian crops over 35 years, causing in the last decades a series of severe epidemics that have strongly impacted crop yields (Arbeláez, 1999). The costs of downy mildew control in the Bogotá Plateau are calculated by the growers in approximately US$ 2.31 m^2 $year^{-1}$. These expenses are distributed as follows: 68.8% to symptomatic plant material removal workforce, 30.3% to chemical control and 0.86% to operate horizontal air flow systems when installed.

P. sparsa develops sporangiophores and sporangia below the surface of downy mildew spots when humidity is relatively high (Francis, 1981). Under optimal conditions, *P. sparsa* can quickly spread over the whole field (Schulz and Debener, 2007). Different authors have reported the presence of oospores in infected leaves, sepals, flowers, buds and stems (Fraymouth, 1956; Stahl, 1973; Horst, 1983; Xu and Pettitt, 2003; Gómez and Filgueira, 2012). In some downy mildews like *Hyaloperonospora parasitica* in *Arabidopsis*, *Plasmopara viticola* in grapevine or *Peronospora manshurica* in soybean, the infection of new plants occurs via oospores which have over-wintered in leaf debris in the soil and the

successive cycles of leaf infection occurs by sporangia (Populer, 1981; Dunleavy, 1981; Slusarenko and Schlaich, 2003). In rose downy mildew, the role of oospores in disease transmission is not so clear. The main source of inoculum corresponds to sporangia produced in infected leaves (Francis, 1981). The presence of different *P. sparsa* races in roses has not been reported to date (Schulz and Debener, 2007), in contrast with *Peronospora farinosa* f. sp. *spinaciae* (syn. *Peronospora effuse*), the downy mildew of spinach (Brandenberger et al., 1994; Satou et al., 2006; Irish et al., 2007) or with *Plasmopara halstedii* in sunflower (Gulya et al., 1991).

SSCP (Single Strand Conformational Polymorphism) analysis suggested homogeneity among isolates of *P. sparsa* taken from four localities at the Bogota Plateau (Ferrucho, 2005). However, in this framework the analysis of ITS2 (Internal Transcribed Spacers) demonstrated nucleotide differences among isolates. For its part, sequence analysis showed a mutation point in some clones, which was recognized by the enzyme *PvuII* in 35 isolates, thus allowing the identification of mixed infections as two variants within a sample (Ferrucho, 2005). In turn, RFLP (Restriction Fragment Length Polymorphism), RAPD (Randomly Amplified Polymorphic DNA) and RAMS (Random Amplified Microsatellites) analyses of 35 Colombian isolates from two production areas also indicated low variability among isolates (Ayala et al., 2008), which allows concluding that the population of *P. sparsa* in Colombia is predominantly clonal. Epidemiological investigations aimed at assessing the effects of temperature and light on *P. sparsa* development have shown optimal and critical values (Giraldo et al., 2002; Soto and Filgueira, 2009), as well as responses from pathogen isolates (Varila, 2005).

To date, the studies conducted to investigate *P. sparsa* development in roses have considered single or diverse sources of inoculum infecting one cultivar while others have evaluated different rose cultivars infected by one isolate. Though the genetic diversity of *P. sparsa* seems to be low, few studies have contributed to characterize populations of the pathogen affecting commercial crops, in terms of important biological aspects for the selection of control strategies. Thus, the aims of this study were: (i) microscopical evaluation of *P. sparsa* isolates from different locations at the Bogotá Plateau in two rose cultivars and (ii) biological characterization of the obtained isolates by aggressiveness assessment parameters.

2.2 Materials and methods

2.2.1 Plant material

Adult rose plants of the cv. Sweetness® belonging to the grandiflora class (Jackson & Perkins, Hodges, South Carolina USA) and cv. Elle® var. Meibderos plants (Meilland International SA, Le Luc-en-Provence, France), Hybrid tea rose, were used as sources of plant material for the experiments. The plants were grown under glasshouse conditions, 16 h photoperiod and average temperatures of 23°C/18°C (day/night) in 10 L pots containing a 3:1 mixture of soil and Profi-substrat Typ ED73 (Gebrüder Patzer GmbH & Co Sinntal-Jossa, Germany), where they were regularly watered and fertilized. Juvenile leaves harvested from the plants immediately before the experiments were used to study the development of the isolates under controlled conditions. After being harvested, the leaves were washed twice with tap water and then rinsed with distilled sterile water. Five leaf discs of 2 cm diameter of each cultivar were placed in the Petri dishes with the adaxial side in contact with wet filter paper (100% RH).

2.2.2 Isolates of Peronospora sparsa and inoculation

Leaves affected by downy mildew were collected during epidemics of the disease from seven Colombian commercial plantations in the year 2010. The sites selected for the sampling were located in the Bogotá Plateau (04°51'N; 74°04'W) at an altitude of 2,600 m.a.s.l. Average annual rainfall is 900 mm with variations along the year and over the region; daily average temperature is 13.5°C with monthly variations of 1°C and respective minimum and maximum records of -5.0°C and 25°C and during certain months of the year (POT, 2000). The location of the sampling sites is presented in Fig. 2.1. The selected crops were grown in conventional unheated plastic greenhouses, which are typical in the cut rose production of this area. The farmers were asked about the type of fungicides and other practices regularly employed to control downy mildew, which were found to be similar in all plantations. In all cases, symptomatic leaves and other parts of the plants were removed almost daily during epidemics of the disease and regularly along the crop cycle. In addition, partial aperture of the lateral areas of the greenhouse was used to improve air movement through the crop, thus decreasing relative humidity inside the greenhouse. Information related to the origin of the isolates from commercial crops is presented in Appendix 1. An additional isolate of *P. sparsa* (Ps 4) available at the phytopathology lab of the Universidad Nacional de Colombia (collected by Viviana Romero) was included in the study. This isolate was obtained during epidemics of downy

mildew in a commercial crop at the Bogota Plateau in 2008, from rose plants cv. Charlotte® that had been found to be susceptible to *P. sparsa,* but the site of origin was not recorded.

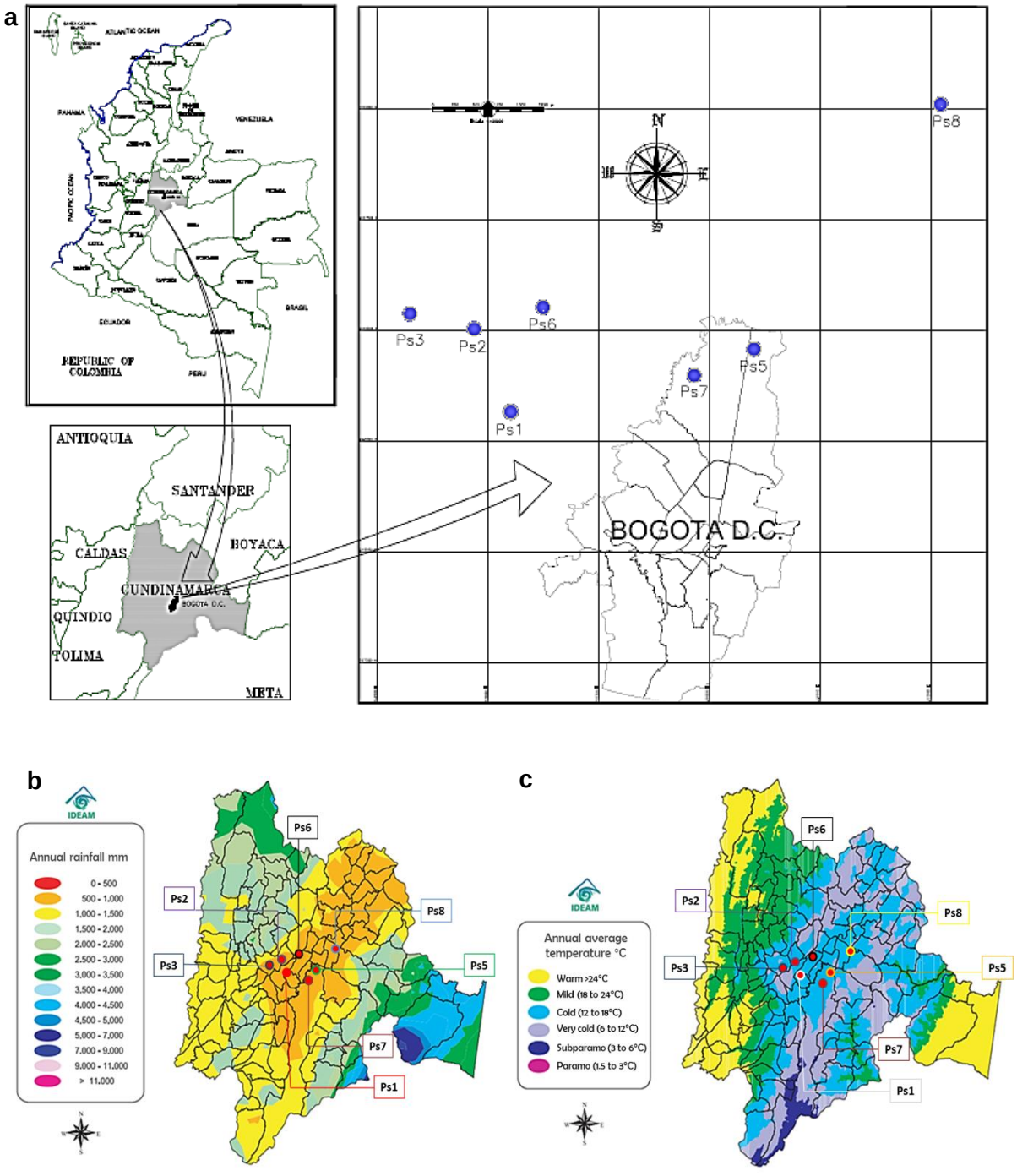

Figure 2.1 Sampling sites of *Peronospora sparsa* in commercial rose crops at the Bogotá Plateau, department of Cundinamarca in Colombia and their location according to different climatic areas of the region: **a**, location of the sampled commercial crops at the Bogota Plateau; **b**, distribution of annual rainfall in Cundinamarca; **c**, distribution of annual average temperature in Cundinamarca; b. and c. modified from Institute of Hydrology, Meteorology and Environmental Studies, IDEAM (2005). Ps: sampling sites.

Each sample consisted of 30 or 50 rose leaves showing typical disease symptoms. One sample of susceptible cultivars located in greenhouse areas where the disease was usually severe was obtained at each site. The leaves were wrapped in humid paper, individually packed in polyethylene bags, leveled and kept in cool boxes during transportation. Under laboratory conditions, sporulation of *P. sparsa* was promoted by keeping symptomatic leaves in plastic boxes under elevated humidity conditions (100% RH). Then, sporangia produced on the leaves of each sample were collected in distilled water, inoculated on fresh rose leaflets and maintained under controlled conditions. After five cycles, seven-day sporangia from each isolate were separately collected in sterile distilled water. Suspensions containing 5.0 x 10^4 sporangia per ml were adjusted with a Fuchs-Rosental hemocytometer and used as source of inoculum. Two 15 µl drops of the suspension were placed in the center of the abaxial side of the discs (Fig. 2.2a) and then uniformly distributed using a soft brush to cover the whole leaflet. After inoculation, the Petri dishes were stored in a growth chamber at 18°C/16°C (day/night) and under a 16 h daily photoperiod.

2.2.3 Biological characterization of Peronospora sparsa isolates

Daily evaluations of presence of sporulation on the leaf surface were conducted under the stereo microscope (Leica S4E, Wetzlar, Germany) for nine days. The latent period, *i.e.*, the number of days to the production of sporangia on the leaf surface (Parlevliet, 1979) was assessed. It was established when 50% of the discs per Petri dish presented sporangiophores with sporangia. Incidence of sporulation on leaf discs was daily determined. Each disc was divided in four segments and the presence of sporangiophores with sporangia per segment was established (Fig. 2.2b). Then, the area under the disease progress curve (AUDPC) for the incidence of sporulation was estimated using the trapezoidal method (Campbell and Madden, 1990), through the formula $AUDPC = \sum_{i=1}^{n} \left(\frac{y_i + y_{i+1}}{2}\right)(t_{i+1} + t_i)$, where *y* corresponded to the incidence of sporulation, and *t* to the evaluation time. The density of sporangia on the leaf surface was daily assessed, thus establishing the sporulation index (SI). SI was evaluated in the four segments from each leaf disc, and it was calculated as follows: $SI = [(0 \times n) + (1 \times n) + (2 \times n) + (3 \times n)] / \sum N$, where *n* in each factor corresponds to the number of segments of the leaf with no sporulation (0), scarce (1), intermediate (2) or abundant (3) sporulation and N represents the total number of leaf segments. $AUDPC_{SI}$ was also estimated for this variable. The production of sporangia per square centimeter of leaf was evaluated 9 days after inoculation (dai). The sporangia of the five discs of each

Petri dish were collected in 5.0 ml of sterile distilled water using a Vortex-Genie 2 (Scientific Industries, Bohemia N.Y, USA) at 600 rpm during one minute. The number of sporangia per ml was calculated using a Fuchs-Rosental hemocytometer. In order to assess the number of oospores produced in the leaf tissue, infected leaves were cleared in chloral hydrate 9 dai and for a period of 15 days (Bruzzes and Hasan, 1983; Jende, 2001), then stained in 0.01% acid fuchsin (Gerlach, 1977) and observed under microscope (Leitz DMRB; Leica, Wetzlar, Germany) equipped with Nomarski-interference-contrast. Oospores were quantified using the fine focus mechanisms of the microscope to examine the leaf from the upper to the lower epidermis. The number of oospores was counted at five sites of the leaf at random using a grid of 0.175 mm^2, which is available in the measuring tools of the Diskus 4.2 software (Hilgers, Königswinter, Germany) (Fig. 2.2c).

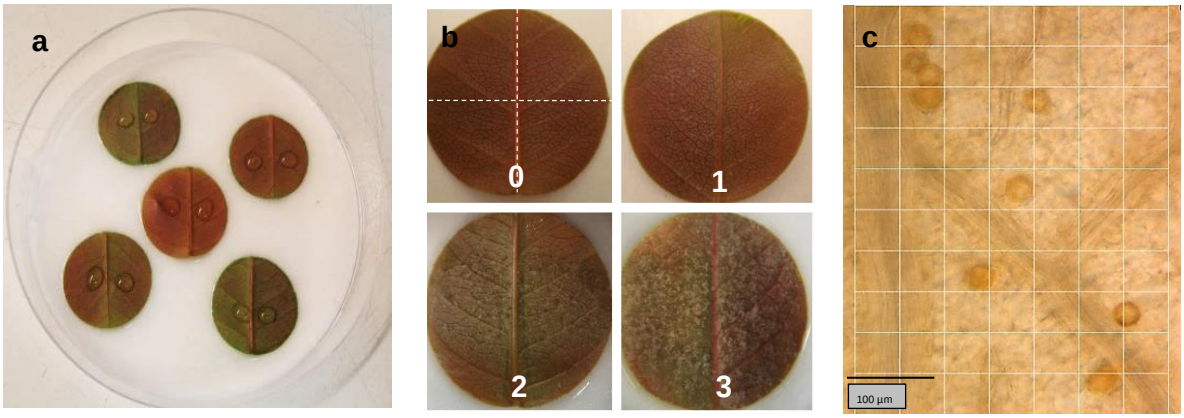

Figure 2.2 Presence of sporangia and oospores in leaf tissue measured to evaluate isolates of *Peronospora sparsa* on rose leaves cvs. Elle® and Sweetness®: **a**, leaf discs inoculated with a suspension of sporangia; **b**, leaf discs showing different levels of sporulation index under stereo microscope, 0: non-sporulating disc depicting the leaf segments evaluated, 1: scarce, 2: intermediate and 3: abundant level of sporulation; **c**, leaf area used for counting the number of oospores in leaf tissue under light microscope (20X).

2.2.4 Statistical analysis

The statistical analysis was conducted using the Superior Performing Software System SPSS 21.0 (SPSS Inc., Chicago, IL, USA). GLM univariate analyses were conducted. When F-values were significant, mean comparisons were performed (Tukey test, $P \leq 0.05$). The experiments were repeated three times and five replicates per isolate and cultivar were used.

2.3 Results

2.3.1 Development of isolates of Peronospora sparsa in rose leaves

2.3.1.1 Latent period

In cv. Elle® the first sporangia were observed 5.6 dai and in cv. Sweetness® 5.8 dai. The cultivar had no significant effect and no interaction was detected between cultivars and isolates (Table 2.1). In cv. Sweetness®, significant differences were observed between isolates (P = 0.01). In this cultivar, isolate Ps 4 had a shorter latent period (5.3 dai) than isolates Ps 5 and Ps 7 (6.3 dai). In cv. Elle®, no significant differences were detected between isolates (Fig. 2.3a).

2.3.1.2 Incidence of sporulation

No significant differences were observed between the isolates of *P. sparsa* in the AUDPC of the incidence of sporulation. Contrastingly, cultivars showed a highly significant effect (P = 0.00), which did not depend on the isolate (Table 2.1). The AUDPC of the incidence of sporulation values were higher in cv. Elle® than in cv. Sweetness® (Fig. 2.3b).

2.3.1.3 Sporulation index (SI)

As an indicator of the abundance of sporulation on the leaf surface at the beginning of pathogenesis (5 dai) and at the end of the study (9 dai), SI was significantly influenced by the rose cultivar (P = 0.00) in both periods. The isolates of *P. sparsa* had a significant effect (P = 0.03) on cv. Sweetness® (Fig. 2.3c, d) 9 dai. The highest value was observed in isolate Ps 4 and the lowest one in Ps 5 and differences between these isolates were significant. No interaction was observed between the cultivar and the isolates of the pathogen in both periods of evaluation (Table 2.2). The density of sporulation on the leaf surface analyzed as the $AUDPC_{SI}$ was significantly different for the two rose cultivars (P = 0.00), the highest value corresponding to cv. Elle®. The isolates were not significantly different and no interaction was detected between cultivars and isolates (Table 2.1).

2.3.1.4 Production of sporangia on rose leaves

The cultivar (P = 0.01) and the isolate (P = 0.01) had significant effect on the production of sporangia, but showed no significant interaction (Table 2.1). Differences between isolates

were only observed in cv. Elle®, where the amount of sporangia produced by isolate Ps 4 was higher than that observed in Ps 1 (Fig. 2.4a). No differences between isolates were observed in cv. Sweetness®.

2.3.1.5 Oospores production in leaf tissue

The production of oospores in leaf tissue 9 dai was significantly influenced by the rose cultivar (*P* = 0.004). No effect of the different isolates of the pathogen was observed. The influence of the cultivar on oospore production was not related to the isolate of the infecting leaf tissue (Table 2.1). The number of oospores in leaf tissue was higher in cv. Elle®, thus contrasting with the values observed in cv. Sweetness® (Fig. 2.4b).

Table 2.1 Development of *Peronospora sparsa* on rose leaves over a period of 9 days after the inoculation.

Variable of development		Source					
		Isolate		Cultivar		Isolate x cultivar	
Latent period	F	2.70		3.40		.864	
	P	.011	*	.066	ns	.536	ns
AUDPC Incidence sporulation	F	2.04		26.34		.184	
	P	.051	ns	.000	**	.989	ns
Sporulation index 5 dai	F	1.07		42.35		.369	
	P	.382	ns	.000	**	.919	ns
Sporulation index 9 dai	F	2.23		65.36		.528	
	P	.033	*	.000	**	.813	ns
AUDPC Sporulation index	F	1.81		69.75		.108	
	P	.086	ns	.000	**	.998	ns
Sporangia/cm^2	F	2.80		102.60		.625	
	P	.008	**	.000	**	.735	ns
Number of oospores	F	1.20		8.35		.531	
	P	.303	ns	.004	**	.811	ns

F: values of F-test; *P:* significance value; significance level: ns = no significant (*P* ≥ 0.050); * = significant (*P* ≤ 0.05); ** = highly significant (*P* ≤ 0.01)

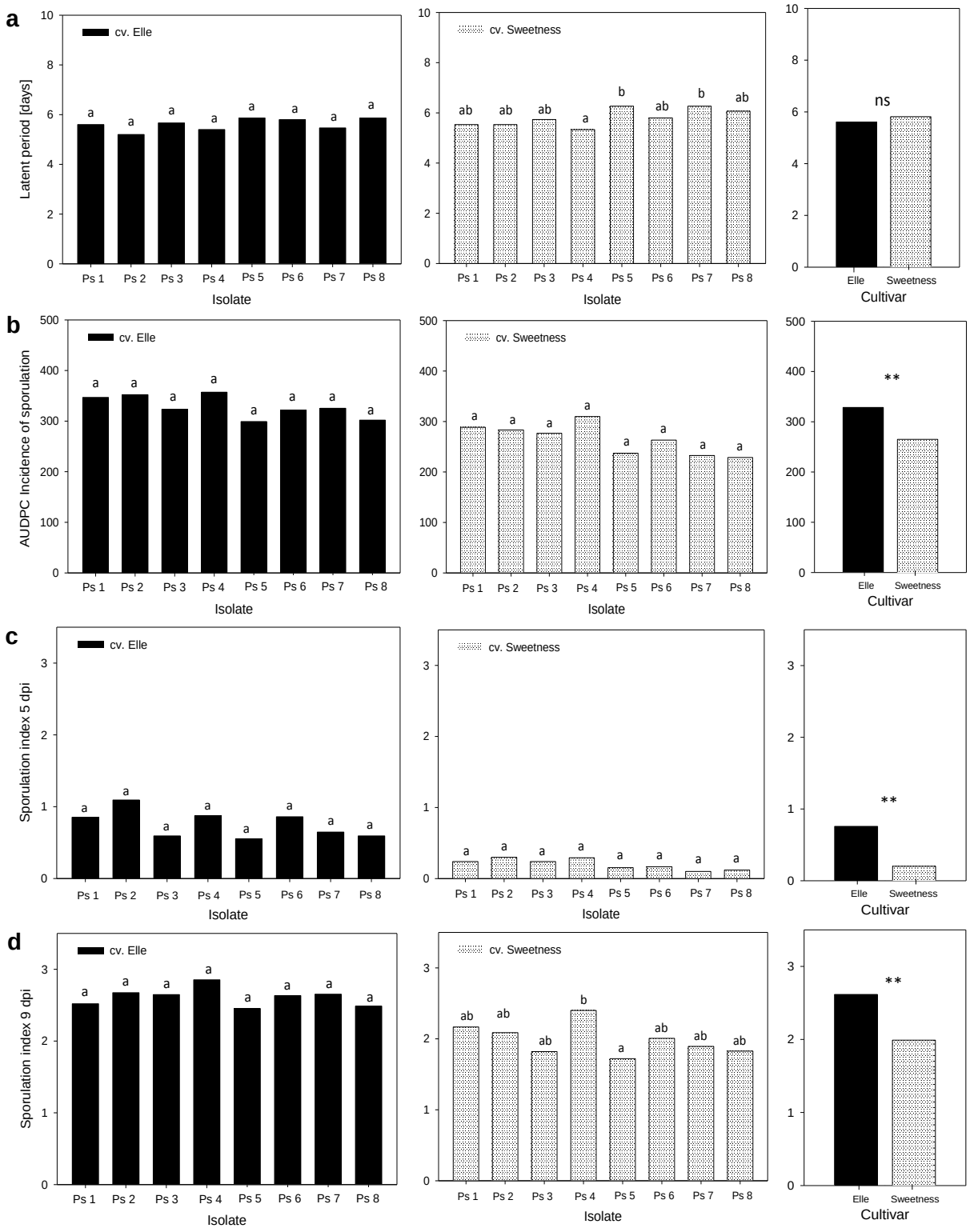

Figure 2.3 Development of isolates of *Peronospora sparsa* on rose leaves cv. Elle® and cv. Sweetness®: **a,** latent period; **b,** incidence of sporulation; **c,** index of sporulation 5 dai; **d,** index of sporulation 9 dai. Values followed by the same letter are not significantly different (Tukey test, $P \leq 0.05$). Significance level of F-test: ns = no significant ($P \geq 0.05$); ** = highly significant ($P \leq 0.01$).

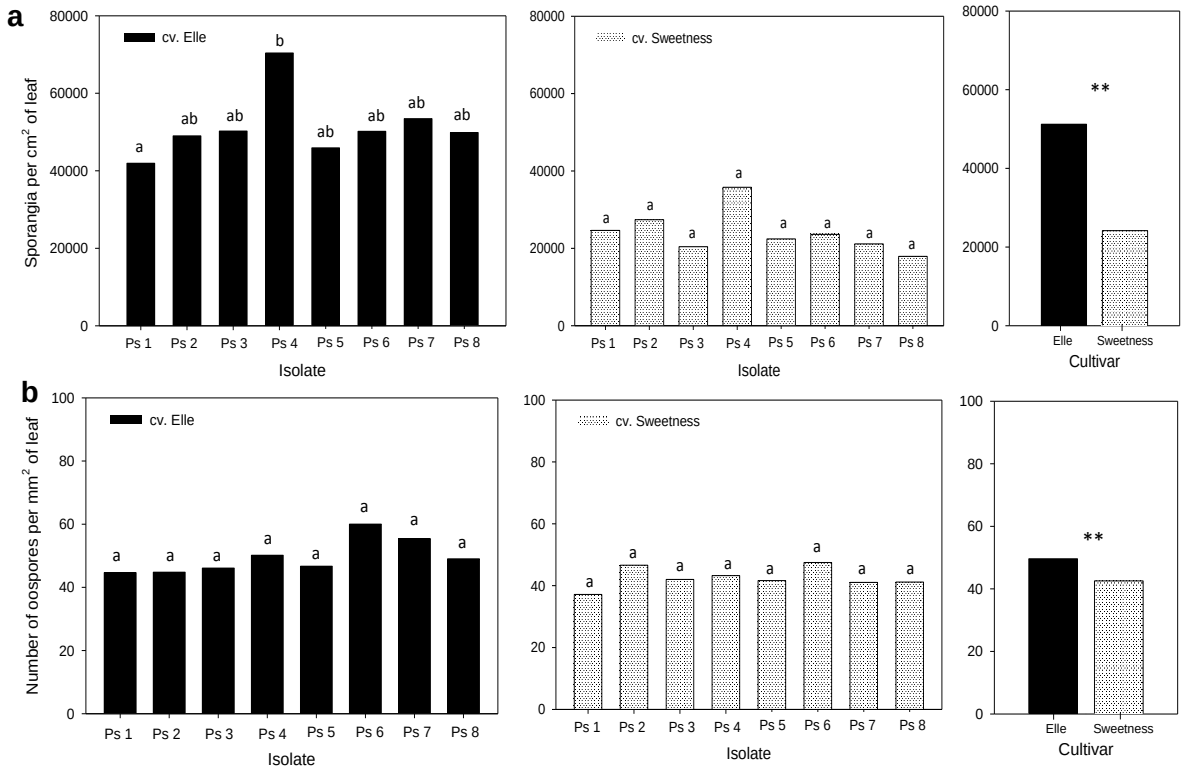

Figure 2.4 Production of sporangia and oospores of *Peronospora sparsa* in rose leaves cv. Elle® and cv. Sweetness®: **a**, production of sporangia; **b**, production of oospores in leaf tissue. Values followed by the same letter are not significantly different (Tukey test, $P \leq 0.05$). Significance level of F-test: ns = no significant ($P \geq 0.05$); ** = highly significant ($P \leq 0.01$).

2.4 Discussion

All the evaluated isolates were found to be pathogenic both in cv. Elle® and cv. Sweetness®. The statistical analyses revealed no interactions between isolates and cultivars. The results showed a fast and profuse development of the pathogen isolates from all the sampling sites and only slight variations were observed among them. The main differences were observed between cultivars. The isolates produced different amounts of sporangia and oospores on the leaves of cv. Elle® and cv. Sweetness®. Cv. Elle® was found to be highly susceptible to *P. sparsa* infection, whereas cv. Sweetness® may just be considered as a susceptible cultivar based on the classification used by Breese et al. (1994) in *Rubus* sp. infected by *P. sparsa*. All the studied variables were significantly higher in cv. Elle®, except for the latent period, which was similar in both cultivars.

The results suggest that slight differences between isolates of *P. sparsa* may be detected under controlled conditions. Interestingly, some differences were observed in cv.

Sweetness®. The variables assessed on the leaf discs allowed the characterization of the different isolates of *P. sparsa* and to differentiate rose cultivars by their susceptibility. After inoculating leaf discs of several cultivars of *Rubus* sp. with isolates of *P. sparsa* (syn. *Peronospora rubi*), Breese et al. (1994) not only found significant differences between cultivars, but also observed oospores in the leaf tissues of all cultivars. Based on the sporulation index, they established that hybrid berries (blackberry x red raspberry) were more susceptible than blackberries and red raspberries. On the contrary, Sakr (2011) found significant differences between *P. halstedii* (sunflower downy mildew) pathotypes, considering the percentage of infection, the latent period and the sporulation density as aggressiveness criteria.

The isolates of *P. sparsa* inoculated in cv. Elle® were similar for most of the measured parameters. Only in the production of sporangia, two isolates showed different values between them. In cv. Sweetness®, one of these isolates (Ps 4) showed a shorter latent period than that of isolates Ps 5 and Ps 7. Differences between these isolates were also observed in the SI as assessed 9 dai, when Ps 4 showed a higher value than Ps 5. Though all the isolates developed effectively in cv. Sweetness®, isolates Ps 4 and Ps 5 differed in some parameters but were similar in the rest of them. Varila (2005) observed a similar response from seven isolates of *P. sparsa* inoculated on leaf discs of rose cv. Charlotte® incubated at different temperatures. Germination of sporangia, latent period and production of sporangia were found to be similar among isolates. Only one isolate showed differences at 10°C, and this particular result was related to the site of origin of the isolate. The latent period of *P. sparsa* observed by Varila (2005) in cv. Charlotte® at 16°C was 4.7 days, which contrasts with the respective 5.6 and 5.8 days recorded for cv. Elle® and cv. Sweetness® in the current study. These differences may be mainly explained by the cultivars. Although both studies evaluated isolates of *P. sparsa* from the Bogotá Plateau, the cultivars, the time and the sampling sites were different. Yet, the results reveal a short latent period of *P. sparsa* in susceptible cultivars and a similar development of isolates regardless of their geographic origin. To date, the biological characterization of isolates conducted in this study, together with the results obtained by Varila (2005), show that isolates do not vary significantly in their aggressiveness.

The Colombian isolates of *P. sparsa* have shown low genetic diversity for the ITS2 region, the variation of the pathogen being limited to two genotypes which were only detectable when PCR (Polymerase Chain Reaction) products were digested with the enzyme *PvuII.* These results suggested the presence of mixed infections as two variants within a sample (Ferrucho, 2005). Using three different molecular markers and isolates from two regions,

Ayala et al. (2008) confirmed the low genetic diversity of the pathogen as reflected in the few genotypes they observed. On the contrary, considerable genetic variability was found in Finish isolates of *P. sparsa* (syn. *P. rubi*) obtained from arctic bramble (*Rubus arcticus* subsp. *arcticus*) and cloudberry (*R. chamaemorus*) plants and analyzed for AFLP (Amplified Fragment Length Polymorphism). Moreover, no genetic differentiation was observed based on geographic origin or host plant (Lindqvist-kreuze et al., 2002). Although the occurrence of oospores in arctic bramble required additional study, the authors suggested that sexual reproduction of *P. sparsa* occurs in Finland. The slight differences in some biological aspects like the latent period or the production of sporangia by some isolates of *P. sparsa* observed in this study and also by Varila (2005) suggest the need for further studies to clear the possible presence of biotypes of the pathogen in the Bogotá Plateau population and in other regions.

Strong homogeneity of host plants and environmental conditions may explain the low diversity found for *P. sparsa* in the Bogotá Plateau so far. The control measures and the semi-controlled conditions of Colombian rose crops might be favoring the prevalence of one genotype (Ferrucho, 2005). Indeed, Anderson and Kohn (1995) highlighted that the ability of asexual propagules to remain in plants, which, together with the strong adaptive fitness of some clones, might contribute to the clonal genetic structure of the population of a pathogen. Populations of sexual pathogens usually exhibit higher genotype diversity; the presence of new genotypes could be restricted by management strategies that limit the occurrence or persistence of sexual reproduction (McDonald and Linde, 2002). Although Colombian isolates produce oospores under controlled conditions, these structures have not been observed under field conditions. Therefore, the homogeneity of *P. sparsa* populations may be determined by the predominance of asexual reproduction (Ferrucho, 2005).

In the current study, the isolates of *P. sparsa* were obtained during epidemics of downy mildew from plants between 2.0 and 10 years old managed with similar control strategies. In addition, the sampling sites were located in the same climatic region (IDEAM, 2005). Similarities in the biological characterization of the isolates might be due to the homogeneity of the conditions under which *P. sparsa* develops, as pointed out by Ferrucho (2005). Francis (1981) mentioned that oospores in *Rosa* sp. are probably not essential for disease transmission when compared to mycelium carry-over. As the role of oospores in the disease cycle is not clear, the presence of oospores in leaf tissues becomes an interesting parameter to be considered in studies of this pathogen.

Collections of modern cut rose cultivars show uniform characteristics including bud and flower shape, stem length, and thorniness, all of them determined by selection processes that look for the same phenotypes. On the other hand, disease resistance has received little attention in breeding programs (De Vries and Dubois, 1996). This observation may coincide with the response of cvs. Elle® and Sweetness®, both found to be susceptible to *P. sparsa*. In addition, in a study on 120 Hybrid tea, miniature, Polyantha and Floribunda cultivars evaluated under field conditions, they were all infected by *P. sparsa* (Wisniewzca-Grzeszkiewicz and Wojdyla, 1996). In a screening of wild rose accessions and garden rose cultivars for resistance to *P. sparsa* as assessed through sporangiophore production in detached leaves, just 15% of the accessions were found to be resistant (Schulz and Debener, 2007; Schulz et al., 2009). In commercial crops, five to seven year old rose plants need to be replaced (Hu, 2001). Although the introduction of new cultivars is desirable, prominent cultivars bearing resistance to downy mildew are not available yet. Consequently, the disease will continue to affect commercial cut rose crops.

In the current study, *P. sparsa* isolates from commercial crops of the Bogotá Plateau did not vary with regards to the studied biological parameters. Although a few isolates revealed particular differences, most of the variables showed similar values. Hence, it can be said that their aggressiveness in cvs. Elle® and Sweetness® is similar. Therefore, comparable results may be expected in other susceptible cultivars after inoculation of Colombian isolates. Nevertheless, *P. sparsa* isolates grown in more diverse climatic areas and under contrasting plant protection methods may differ in their biological parameters. In addition, the evaluation of an important number of cultivars for their response to *P. sparsa* infection may be of interest not only for rose breeding programs but also for growers, in as much as it allows the selection of more resistant cultivars and the reduction of chemical treatments. Further studies aimed at understanding the epidemiological significance of oospores in rose downy mildew are also needed.

3. HISTOLOGICAL STUDY OF *Peronospora sparsa* INFECTION AND DEVELOPMENT IN ROSE LEAVES

3.1 Introduction

Rose downy mildew caused by *Peronospora sparsa* has lately become an important disease in cut rose nurseries and greenhouses, especially in those with no control of environmental conditions. As other downy mildews, *P. sparsa* is favored by cool humid conditions and long wet periods (Xu and Pettitt, 2004; Aegerther et al., 2003; Restrepo and Lee, 2009). Leaves, stems, peduncles and flowers can be infected. Dark-brown purple angular spots that may turn yellow, as well as premature leaf abscission are typical symptoms. In infected flowers and stems, purple brown lesions are common, accompanied by malformed floral buds (Aegerter et al., 2003; Xu and Pettitt, 2003). Similar symptoms have been described in *Rubus* sp. infected by *P. sparsa* (Aegerter et al., 2002).

Downy mildew sporulation occurs under high relative humidity, mainly in the dark and usually on green tissues (Yarwood, 1943; Populer, 1981; Ingram, 1981). Sporangia of *P. sparsa* have been observed to germinate from 2°C to 18°C and little or no germination takes place above 26°C (Breese et al., 1994; Xu and Pettitt, 2004). In rose, *P. sparsa* sporulates on leaf undersurfaces (Francis, 1983). The coenocytic mycelium of the Peronosporales produces intercellular hyphae which grow between host cells and ramify in all directions. Haustoria of most of the species of *Peronospora* are filamentous and multinucleate, developing into extensively absorbing surfaces through profuse branching (Fraymouth, 1956). Filamentous biotrophic pathogens penetrate host cell walls, but hyphae remain surrounded by a host derived plasma membrane (Lu et al., 2012). After infection, high incidence of intercellular mycelium has been reported in leaves of rose and *Rubus* sp. infected by *P. sparsa* (Breese et al., 1994; Williamsom et. al., 1995). In a susceptible cultivar of grapevine, intercostal areas of leaves were completely colonized with mycelium of *Plasmopara viticola* three days after inoculation (Unger et al., 2007). Likewise, intercellular mycelia of *P. sparsa* isolated from rose have been observed to quickly and extensively colonize tummelberry leaf discs (Breese et al., 1994). *P. sparsa* oospore formation in the leaf mesophyll has been observed as well (Breese at al., 1994; Xu and Pettitt, 2003; Gomez and Filgueira, 2012). Fraymouth (1956) mentioned

rapid increase in the volume of hyphae growing under the lower epidermis potential to disrupt the organ and contribute to leaf shrivelling, which is a common symptom in many downy mildews.

A limited number of investigations about *P. sparsa* infecting roses have been conducted, and information on related downy mildews is normally used to understand the disease. Therefore, additional studies about the development of the pathogen and the disease are still needed. Due to the importance of understanding the dynamics of the pathogen in plant tissues a precise cytological and histological description of the *P. sparsa* - *Rosa* sp. interaction is necessary. To expand the knowledge on this topic, the aims of this study were: (i) the histological characterization of leaf infection and colonization by *P. sparsa,* making use of different microscopic techniques, (ii) the study of the adaxial and abaxial infection processes and (iii) the visualization of pathogen ultrastructures in infected tissues.

3.2 Materials and methods

3.2.1 Plant material

Hybrid tea rose plants of cv. Elle® Var. Meibderos (Meilland International SA, Le Luc-en-Provence, France) were employed for the experiment. The plants were grown in glasshouse under 16 h photoperiod and average day/night temperatures of 23°C/18°C. They were planted in 10 L pots containing a 3:1 mixture of soil and Profi-substrat Typ ED73 (Gebrüder Patzer GmbH & Co Sinntal-Jossa, Germany), where they were regularly watered and fertilizer. Leaves at three maturity stages were employed for the study. They were harvested and rinsed once with tap water and twice with distilled sterile water immediately before *P. sparsa* inoculation. Then, 20 mm leaf discs were cut and placed in Petri dishes with wet filter paper (100% RH) to track the progress of the infection.

3.2.2 Pathogen and inoculation

Isolate Ps 6 of *P. sparsa,* obtained from a commercial rose crop and maintained on leaflets under laboratory conditions was used as source of inoculum. Seven-day sporangia were collected in distilled sterile water. Using a Fuchs-Rosental hemocytometer, the suspension was adjusted to 1.0×10^5 sporangia per ml. Rose leaves were inoculated on the abaxial and adaxial sides with two 15 µl drops of the suspension placed in the center and then distributed uniformly using a soft brush to cover the whole

disc. In addition, abaxial inoculation of intermediate and mature leaves was conducted. After inoculation, the Petri dishes were kept at 18°C/16°C day/night temperatures and 16 hours of light in a growth chamber. To observe if *P. sparsa* produced sporangia on the adaxial side of the leaf, the exposure of the leaf surfaces in the Petri dishes was modified. After adaxial inoculation, one group of leaflets was placed with the inoculated side facing up during the whole study, while a second group of leaflets was laid upside down 48 hours after inoculation (hai), thus exposing the abaxial side in the Petri dish. Conversely, the abaxially inoculated leaflets were laid with the inoculated side facing up during the whole study, while some others were turned over 48 hai, thus exposing the adaxial side in the Petri dish.

3.2.3 Assessment of the infection process

The infection and development of *P. sparsa* in rose tissues was tracked by processing, staining and mounting the leaf material for microscopical observation. Inoculated leaves were observed under epifluorescence, bright light, interference contrast and transmission electron microscopy (TEM). Structures of the pathogen were observed in samples taken from inoculated leaves and processed for further microscopical observations, 12 hai and every 24 hours for seven days and then ten days after inoculation (dai). To visualize the formation of sporangia on the leaf surfaces daily evaluation of inoculated leaves was conducted under the stereo microscope (Leica S4E, Wetzlar, Germany).

3.2.4 Histological techniques and microscopy

The development of *P. sparsa* on the leaf surface was observed in 1.0 cm^2 fresh leaf segments cut out from inoculated leaves, stained with 10 µl of a 0.01% solution of the fluorescence stain blancophor (Gachomo, 2004), and observed directly in a photomicroscope (Leitz DMRB; Leica, Wetzlar, Germany) equipped with UV-excitation system for epifluorescence.

Structures of the pathogen in the leaves were observed in 12 mm diameter leaf discs taken from inoculated leaves and cleared by treating the tissue in saturate chloral hydrate (AppliChem) (2.5 g ml^{-1} water) (Bruzzes and Hasan, 1983; Jende, 2001) for seven to ten days at room temperature (20 ± 3°C). Then, the tissue was stained for 48 hours in 0.01% acid fuchsin (Fluka) (10 ml phenol, 10 ml lactic acid, 10 ml glycerin, 10 ml distilled water) (Gerlach, 1977). Microscopical observations were carried out using a Leitz DMRB photomicroscope equipped with Nomarski-interference-contrast.

For further histological observations, semi-thin sections were prepared from 0.2 mm^2 leaf blocks taken from infected leaves. Those samples were fixed in a Karnosky´s fixative solution containing 2% paraformaldehyde (SiGMA) and 2% glutaraldehyde (AppliChem) in a 0.2 M sodium cacodylic acid sodium salt trihydrate buffer pH: 7.2 (Fluka) at room temperature for two hours (Karnovsky, 1965). After washing the material seven times in the cacodylic acid sodium salt trihydrate buffer (pH: 7.2) for 15 minutes each, and then in a 2% osmium tetraoxide (ROTH) solution for 1.0 hour, it was washed again in the cacodylic acid sodium salt trihydrate buffer (pH: 7.2). The subsequent dehydration process was done in a graded ethanol (AppliChem) water bi-distilled series (15, 30, 50, 70, 90 and 100%). The material was then washed twice (10 minutes each) in propylene oxoide 99.5% (ALDRICH). The embedding media corresponded to a firm standard ERL medium (8.2 g ERL 4221 Cycloaliphatic epoxide resin), 6 g D.E.R. 736 (Diglycidyl ether of Polypropylene glycol), 11.8 g NSA (Nonenyl succinic anhydride) and 0.2 g DMAE (Dimethylaminoethanol) employed according to Spurr (1969). Samples were embedded in low viscosity Spurr (SiGMA-ALDRICH) in different propylene oxoide pure Spurr ratios: 3:1, 1:1, 1:3 and left overnight at 70°C. Then, the samples were polymerized in 100% Spurr in embedding trays (Agar-Aids) at 70°C for 10 h. The material was sectioned to 500 nm wide with a 45° glass knife using an ultra-microtome (Reichert-Jung Ultramicrotome Ultracut E; Leyca Microsystem, Nussloch, Germany) and then stained in 1% toluidine blue for one minute (AppliChem), according to the methodology modified from Gerlach (1977) (0.5 g toluidine, 0.5 g sodium tetraborate, 50 ml bi-distilled water) and finally rinsed in water to remove the excess of colorant. The sectioned leaves were then mounted and sealed dry overnight before microscopical observation. Structures of the pathogen were observed under bright field with a Leitz DMRB photomicroscope. Images of the specimens observed under light microscope were recorded digitally with a camera incorporated to the Leitz DMRB Leica light microscope using the software Diskus 4.2 (Hilgers, Königswinter, Germany).

For detailed observations, ultrathin sections (70-75 nm) were prepared using a diamond knife (DiATOME) in a Reichert-Jung Ultramicrotome (Ultracut E; Leyca Microsystem) and then stained for Transmission Electron Microscope (TEM) with 2% uranyl acetate (MERCK) for 5 minutes and with laid nitrate (SiGMA) (1.33 g blei nitrate, 1.76 g nitrium citrate, 30 ml bi-distilled sterile water) for 45 seconds. Ultrastructures were observed under TEM EM109 (Carl Zeiss AG, Jena, Germany). TEM digital images were obtained using a wide-angle dual speed CCD camera (TRS, Moorenwies, Germany) and the software ImagesSP (SysProg & TRS, Moorenwies, Germany).

3.2.5 Statistical analysis

Statistical analysis was conducted using the Superior Performing Software System SPSS 21.0 (SPSS Inc., Chicago, IL, USA). Mean comparisons at a significance level of 95% were done by *t*-test ($P \leq 0.05$). All the experiments were performed at least two times.

3.3 Results

3.3.1 Development of Peronospora sparsa in leaf tissue

3.3.1.1 Abaxial leaf side

3.3.1.1.1 Germination and penetration

Germination of sporangia of *P. sparsa* began 6 hai and most of them germinated 12 and 24 hai. Penetration through the abaxial side of the leaves occurred with formation of appressoria, directly through the leaf cuticle or through leaf stomata (Fig. 3.1a-c). Penetration through stomata was observed between 8 and 10 hai, while penetration by appressorium often took place 12 hai. After penetration, the hyphae grew between epidermal cells. On the leaf surface, the sporangia produced long, superficially ramified germination tubes that attempted to penetrate the leaf tissue even 24 hai (Fig. 3.2e). In some cases, dead cells were visualized after penetration by bright light and fluorescence microscopy as brown cells next to the penetration site (Fig. 3.1c) but this reaction did not limit the infection process. On intermediate maturity leaves, the sporangia germination was observed first 24 hai, and no penetration was detected 72 hai. In contrast, few sporangia germinated on mature leaves 72 hai.

3.3.1.1.2 Colonization of leaf tissue

Intercellular hyphae were observed growing profusely 48 hai in spongy parenchyma (Fig. 3.1d). Hyphae and haustoria colonized adjacent tissue layers and, 96 hai, cells of the opposite epidermal layer had already been infected. Simple filiform haustoria penetrating cell tissues were observed, some exhibiting a short branch at the distal end (Fig. 3.1f). Rapid hyphal growth continued and 120 hai the mesophyll of the leaf was extensively colonized. In cross sections taken 144 hai, the pathogen was observed infecting cells of all tissue layers (Fig. 3.3). On intermediate maturity leaves, the first hyphae and haustoria were observed 144 hai, profuse growth in different tissue layers taking place 168 hai.

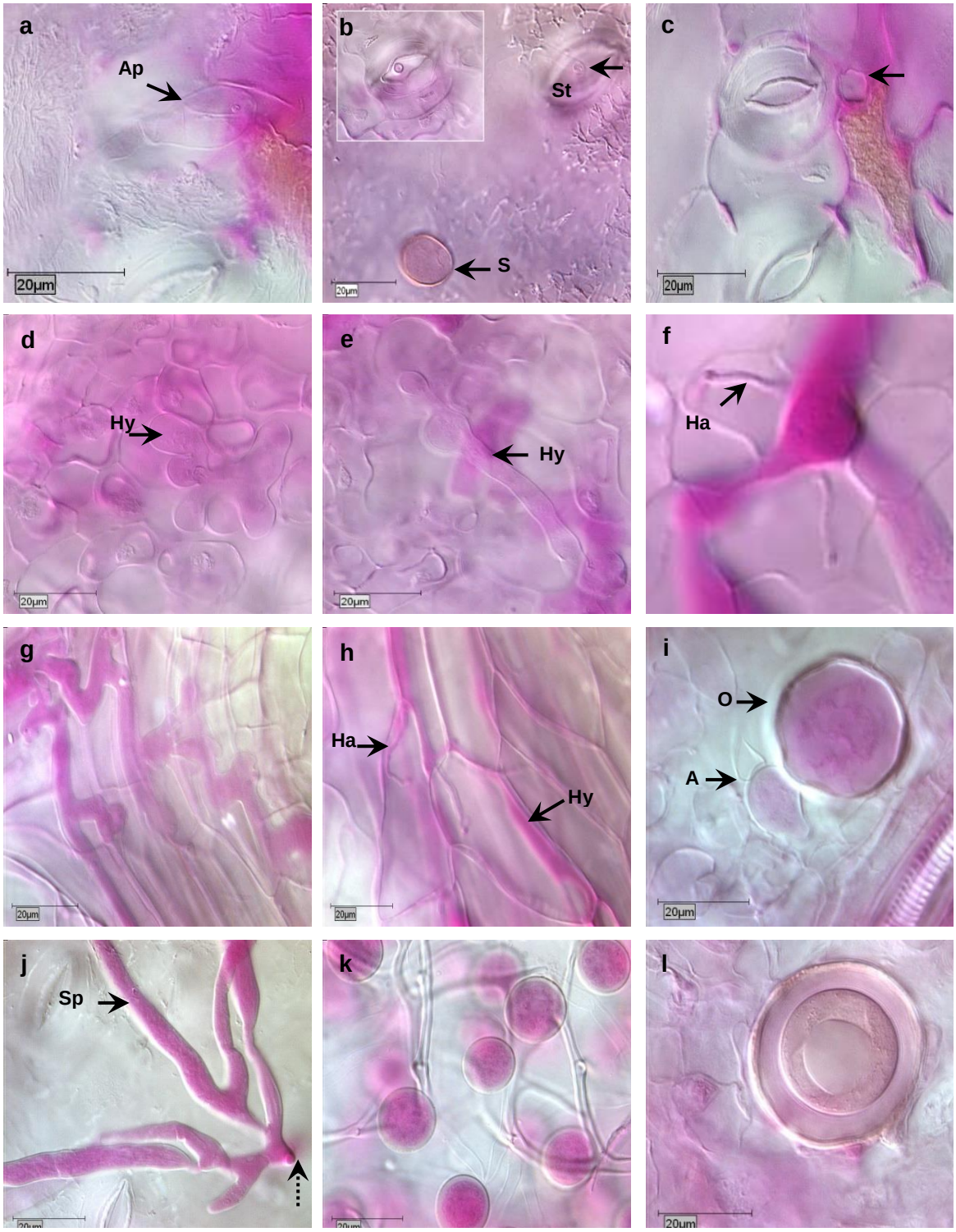

Figure 3.1 *Peronospora sparsa* infection in rose leaf tissue visualized by interference contrast microscopy: **a**, direct penetration with appressorium 12 - 24 hai; **b**, penetration through stoma 8 - 12 hai; **c**, leaf cuticle penetrated 24 hai; **d**, first intercellular hyphae in mesophyll cells 48 hai; **e**, profuse growth of hyphae in spongy parenchyma 72 hai. **f**, detail of haustorium; **g**, thick fasciated hyphae crossing leaf veins 96 hai; **h**, haustorium and hyphae along leaf veins 96 hai; **i**, antheridium and oogonium formed 144 hai in spongy parenchyma; **j**, sporangiophore produced through stoma (dotted arrow) 144 hai; **k**, sporangia 168 hai; **i**, oospore 168 hai. A, antheridium; Ap, appressorium; Ha, haustorium; Hy, hypha; S, sporangium; Sp, sporangiophore; St, stoma; O, oogonium.

Scarce hyphal growth inside the tissue of mature leaves was observed 168 hai and colonization of *P. sparsa* was restricted to few sites of the leaf. Hyphal growth was not limited by leaf veins. Mycelia expanded parallel to the main veins and fasciated hyphae were observed surrounding the leaf veins when the pathogen spread to a new mesophyll area. Filiform haustoria were observed infecting cortical cells of the tissue surrounding the veins (Fig. 3.1h). In midribs, hyphae and haustoria were mainly observed in collenchyma tissues under epidermal cells (Fig. 3.3c, d). Under the conditions of the experiments, neither hyphae nor haustoria were observed infecting leaf xylem or floem cells, but they were observed densely infecting bundle sheath cells (Fig. 3.3h).

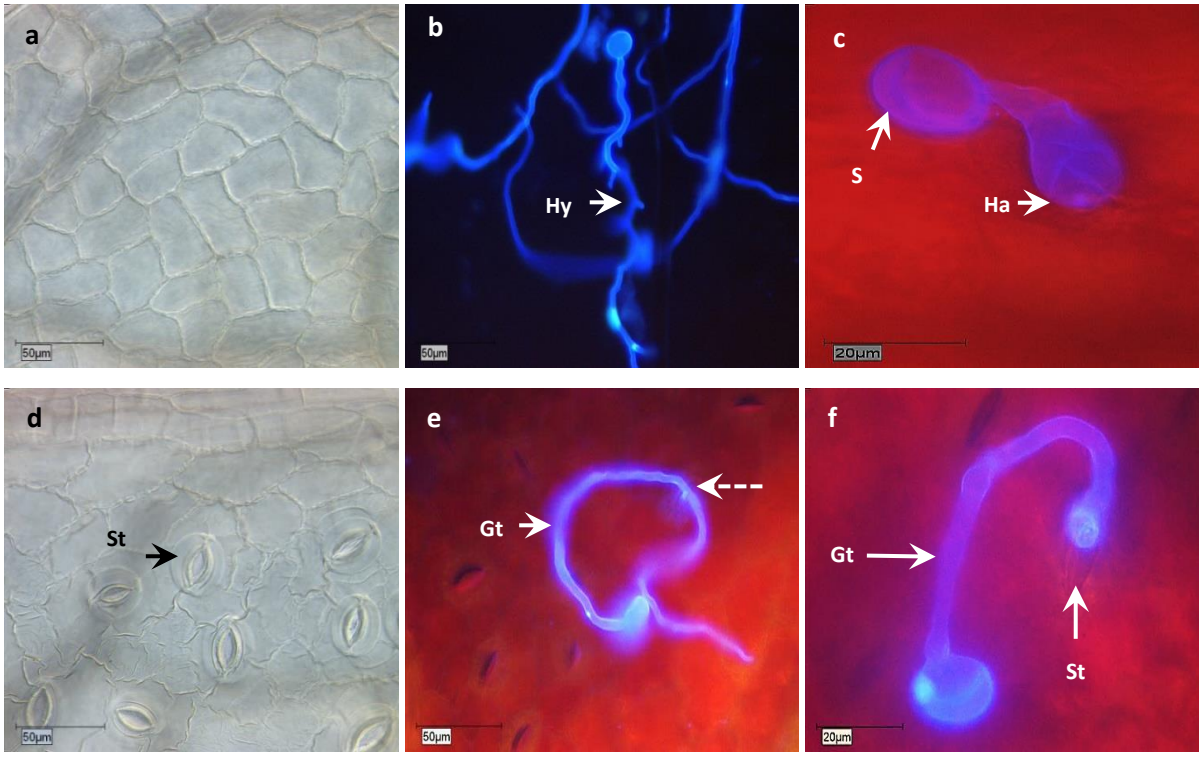

Figure 3.2 Infection of *Peronospora sparsa* on adaxial (a, b and c) and abaxial (d, e and f) leaf side of rose visualized by fluorescence microscopy and leaf surfaces observed by interference contrast microscopy: **a**, leaf side without stomata; **b**, elongated germination tubes 24 hai; **c**, direct penetration 12 hai; **d**, leaf side with stomata; **e**, germinated sporangium 24 hai with a branch attempting to penetrate a stoma (dotted arrow); **f**, germination tube penetrating through a stoma 48 hai. Gt, germination tube; Ha, haustorium; Hy, hypha; S, sporangium; St, stoma.

3.3.1.1.3 Formation of sporangia and oospores production

Sporangiophores branched dichotomic according to the typical specie morphology. First sporangiophores and lime shaped sporangia were produced 120 hai through stomata located only on the abaxial side of the leaves. The first antheridia and oogonia were observed 144 hai (Fig. 3.1i). A dense deposition of hyphae in substomatal cavities,

profuse production of sporangia, total tissue colonization by intercellular hyphae and presence of oospores took place 168 hai (Fig. 3.1k, l). After abaxial or adaxial infection, the production of sporangia on the abaxial side of the leaf was abundant and covered the leaf surface uniformly. Production of first sporangia of *P. sparsa* varied depending on the maturity of the leaves. On intermediate and mature leaves, sporangiophores and sporangia were observed 10 dai, but density was low on intermediate leaves and scarce on mature leaves.

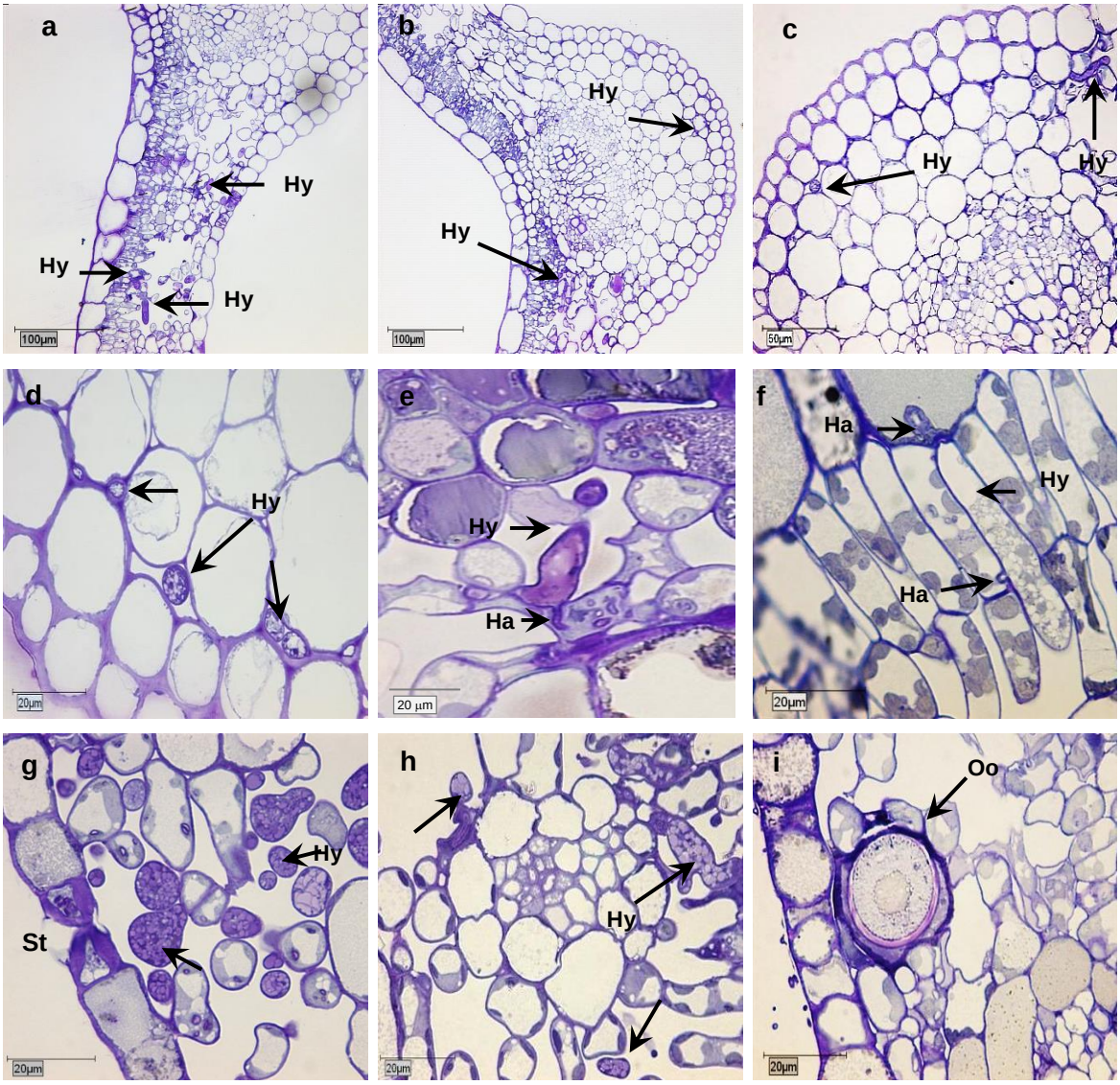

Figure 3.3 Sections of rose leaf tissue infected by *Peronospora sparsa* 7 dai observed by bright light microscopy: **a**, leaf lamina with hyphae in the mesophyll; **b**, leaf midrib surrounded by hyphae; **c**, hyphae in the cortical tissue of a midrib; **d**, detail of hyphae in the cortical parenchyma of a main vein; **e**, hypha and haustorium in mesophyll cell; **f**, hypha penetrating simultaneously a palisade and an epidermal cell; **g**, dense hyphae in stomatal cavity; **h**, hypha surrounding and infecting bundle sheath cells of a secondary vein; **i**, oospore in spongy parenchyma close to low epidermis. Hy, hypha; Ha, haustorium; Oo, oospore; St, stoma.

3.3.1.2 Adaxial leaf side

3.3.1.2.1 Germination and penetration

The first *P. sparsa* sporangia germinated 6 hai, while most of them did so 12 and 24 hai. Elongated and superficially ramified germination tubes attempting to penetrate the leaf tissue were observed until 24 hai (Fig. 3.2b). Direct penetration of the leaf occurred with or without formation of appressoria. Brown cells surrounding the penetration site were also observed by fluorescence microscopy (Fig. 3.2c) but this reaction did not limit the infection. After penetration, the first hyphae grew between epidermal cells (Fig. 3.4).

3.3.1.2.2 Colonization of leaf tissue

Intercellular hyphae and haustoria growing extensively in palisade parenchyma were observed 72 hai. Hyphae of *P. sparsa* expanding superficially under the upper cuticle were observed 72 hai with formation of haustoria in epidermal cells (Fig. 3.4b, c). Subsequently, the leaf tissue was colonized not only by intercellular hyphae in mesophyll cells but also by hyphae growing profusely on the upper epidermis. Hyphae and haustoria infecting the

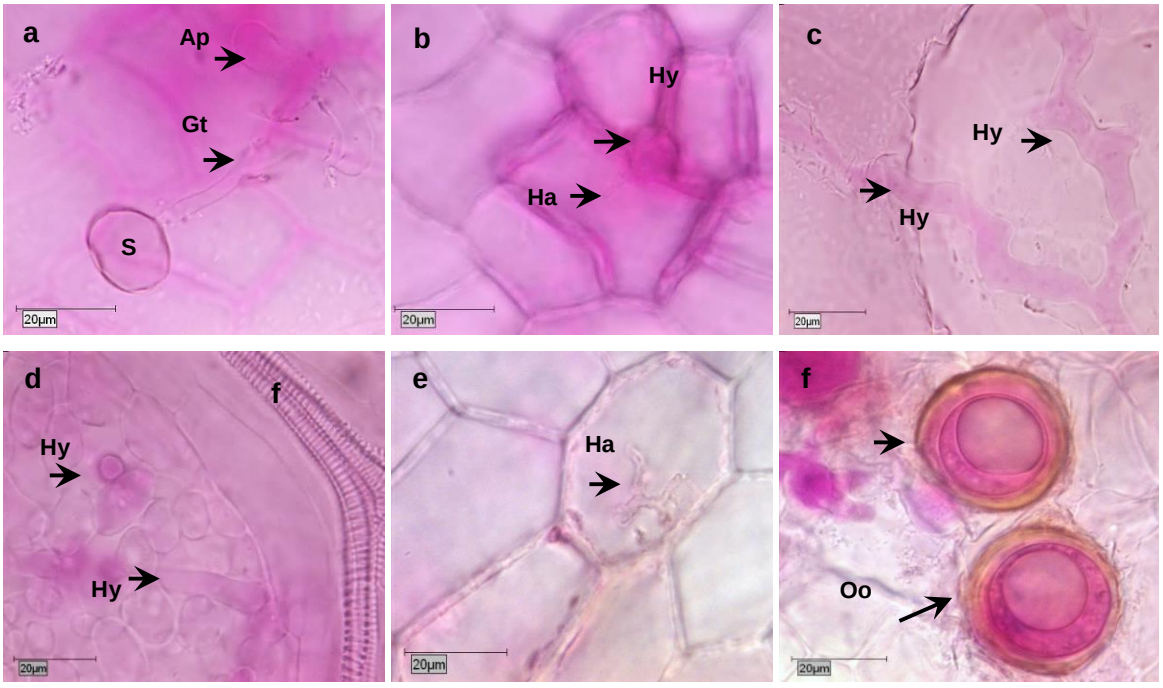

Figure 3.4 Development of *Peronospora sparsa* after adaxial inoculation of rose leaves observed by contrast interference microscopy: **a**, penetration after appressorium formation 12 hai; **b**, haustoria in epidermal cell; **c**, hyphae growing superficially under the cuticle; **d**, intercellular hyphae growing in spongy parenchyma 96 hai; **e**, detail of an haustorium; **f**, oospores formed 120 hai under the cuticle. Ap, appressorium; Gt, germination tube; Ha, haustorium; Hy, hypha; S, sporangium; Oo, oospore.

opposite epidermal layer were observed 96 hai. Intercellular mycelia colonized all tissue layers and expanded under the upper epidermis 120 hai (Fig. 3.4d, e).

3.3.1.2.3 Formation of sporangia and oospores production

The first sporangiophores and oospores were formed under the cuticle 120 hai (Fig. 3.4f). In later stages of pathogenesis, oospores were formed in spongy parenchyma tissue. Sporangiophores branched profusely on the adaxial side of the leaf since their earlier stages. Produced between the intercellular spaces of epidermal cells, they were mainly located on the borders of the polygonal reticule formed by secondary and tertiary veins (Fig. 3.5a, b). Thick, ramified, superficially formed hyphae were visualized by fluorescence at the site where sporangiophores were produced (Fig. 3.5c, d).

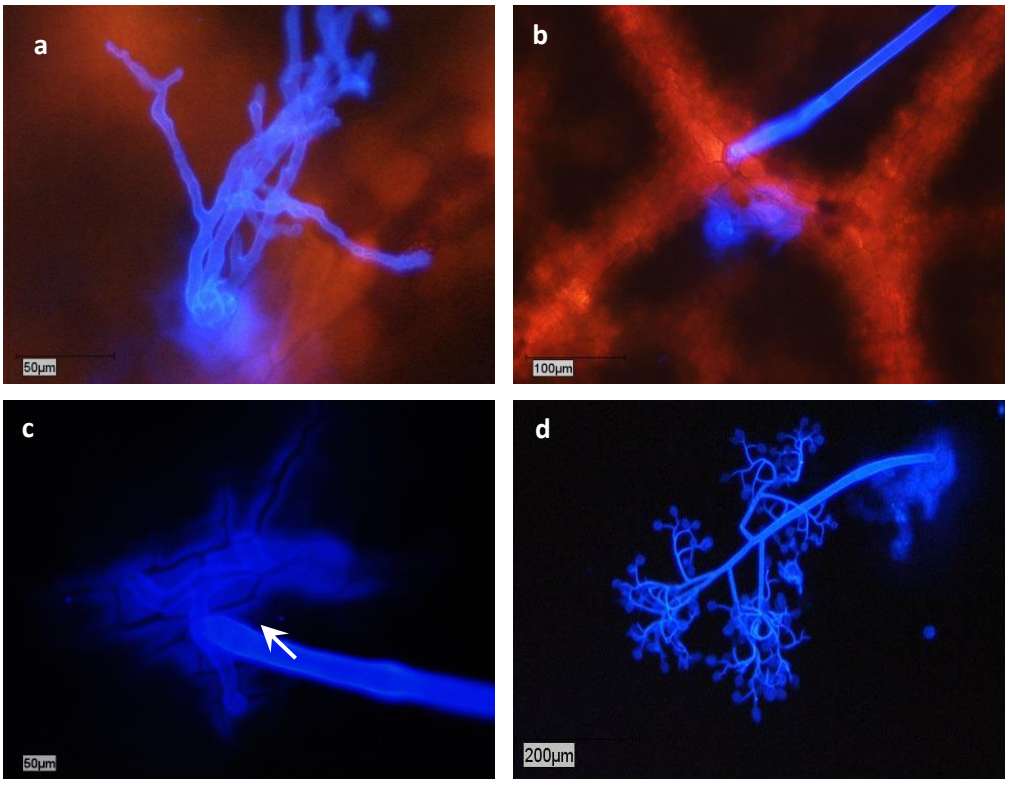

Figure 3.5 Development of sporangiophores and sporangia of *Peronospora sparsa* on adaxial side of rose leaves visualized by fluorescence microscopy: **a**, sporangiophore coming through leaf cuticle; **b**, elongated sporangiophore produced in a cell of the leaf vein **c**, detail of branched hyphae growing superficially under cuticle tissue; **d**, detail of a complete sporanghiophore with sporangia produced through upper cuticle.

The latent period (number of days to sporulation) was similar for the abaxial and adaxial sides of the leaf. However, the minimum and maximum numbers of days varied slightly according to the side of the leaf where inoculation or sporulation took place (Table 3.1).

Table 3.1 Sporulation of *Peronospora sparsa* after adaxial and abaxial inoculation of leaves of rose cv. Elle®.

	Sporulation			
	Adaxial		*Abaxial*	
Inoculation	Time	Grade*	Time	Grade*
Adaxial	5-8 dai	1	6-7 dai	3
Abaxial	5-6 dai	2	4-6 dai	3

* = Grade of sporulation: 0, absent; 1, slight; 2, intermediate; 3, abundant
dai = days after inoculation

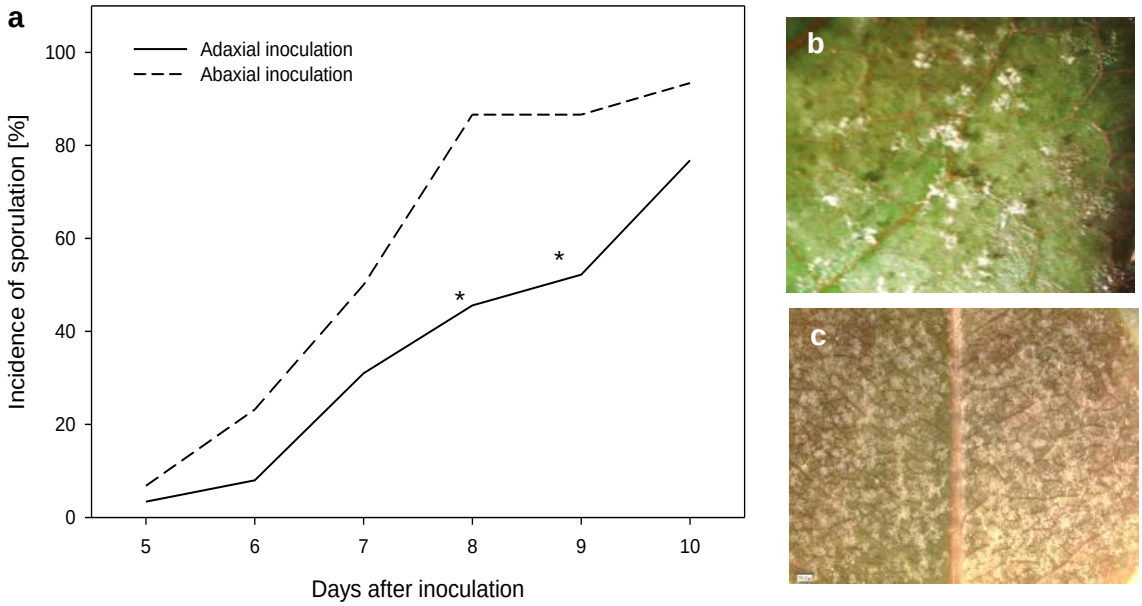

Figure 3.6 Formation of sporangia of *Peronospora sparsa* on leaves of rose cv. Elle® after adaxial and abaxial inoculation visualized under stereo microscope: **a**, incidence in percentage of discs showing sporulation on the abaxial side of leaves after adaxial or abaxial inoculation; **b**, adaxial sporulation 10 dai; **c**, abaxial sporulation 10 dai. Asterisk represents values significantly different (*t*-test, $P \leq 0.05$).

Production of sporangia on the adaxial side of the leaf took longer following either adaxial or abaxial inoculation. After abaxial infection, the production of sporangia was observed to be faster, especially on the abaxial surface. The incidence of abaxial sporulation following abaxial inoculation was significantly higher 8 and 9 dai, when compared to that following adaxial inoculation (Fig. 3.6a). Moreover, the density of sporangiophores observed on the adaxial side of the leaves was notably lower due to the absence of stomata facilitating sporangiophores formation (Fig 3.6b).

3.3.2 Ultrastructure of Peronospora sparsa in leaf tissue

Infected leaf tissue observed under the Transmission Electron Microscope showed abundant intercellular mycelium especially between mesophyll cells (Fig. 3.7a,b) and elongated haustoria penetrating the host by cell membrane invagination, in continuous contact with the host plasma membrane (Fig. 3.7c, 3.8). Hyphae simultaneously penetrating different cells with haustoria were observed. Besides, more than one haustorium per cell seems to be possible as a result of penetration from different sides (Fig. 3.8c). A light electron dense juvenile hypha illustrates sporangiophore formation through a stoma (Fig. 3.7d). Epidermal cells were densely penetrated on the adaxial side around sporulation time (Fig. 3.8c).

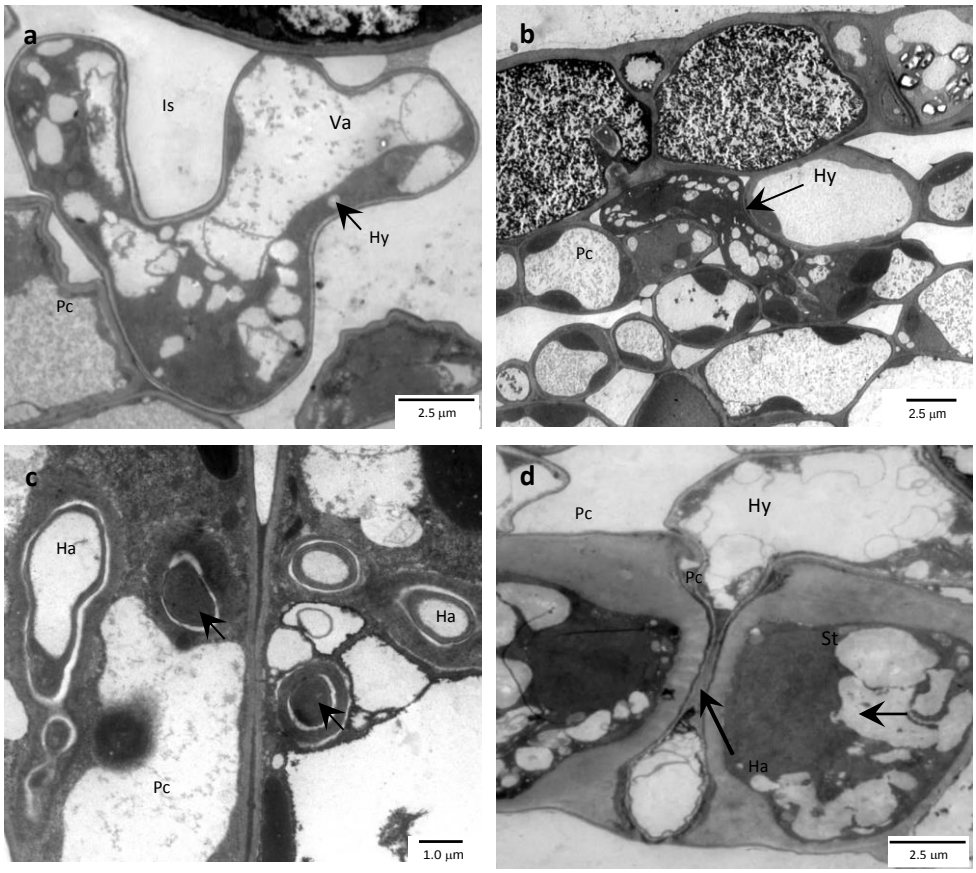

Figure 3.7. Development of structure of *Peronospora sparsa* in leaf tissue of rose cv. Elle® 7 dai visualized by Transmission Electron Microscope: **a**, hypha in intercellular spaces of spongy parenchyma; **b**, hyphae under epidermal cells; **c**, haustoria in parenchyma cell; **d**, hypha penetrating stomatal cavity. Ha, haustorium; Hy, hypha; Is, intercellular spaces; Pc, plant cell; St, stoma cells; Va, vacuole; N, nucleus.

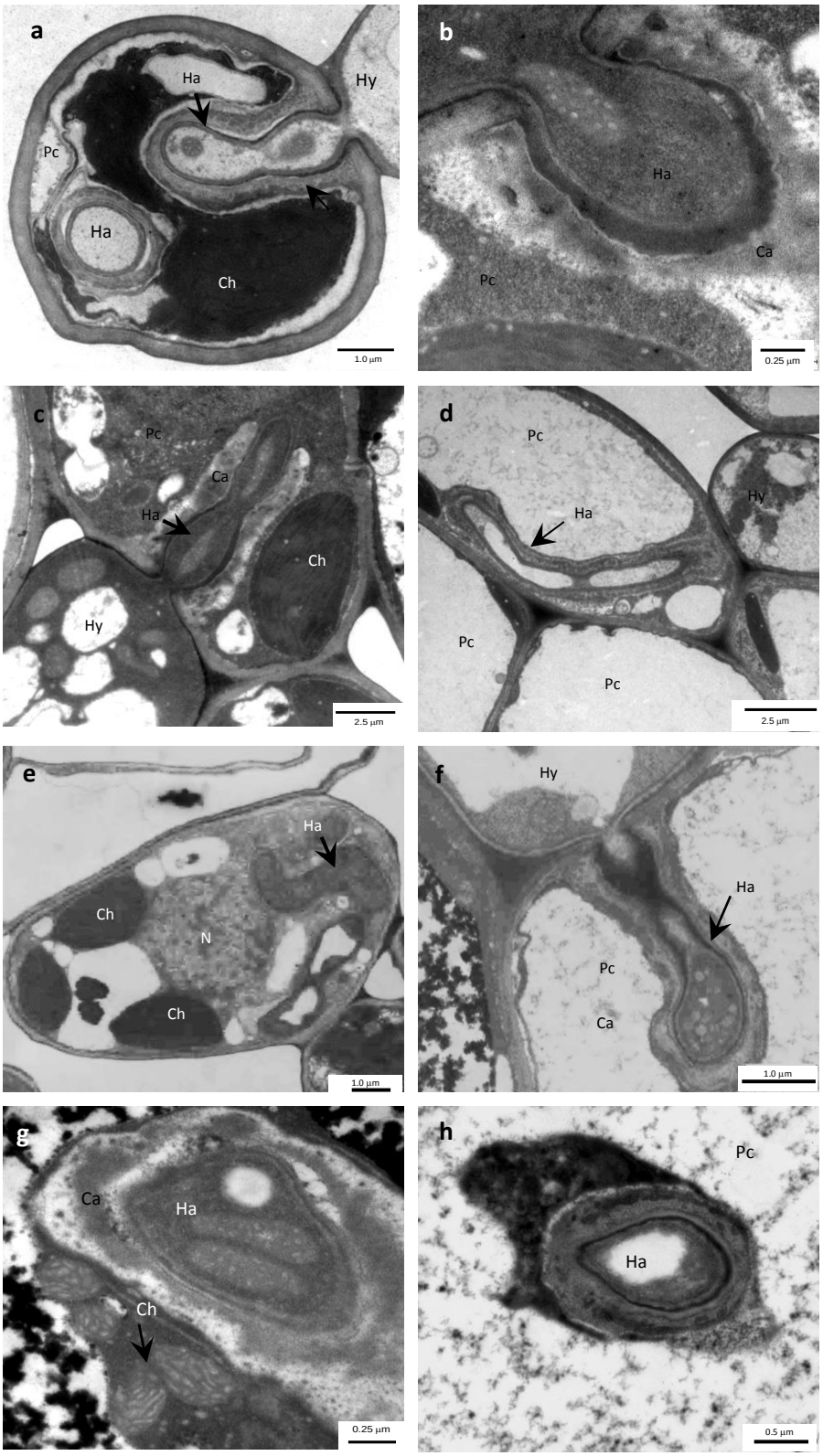

Figure 3.8 Development of structures of *Peronospora sparsa* in leaf tissue of rose cv. Elle® 4 and 10 dai visualized by Transmission Electron Microscope: **a**, haustorium in spongy parenchyma cell 4 dai; **b**, detail of an haustorium 4 dai; **c**, detail of an haustorium 4 dai incompletely covered by an electron dense material; **d**, haustorium penetrating bundle sheath cell 4 dai; **e**, mesophyll cell with haustorium 10 dai; **c**, haustorium in mesophyll cell 10 dai; **f**, cross section of an haustorium 4 dai; **g**, cross section of an haustorium 10 dai; Ca, callose; Ch, chloroplast; Ha, haustorium; Hy, hypha; Pc, plant cell; Va, vacuole; N, nucleus.

Haustoria were observed in early stages of pathogenesis and the transversal sections showed ramified haustoria inside the cells. An electron dense deposit surrounding haustoria formation was observed in different stages of their development (Fig. 3.8b, c). Since early stages of infection, haustoria were visualized in palisade and spongy parenchyma cells. In all the observed materials, structures penetrating cell tissues presented a constriction at the base similar to a neck, while the host protoplasmic membrane was intact. These facts suggest that *P. sparsa* entered the leaf cell in the form of haustoria. Differences were observed in the electron dense material content of haustoria produced 4 dai and in later stages of infection (Fig. 3.8g, h). Ten days after inoculation, no collapsed cells were observed even in densely infected tissues, while the arrangement of cellular organelles was not altered (Fig. 3.8e).

3.4 Discussion

The current findings describe the entry of *P. sparsa* through the abaxial and adaxial sides of rose leaves and its subsequent development. The ramified germination tubes that attempted to penetrate the leaf tissue suggest that the number of infection sites after one single sporangium germinates is not restricted to one. On the abaxial leaf surface, penetration through stomata was observed before direct penetration. This may explain the faster development of the pathogen after abaxial inoculation of *P. sparsa*.

The cells were densely penetrated with filiform haustoria after abaxial and adaxial inoculation. In addition, the observations suggest that more than one haustorium per cell may be produced in the susceptible cv. Elle®. Similar haustoria to those observed in rose, but exhibiting one or two branches at the distal end, were found by Williamson et al. (1995) in *Rubus* sp. infected by *P. sparsa* (syn. *P. rubi*). Colonization of leaf tissue by subcuticular hyphae, fast formation of superficial oospores and sporulation of *P. sparsa* through epidermal cells were important events that followed the adaxial infection. These results indicate that the leaf surface may play an important role in the disease progress, mainly because under natural conditions, deposition of sporangia may take place principally on the adaxial leaf side.

Rose leaf maturity was important in the infection and development of *P. sparsa.* Leaf age restricted the progress of the pathogen and the structures produced. Although the infection of *P. sparsa* succeeds in the three stages of maturity, the development of the pathogen was limited in the older leaves in comparison to the infection of young leaves.

Reuveni (1998) observed age-related resistance in *Vitis vinifera* infected by *Plasmopara viticola.* Mature leaves were more resistant to infection in comparison to young leaves, and this reaction was associated with higher β-1-3-glucanase and peroxidase activities in older leaves as defense mechanisms. Other factors may be related with cell wall and cuticle thickness and deposition or activity of other compounds like lignin, as reported by Vance et al. (1980).

After abaxial or adaxial inoculation, *P. sparsa* produced sporangiophores and sporangia on both sides of the leaf. In contrast with the adaxial infection, stomata facilitated not only the penetration of the leaf but also a dense and fast production of sporangia. This may be explained by a higher number of infection sites by direct penetration and penetration through stomata on the abaxial side, both contributing to a faster development of the pathogen. Even though sporangia were produced faster and more densely on the lower side of the leaf, adaxial sporulation did occur, and it may be considered as a possible event during the development of the disease. Adaxial sporulation of *P. sparsa* had not been observed and described until now. Indeed, Breese et al. (1994) only observed sporangiophores of *P. sparsa* on the abaxial epidermis of *Rubus* sp. and *Rosa* sp. leaves, while Xu and Pettitt (2003) mention that sporulation of *P. sparsa* occurs on the lower surface.

Breese et al. (1994) report the presence of oospores in leaves of *Rubus* sp. and *Rosa* sp.. Williamsom et al. (1995) observed oospores in leaves of *Rubus* sp. grown *in vitro,* while Xu and Pettitt (2003) recorded the presence of oospores of *P. sparsa* in rose leaf discs one week after inoculation. Twenty six µm diameter (in average) oospores of *P. sparsa* were produced in rose cv. Elle® between 5 and 7 dai. The diameter of these oospores falls into in the range reported for *P. sparsa* (syn. *P. rubi*) in *Rubus* sp. (Hall and Gardener, 1982; Williamsom et al., 1995). In the current study, oospores of *P. sparsa* were profusely formed following adaxial inoculation, not only in spongy parenchyma but also under the leaf cuticle. Moreover, hyphae growing superficially after adaxial inoculation were observed. These results suggest that a superficial development of *P. sparsa* takes place under the leaf cuticle, probably related with tissue damage. Fraymouth (1956) mentioned that the upper cuticle and epidermis of the leaf may be damaged due to the growth of some downy mildews, thus explaining the severity of the symptoms.

Studies conducted until now confirm the ability of *P. sparsa* to quickly colonize rose leaf tissue. Rapid colonization of leaves by other downy mildews has been well documented. Using fluorescence microscopy, Breese et al. (1994) observed an extensive colonization

of tummelberry leaf discs by intercellular mycelium of *P. sparsa* isolated from rose. The mesophyll of *Rubus* sp. leaves was observed to be extensively colonized by intercellular hyphae of *P. sparsa* (syn. *P. rubi*), which formed simple dichotomous haustoria (Williamsom et al., 1995). A similar pattern of rapid growth of *P. sparsa* in rose was observed by Gómez and Filgueira (2012). Nevertheless, in this study *P. sparsa* developed faster in leaves of cv. Charlotte® plants grown *in vitro,* than in those of cv. Elle® plants. The differences can be mainly explained by the cultivar and the infected tissue. In fact, Breese et al. (1994) stressed the high susceptibility of micropropagated hybrids of *Prunus lauraceus* to *P. sparsa,* suggesting that juvenile tissue is exceptionally sensitive to the infection, probably due to the fact that the leaf cuticle and epicuticular waxes are still poorly developed. Lebeda and Reinink (1991) found differences in the germination of sporangia, the speed of infection and the structures developed by *Bremia lactucae* in cultivars of lettuce. Cohen et al. (1989) also observed histological differences in the infection process of *Pseudoperonospora cubensis* in muskmelon cultivars.

In the current study, sporangiophores covering the complete leaf surface of inoculated rose leaves indicated that *P. sparsa* colonized the whole leaf lamina. In the process of extensive colonization by *P. sparsa,* hyphae growing parallel to the veins, together with the presence of thick fasciated hyphae expanding over the leaf veins, confirm the ability of the pathogen to spread through leaf tissues. In a study on tummelberry, a similar kind of hyphae (described as fan-shaped, branched and fasciated) was observed by Williamsom et al. (1995), associated with leaf veins within intercellular spaces of parenchyma cells infected by *P. sparsa* (syn. *P. rubi*). In the inspected material of rose, the bundle sheath cells of main, secondary and primary veins were surrounded and infected with filiform haustoria and the mycelium of the pathogen grew and expanded along vascular vessels. No hyphae or haustoria were detected infecting floem or xylem cells. In a histological observation of rose leaves from different sources, Xu and Pettitt (2004) did not observe invasion of vascular vessels. Contrarily, Gómez and Filgueira (2012) reported *P. sparsa* haustoria in xylem vessels of infected rose leaves as observed by light microscopy in manually prepared cross cuts. Williamson et al. (1995) observed *P. sparsa* (syn. *P. rubi*) growing extensively on interveinal tissue but rarely penetrating the vascular tissue.

Haustoria invaded the cells of the studied tissues without altering their structure. In electron micrographs, no cellular damage of palisade or spongy parenchyma cells was observed in heavily infected leaf material even 10 dai. Through different techniques, the histological observations showed the quick, invasive, and profuse growth of *P. sparsa* in rose leaves. The results showed a particular interaction of the pathogen with leaf tissues

and the ability to complete its life cycle by adaxial sporulation through the cuticle. These results provide new information about the adaxial and abaxial infection by the pathogen and its development. These findings constitute a close up into rose histology as infected by *P. sparsa,* thus contributing to the understanding of the localization and spread of the pathogen in different leaf tissues. In addition, the observed ultrastructures provide a first insight into the *Rosa* sp. - *P. sparsa* interaction. To date, the studies on downy mildew in roses have provided important knowledge on the topic. Nevertheless, it is necessary to perform complementary histological studies in adult rose plants involving other approaches to get a broader view of this interaction.

4. MONITORING OF LOCALIZED DOWNY MILDEW INFECTION AND DEVELOPMENT OF SYMPTOMS IN ROSE

4.1 Introduction

Downy mildew caused by *Peronospora sparsa* is considered one of the most important diseases affecting greenhouse cut rose production in the tropics. Pathogens of this group are considered to cause devastating plant diseases, which under optimal environmental conditions may lead to total loss of the crop. In addition, development of epidemics in affected crops can take place in short periods of time that may vary within four and seven days after appearance of the first diseased plants (Hildebrand and Sutton, 1985; Urban et al., 2007). As previously reported for other downy mildews, the growth of *P. sparsa* in *Rubus articus* is favored by cool and moist conditions (Lindqvist, et al., 1998).

The importance of rose downy mildew is also related to the difficult detection of the disease in early stages of spore production (Wheeler, 1981), which might take place in green tissues without any other indication of infection (Xu and Pettitt, 2003). Symptoms of the disease are found in leaves, stems, peduncles, calices, and petals. The infection is commonly limited to young apexes (Aegerter et al., 2002). The first signs of the disease are angularly-edged, purple-red spots that evolve into dark brown lesions followed by defoliation of affected plants.

The frequent appearance of the disease in “hot spots” and the tendency for severe symptoms to appear suddenly under favorable conditions supports the hypothesis that the pathogen overwinters in the plant probably as dormant mycelium (Xu and Pettitt, 2004). The ability of downy mildew to form systemic infections in a wide range of herbaceous plants is well known (Populer, 1981), e.g., *Pisum sativum* infected by *Peronospora viciae* (Tylor et al., 1990), *Rubus* spp. by *Peronospora sparsa* (syn. *P. rubi)* (Tate, 1981) and *Nicotiana* spp. by *Peronospora tabacina* (Reuveni et al., 1986). In raspberry, *P. sparsa* (syn. *P. rubi)* has been observed to infect leaves, flowers, fruits and stems, but the spread of the pathogen into vascular tissue was limited (Tate, 1981). In pea downy mildew, although foliar lesions are more common, systemic infection causes important yield losses. In this crop, *P. viciae* was observed in the stem cortex, vascular tissue and the central lumen. Symptomless invasion of stem tissues has been observed to result in systemic infection indicating that some apical infection may originate from leaf lesions (Taylor et al., 1990). Lindqvist et al. (1998) reported that *P. sparsa* can overwinter in the underground parts of artic bramble. In rose, mycelium of *P. sparsa* may also overwinter in the cortex of stems (Wheeler, 1981; Francis, 1983; Misko and Postnikova, 1989). By PCR

and microscopy, Aegerter et al. (2002) demonstrated the permanence of *P. sparsa* infection in stems, roots, and crown of rose plants with no apparent symptoms. Nevertheless, Xu and Pettitt (2004) did not observe invasion of vascular tissue by *P. sparsa* in affected rose leaves and petioles in the UK. Furthermore, they observed little fungal mycelium in affected leaves from different origins.

Downy mildew is relevant in crop protection programs in rose production, not only because of the difficult management of the disease, but also due to the clonal propagation of roses, which requires to use free pathogen plant material. Since systemic infections for other downy mildews have been confirmed and overwinter spores and mycelia have been found in *Rosa* sp., additional information about the development of the infection is still necessary. This is a crucial aspect to improve control strategies such as timely fungicide application and cultural practices, among others. Thus, the aims of this study were (i) to investigate the spread of *P. sparsa* from localized inoculation on leaves of two rose cultivars, (ii) to assess the effect of leaf maturity on the spread of the pathogen, (iii) to evaluate localized inoculation of the pathogen on leaves and stems of young rose shoots and (iv) to observe the structures of *P. sparsa* that are present in diseased plant tissue.

4.2 Materials and methods

4.2.1 Plant material

Adult plants of cv. Sweetness® class grandiflora (Jackson & Perkins, Hodges, South Carolina USA) and cv. Elle® Var. Meibderos (Meilland International SA, Le Luc-en-Provence, France), Hybrid tea rose, were used as source of plant material for the experiments. The plants were planted in 10 L pots containing a 3:1 mixture of soil and Profi-substrat Typ ED73 (Gebrüder Patzer GmbH & Co Sinntal-Jossa, Germany) and grown in glasshouse under 16 h photoperiod, average temperatures of 23°C/18°C (day/night) and water and fertilizer supplied as necessary. Plant material was harvested immediately before the experiments. For localized inoculation on leaves, three states of maturity were evaluated: young leaves (typically red), intermediate maturity leaves characterized by red-green color, and mature green leaves. During the study, each leaf was kept with the adaxial side in contact with wet filter paper in a Petri dish (Fig. 4.1a). Inoculation of young shoots was conducted on material of cv. Elle® with four to five complete leaves and a small visible bud flower. After harvest, the shoots were placed in 50 ml Eppendorf® tubes with distilled sterile water and sealed at the base with Parafilm®.

4.2.2 Pathogen and inoculation

Sporangia of *P. sparsa* produced on rose leaflets under laboratory conditions were used as source of inoculum. For the inoculation of leaves, three isolates of the pathogen were evaluated, Ps 4, Ps 7 and Ps 8. Seven-day sporangia were collected in sterile distilled water and the density of the inoculum was adjusted to 1.0 x 10^5 sporangia per ml using a Fuchs-Rosental hemocytometer. Two 25 µl drops of the suspension were placed in the center of the abaxial side of the apical leaflets (Fig. 4.1b) and then distributed uniformly using a soft brush to cover a 0.5 cm stripe in the middle of the leaflet. To observe the directionality of *P. sparsa* spread, the middle and distal leaflets of the leaf were inoculated separately. Control leaves were mock inoculated with sterile distilled water. After inoculation, the Petri dishes were stored in a growth chamber at 18°C/16°C day/night temperatures and 70±10% RH.

The shoots were inoculated with the isolate Ps 4 of the pathogen. The apical leaflets were inoculated on the lower leaf surface with 25 µl of the suspension of sporangia using a soft brush. On the stems, a separate group of shoots was inoculated, placing 200 µl of the inoculum in contact with the stem for a period of 48 hours. For this purpose, a small conic container made of Parafilm® was fixed at the inoculation site to keep the inoculum on a 0.5 cm stripe during this time. Control shoots were mock inoculated with sterile distilled water. Then, inoculated and non-inoculated shoots were placed for a period of 48 hours at 10°C and 100% RH conditions to ensure pathogen infection. Next, they were kept in growth chamber under 18°C/16°C day/night temperatures and 70±10% RH.

4.2.3 Presence of the pathogen and disease evaluation

Three days after inoculation (dai), presence of sporulation on the leaf surface was observed daily under the stereo microscope (Leica S4E, Wetzlar, Germany) for fifteen days. The distance in millimeters between the inoculation site and the farthest site of the leaf with presence of sporangiophores bearing sporangia of *P. sparsa* was measured. To report sporulation, the leaf parts were identified as shown in Fig. 4.1b. In addition, 20 dai, the number of oospores in leaves and petioles was quantified under the light microscope (Leitz DMRB; Leica, Wetzlar, Germany). The number of oospores produced at the inoculation site was counted in a grid of 0.175 mm^2, a tool available in the software Diskus 4.2 (Hilgers, Königswinter, Germany) (Fig. 4.1c). Oospores were counted using the fine focus mechanisms of the microscope to examine the sample from the upper to the lower epidermis. In petioles, due to their cylindrical shape, the abundance of oospores was

evaluated visually using a designed scale. The scale considered four degrees of oospore density: 0 (absent), 1 (scarce), 2 (numerous), and 3 (profuse) (Fig. 4.1d). In shoots, the development of the disease was daily monitored by visual assessment of the apical, middle and terminal leaflets, petioles and stems, so as to establish the number of days to the presence of disease symptoms. RBG images were taken to record the progress of the lesions and other visual changes of the tissue.

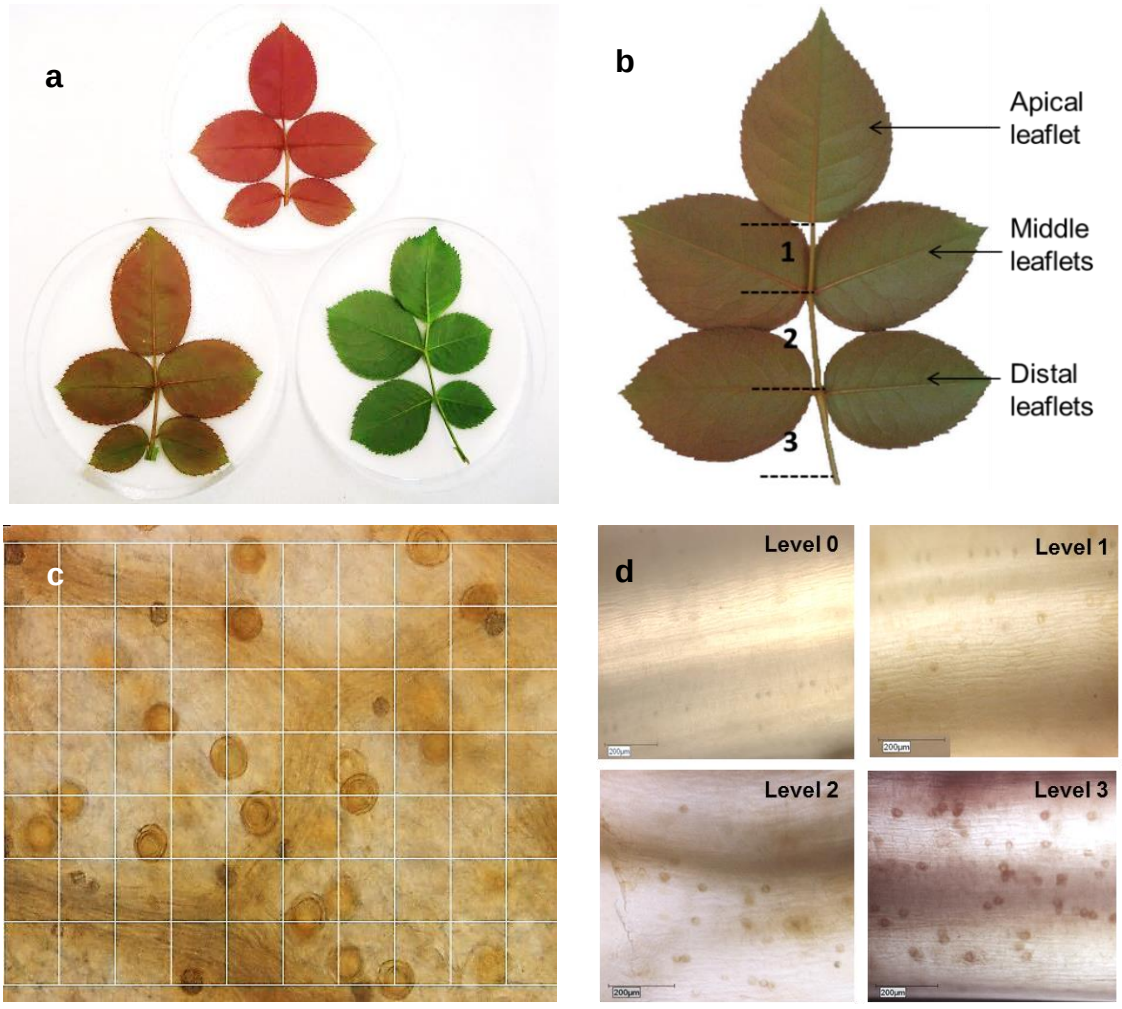

Figure 4.1 Presence of sporangia and oospores in leaf tissue as signs of the development and spread of *Peronospora sparsa* in rose leaves: **a**, maturity stages evaluated: young red color leaves, intermediate leaves reddish green and mature green leaves; **b**, parts of the leaf used to the evaluations; **c**, grid used to quantify oospores at the inoculation site in cleared leaf discs (20X); **d**, scale used to score the abundance of oospores in petioles (10X).

4.2.4 Histological techniques and microscopy

The histological procedures used to process infected leaves, petioles and stems, in order to observe structures of *P. sparsa* in the tissue are described in detail in Chapter 3 (3.2.4).

In general, samples of infected leaves and petioles used to assess oospores in leaf tissue were cleared in chloral hydrate, (Bruzzes and Hasan, 1983; Jende, 2001), stained in 0.01% acid fuchsin (Gerlach, 1977) and observed under the microscope (Leitz DMRB; Leica, Wetzlar, Germany) equipped with Nomarski-interference-contrast. Semi-thin sections (500 nm) were stained with 1% toluidine blue and observed under bright-field. Ultrathin sections (70-75 nm) were stained for observations under Transmission Electron Microscope EM109 (Carl Zeiss AG, Jena, Germany) with 2% uranyl acetate (MERCK) for 5 minutes and with leid nitrate (SiGMA) (1.33 g blei nitrate, 1.76 g nitrium citrate, 30 ml bi-distilled sterile water) for 45 seconds. Images were recorded digitally as explained in Chapter 3 (3.2.4).

4.2.5 Statistical analysis

The statistical analysis was conducted using the Superior Performing Software System SPSS 21.0 (SPSS Inc., Chicago, IL, USA). Data were analyzed by standard analysis of variance and by linear regression. When F values were significant, mean comparisons were performed (Tukey test, $P \leq 0.05$). In addition, independent sample *t*-tests for mean comparisons at a significance level of 95% confidence (*t*-test, $P \leq 0.05$) were carried out. The experiments were performed at least two times with five replicates each.

4.3 Results

4.3.1 Development of downy mildew from localized inoculation on leaves

4.3.1.1 Presence of sporulation of Peronospora sparsa along the leaves

After localized inoculation of apical leaflets, *P. sparsa* infected the leaves of all the maturity stages evaluated in both cultivars. Nevertheless, sporangia were produced at different times across stages of leaf maturity and rose cultivars. The F values were not significantly different ($P \geq 0.05$) for the isolates evaluated and no interaction was detected between isolates and cultivars or maturity stages. F values were significantly different ($P \leq 0.05$) for cultivars and stages of maturity. Interaction between these two factors was observed (Table 4.1). Therefore, the results correspond to those obtained for the three isolates.

Table 4.1 Analysis of variance for the variables: isolate of *Peronospora sparsa*, cultivar and stage of maturity of rose leaves after localized inoculation of the pathogen.

	Days to sporulation apical leaflet		Distance		Oospores inoculation site	
Source	**F**	***P***	**F**	***P***	**F**	***P***
Isolate	2.11	.131 ns	1.15	.322 ns	1.18	.315 ns
Cultivar	33.20	.000 **	.08	.772 ns	35.40	.000 **
Maturity	55.02	.000 **	72.07	.000 **	8.19	.001 **
Isolate x cultivar	1.83	.171 ns	.87	.426 ns	.83	.441 ns
Isolate x maturity	2.46	.056 ns	.19	.940 ns	.842	.505 ns
Cultivar x maturity	7.91	.001 **	1.65	.200 ns	7.12	.002 **
Isolate x cultivar x maturity	.62	.653 ns	1.14	.344 ns	.23	.921 ns

F: values of F-test; *P:* significance value; significance level: ns=no significant ($P \geq 0.05$); ** = highly significant ($P \leq 0.01$).

Sporangia were observed 5 dai at the inoculation site on young leaves of cv. Elle®, 10 dai on petiole 1, 11 dai on petiole 2 and 14 dai on petiole 3. In cv. Sweetness®, sporulation of the pathogen was observed 6 dai on the apical leaflet, 10 dai on petiole 1, and 13 dai on petioles 2 and 3 (Fig. 4.2). In both cultivars, sporangiophores of the pathogen were observed on middle and distal leaflets one or two days after they were observed on the previous petiole segment. Sporangia of *P. sparsa* on apical leaflets occurred first on young and intermediate leaves of both cultivars, and then on mature leaves. However, the pathogen sporulated faster on young and mature leaves of cv. Elle® than on those of cv. Sweetness®. On mature leaves, *P. sparsa* sporulated later than in young leaflets (three days later in cv. Elle® and six days later in cv. Sweetness®) (Fig. 4.2).

In petioles, the number of days to sporulation was affected by leaf maturity. It was faster on young leaves and no sporangiophores were produced on petioles of mature leaves. In petiole 1, sporulation of *P. sparsa* was similar on young and intermediate leaves for both cultivars. In petiole 2 the number of days to sporulation was shorter on young leaves of cv. Elle®, but similar on intermediate leaves of both cultivars. On petiole 3 the pathogen sporulated at similar periods of time on young leaves, but sporangia were only observed on intermediate leaves of cv. Elle® (Fig. 4.2).

Sporulation on middle leaflets also depended on leaf maturity. In cv. Elle®, this sporulation occurred first on the young leaves and then on the intermediate leaves; in cv. Sweetness®, it took place only in the young leaves. Sporulation on distal leaflets was only present on the young leaves of both cultivars (Fig. 4.2).

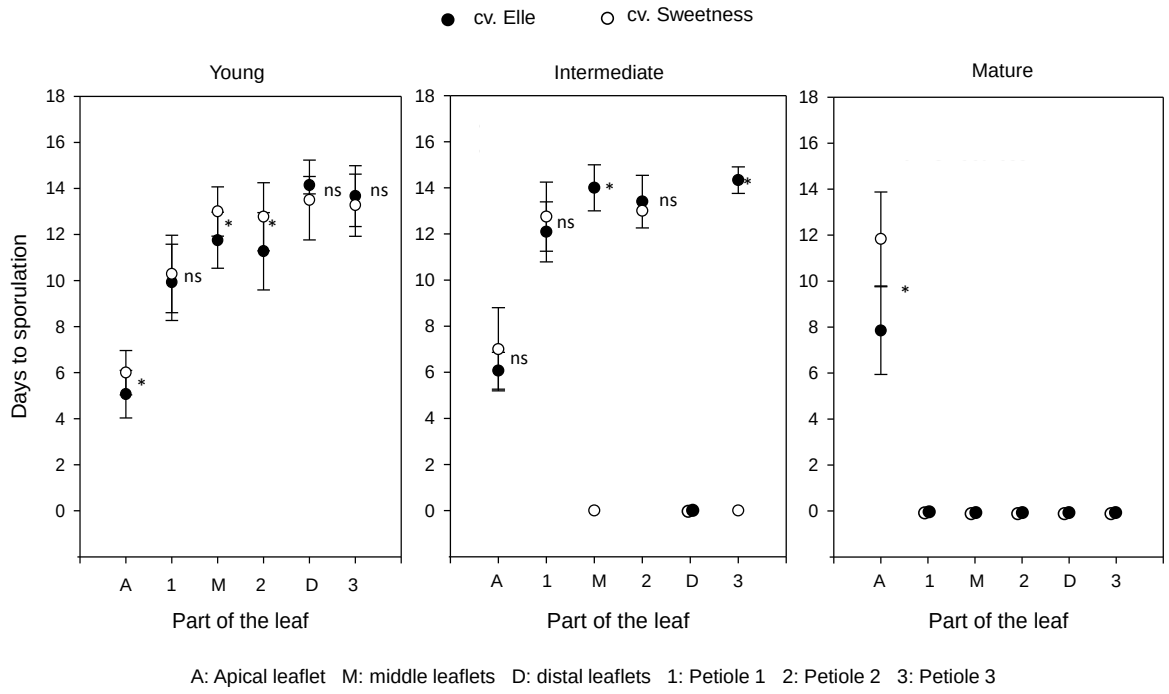

Figure 4.2 Effect of cultivar and leaf maturity on the presence of sporulation of *Peronospora sparsa* on different parts of rose leaves according to Figure 4.1, after localized inoculation on apical leaflets. Error bars represent the standard deviation. Asterisk indicates values significantly different; ns denotes values no significantly different (*t*-test $P \leq 0.05$).

After localized inoculation on single, middle or distal leaflets, *P. sparsa* spread to the apical leaflet and toward the leaf petiole ending without any particular preference. Dense sporulation of the pathogen covered the whole leaf 15 dai. Furthermore, the number of days to sporulation and the spread pattern of *P. sparsa* were similar in both cultivars. These results confirmed the acropetal and basipetal spread patterns of the pathogen in complete rose leaves.

4.3.1.2 Spread of Peronospora sparsa from the inoculation site

The results showed *P. sparsa* spreading from the site of infection and completely covering the young leaves with dense sporulation 15 dai. The equation of linear regression showed the pathogen spreading from the inoculation area on the young leaves of both cultivars 8 dai at similar rates (Fig. 4.3a). On intermediate leaves of cv. Elle® the pathogen spread out from the inoculated area 8 dai and 11 dai in cv. Sweetness® (Fig. 4.3b). On mature leaves of both cultivars the spread of *P. sparsa* visualized as sporangia on the leaf surface was restricted to the inoculation site (Fig. 4.3c). Sporangia on young leaves were observed as far as 70 mm from the inoculation site 15 dai and around 50 mm on intermediate leaves by the same period of time. Fifteen days after inoculation, the cultivar was observed to have no significant effect on the distance covered by sporulation from the inoculation site. Contrastingly leaf maturity did affect this distance.

4.3.1.3 Oospore production in leaf tissue

The amount of oospores produced at the inoculation site in leaves and petioles 20 dai varied depending on the cultivar and on leaf maturity. No significant differences were observed in the number of oospores produced in the young leaves of both cultivars. However, the value was higher in cv. Elle® in intermediate and mature leaves, in contrast with cv. Sweetness®. Furthermore, in cv. Elle® the amount of oospores at the inoculation site was similar in the three stages of maturity. On the contrary, in cv. Sweetness® the number of oospores produced declined with leaf maturity (Fig. 4.4). In leaf petioles, high oospore index values were observed in young and intermediate leaves of cv. Elle®. In cv. Sweetness® high values were only observed in young leaves. In mature leaves, low indexes were scored by both cultivars (Fig. 4.5). No differences were observed in oospore abundance along the segments of the leaf petioles of young leaves. In intermediate leaves, the index of oospores was higher in petiole 1 in comparison to the other segments of the petiole. In mature leaves, oospores, which exhibited low counts, were only observed in petiole 1 of both cultivars 20 dai (Fig. 4.6a, b). Presence of oospores in petioles confirmed the spread of *P. sparsa* along rose leaves. Oospores were densely produced in leaf areas with profuse sporulation or in their proximities. Presence of oospores 20 dai in petiole segments where sporulation had not been observed suggests the intercellular spread of mycelia and the possibility to produce scarce oospores in late stages of the disease in more mature leaf tissues.

4.3.2 Development of downy mildew from localized inoculation on shoots

4.3.2.1 Presence of disease symptoms

After localized inoculation of *P. sparsa* on apical leaflets, typical symptoms of downy mildew were first observed at the site of inoculation 10 dai, then on neighboring leaflets 22 dai and later on stems 28 dai (Fig. 4.7). The first visible symptoms of *P. sparsa* infection were dull apical leaflets that looked weighty and tended to decrease the angle with the stem in comparison to healthy ones. Then, the color of the leaflet changed to brown, followed by presence of irregular brown-purple spots that turned to yellow-green angular shaped lesions (Fig. 4.8a, b, c). *P. sparsa* spread from apical to neighboring leaflets in 58.3% of the diseased leaves (Fig. 4.8d, e).

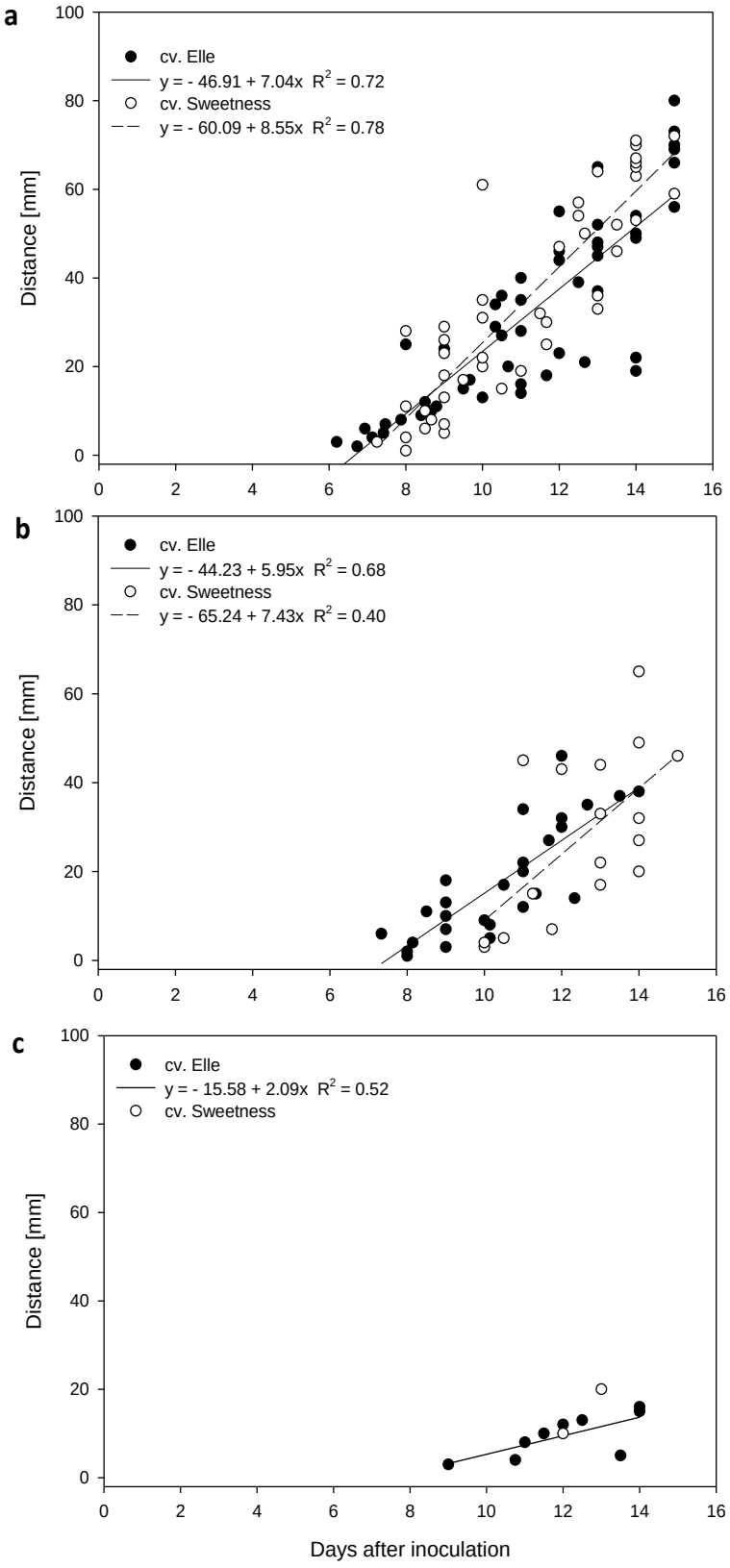

Figure 4.3 Spread of *Peronospora sparsa* over the time measured in distance from the inoculation site on apical leaflets, distance 0, of leaves of two rose cultivars and three stages of leaf maturity: **a**, young leaves; **b**, intermediate leaves and; **c**, mature leaves. Linear regression ($y = b_0 + b_1x$) and the R-square values for each cultivar per stage of maturity are presented.

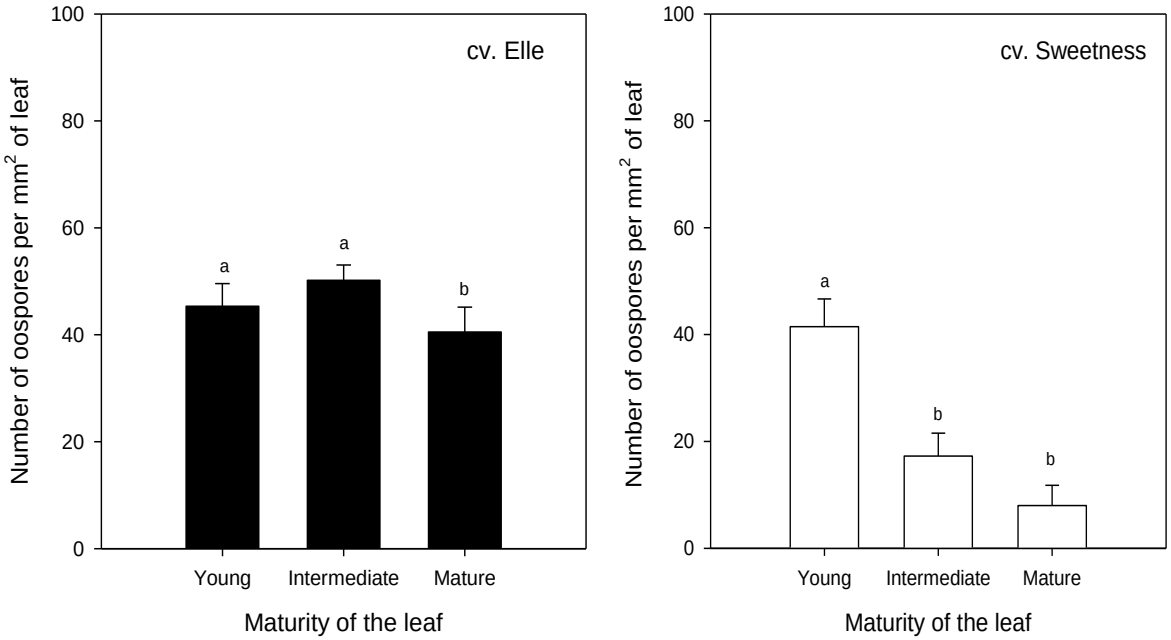

Figure 4.4 Number of oospores in leaf tissue at the inoculation site on apical leaflets in three stages of maturity of rose cv. Elle® and cv. Sweetness® 20 dai. Values followed by the same letter are not significantly different (Tukey test, $P \leq 0.05$). Error bars represent the standard error.

As to the spread from inoculated apical leaflets, 18.3% of them were observed to produce stem symptoms at the leaf insertion point (Fig. 4.8f). Under the conditions of the experiment (≤80% RH), no sporulation was observed. Therefore, the results corresponded to the spread of the pathogen from localized inoculation sites and not to secondary infection of new sporangia.

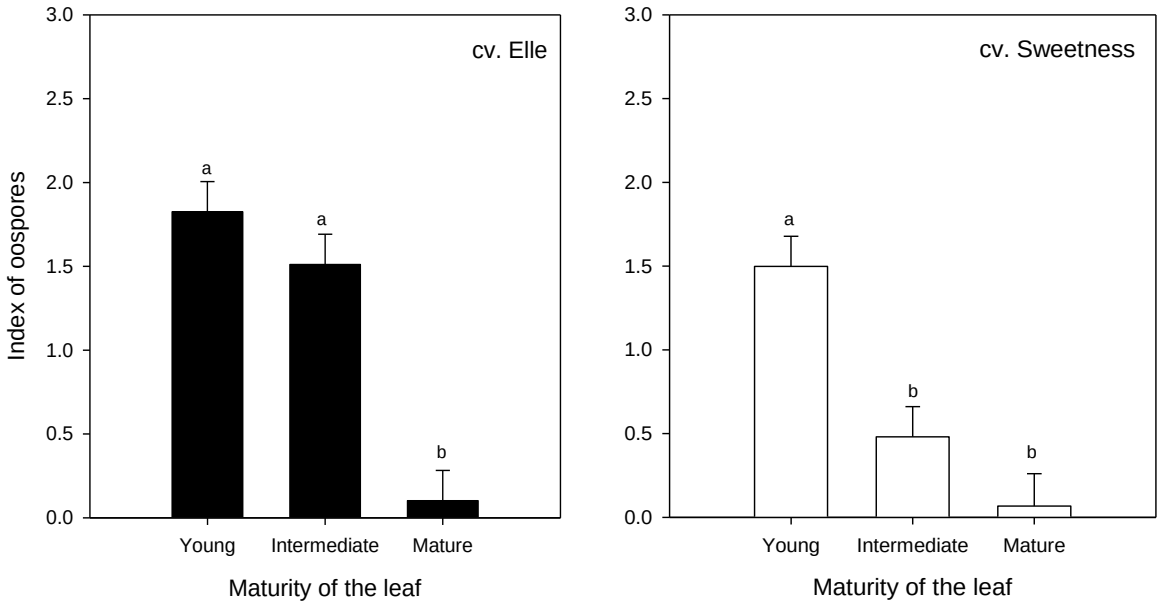

Figure 4.5 Index of oospores in leaf petioles of three stages of maturity of rose cv. Elle® and cv. Sweetness® 20 dai. Values followed by the same letter are not significantly different (Tukey test, $P \leq 0.05$). Error bars represent the standard error.

On stems, symptoms varied from green spots with swollen borders to slightly chlorotic flecks that turned into irregular purple spots which darkened and increased in number or coalesced over time. At the inoculation site, symptoms appeared 18 dai (Fig. 4.8g), spread to higher leaf insertions taking place 34 dai in 50% of the inoculated stems (Fig. 4.8h, i). The colonized leaflets showed typical disease symptoms, first on the proximal leaflets and then on the middle and apical leaflets. In all cases, sporulation was produced on symptomatic leaflets after 24 hours under 100% RH. These results confirm that *P. sparsa* infection in rose shoots can spread from localized infections to the stems.

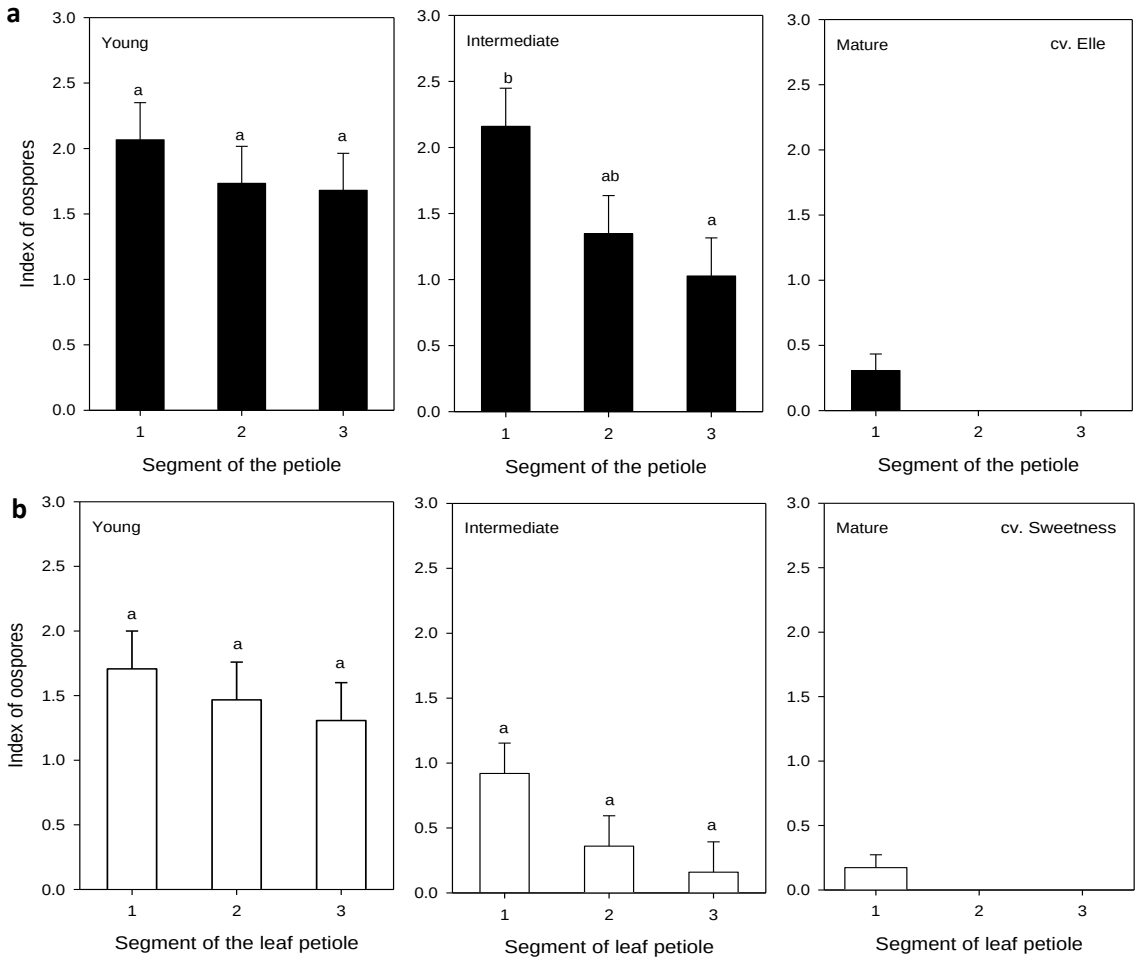

Figure 4.6 Distribution of oospores of *Peronospora sparsa* along segments of leaf petioles of two rose cultivars in three stages of maturity 20 days after inoculation on apical leaflets: **a**, cv. Elle®; **b**, cv. Sweetness®. Values followed by the same letter are not significantly different (Tukey test, $P \leq 0.05$). Error bars represent the standard error.

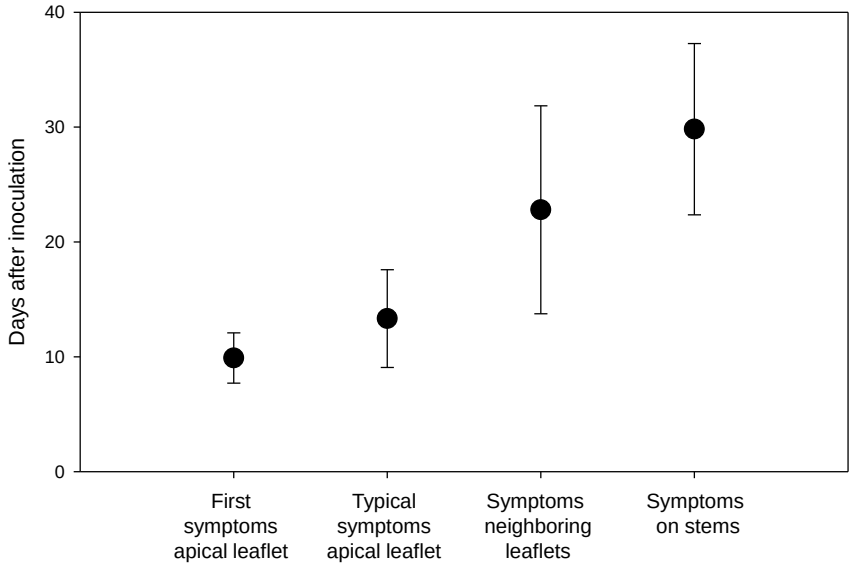

Figure 4.7 Effect of localized inoculation of apical leaflets with *Peronospora sparsa* on the presence of symptoms of the disease in young shoots of rose cv. Elle®. Error bars represent the standard deviation.

4.3.3 Structures of Peronospora sparsa in infected tissue

Intercellular hyphae and haustoria of *P. sparsa* were observed with the first disease symptoms in inoculated apical leaflets and neighboring leaflets that became infected from distal inoculations. In more severe symptoms, high number of haustoria penetrating all tissue layers of leaves was observed (Fig. 4.9). Structures of the pathogen were not observed at the base of inoculated apical leaflets of young, intermediate and mature leaves even 7 dai. This result shows that under the conditions of the study, long distance colonization by *P. sparsa* out of the apical leaflet began 8 dai in young leaves. In leaf petioles, intercellular hyphae and haustoria of *P. sparsa* were observed to be confined to cortical tissue. Hyphae were densely produced at the angular sector of the petiole and in stomatal cavities (Fig. 4.10). On symptomatic stems, hyphae and haustoria were confined to the cortex tissue. Hyphae of *P. sparsa* were observed spreading along cortical cells in longitudinal sections (Fig 4.11).

Under the conditions of the study, *P. sparsa* was found to penetrate cells of the bundle sheath, but not xylem or floem cells in leaves, petioles or stems. Oospores were observed in infected leaves and petioles when the symptomatic material was exposed to 100% RH and sporangia were produced. In the stems, no oospores were observed even in sporulated tissue. Ultrastructures in petioles and stems showed hyphae of *P. sparsa* adapting their size according to available intercellular space. In compact tissues like the

cortex of petioles and stems, hyphae were narrow (Fig. 4.10c and 4.11e) in comparison with the wide hyphae observed in leaf tissues. Petioles and stems were infected by filiform haustoria.

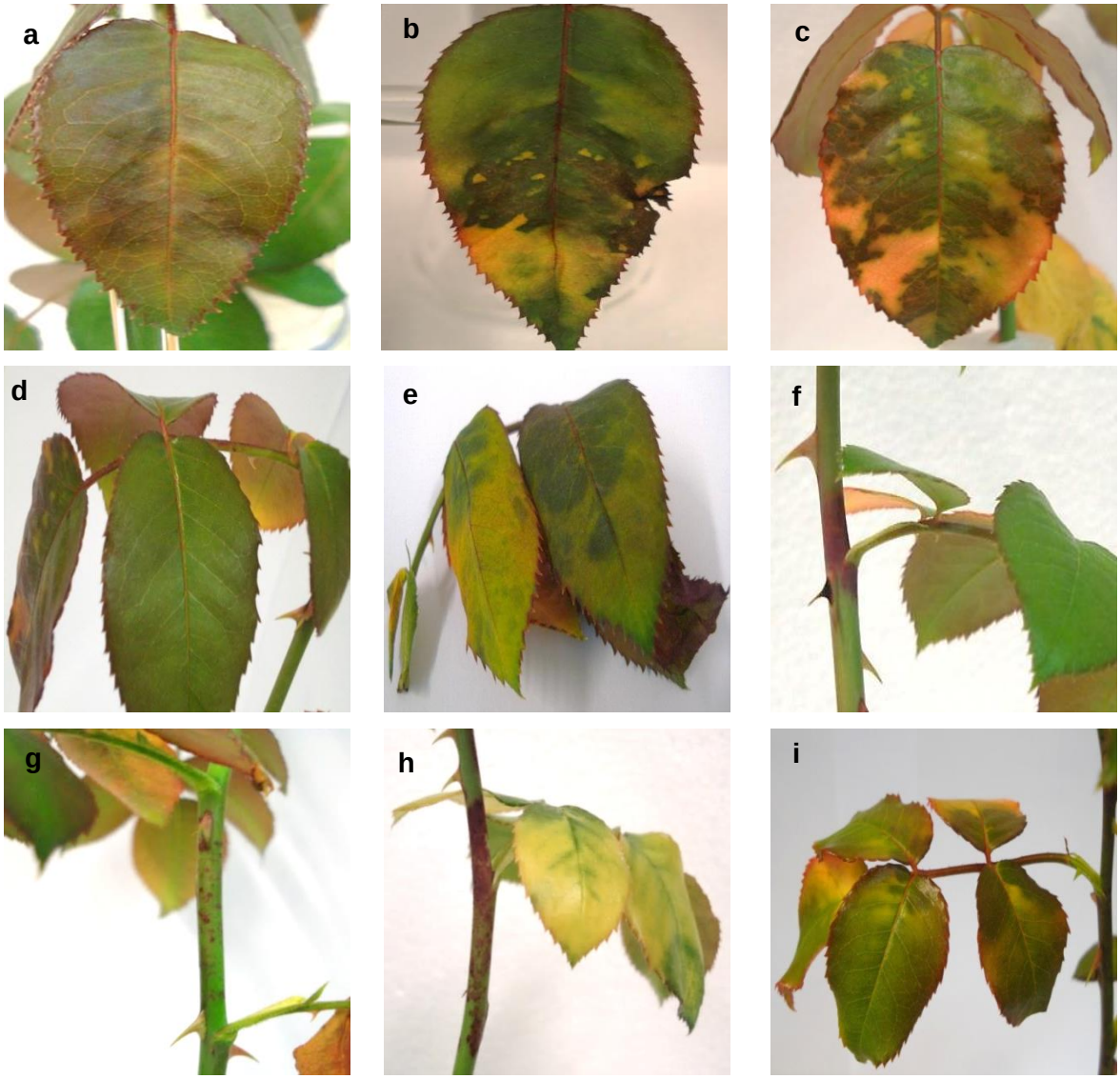

Figure 4.8 Symptoms of downy mildew on rose cv. Elle® after localized inoculations of *Peronospora sparsa* on apical leaflets and stems: **a**, first symptoms on apical leaflet 10 dai; **b**, same leaflet showing typical green purple spots angular shape 12 dai; and **c**, complete leaflet showing green angular spots and chlorotic tissue 16 dai; **d**, infected brown purple petiole 13 dai; **e**, symptoms on neighboring leaflets 22 dai; **f**, symptoms on stems 28 dai as a result of the spread of the pathogen from apical leaflets; **g**, purple lesions on stems 17 dai; **h**, and; **i**, symptoms in higher leaf insertions caused by spread of *P. sparsa*. Days after inoculation: dai.

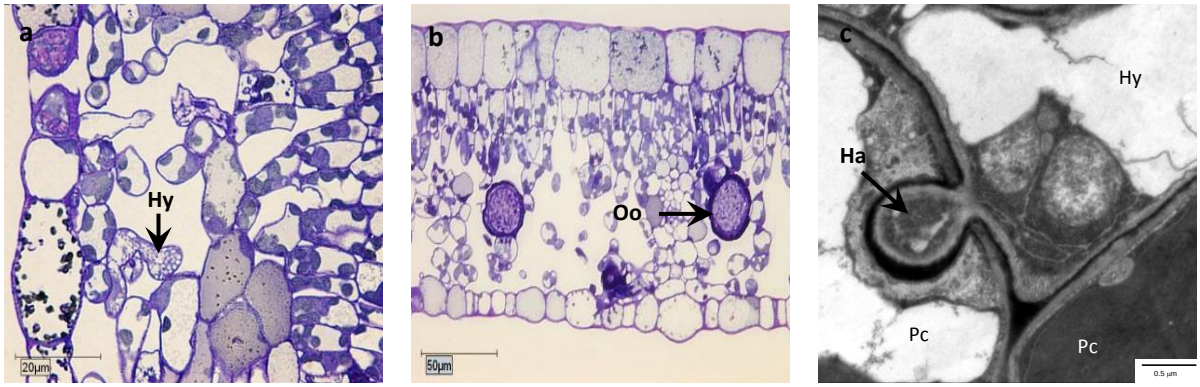

Figure 4.9 Typical infection structures of *Peronospora sparsa* in rose leaves cv. Elle® 8 days after localized inoculation on apical leaflets observed in semi thin sections under light microscope (a, b) and transmission electron microscope (c): **a**, hypha in spongy parenchyma; **b**, oospores produced in the mesophyll of the leaf; **c**, haustorium in mesophyll cell. Hy, hypha; Ha, haustorium; Oo, oospore; Pc, plant cell.

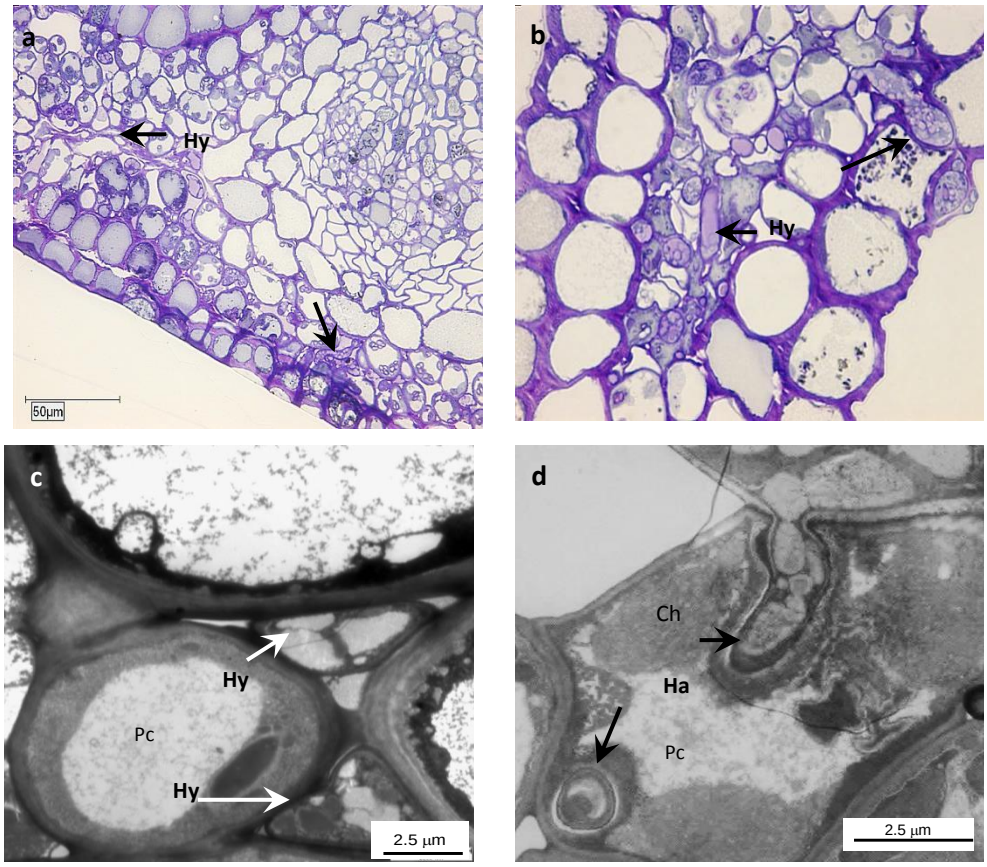

Figure 4.10 Typical infection structures of *Peronospora sparsa* in petioles of rose leaves cv. Elle® 8 days after localized inoculation on apical leaflets observed in semi thin sections under light microscope (a, b) and transmission electron microscope (c, d): **a**, hyphae confined to cortical tissue; **b**, intercellular hyphae in the angular sector of the petiole and thick hyphae the under the cuticle; **c**, narrow intercellular hyphae in cortical tissue; **d**, detail of petiole cell penetrated apparently by two haustoria. Ch, chloroplast; Hy, hypha; Ha, haustorium; Pc, plant cell.

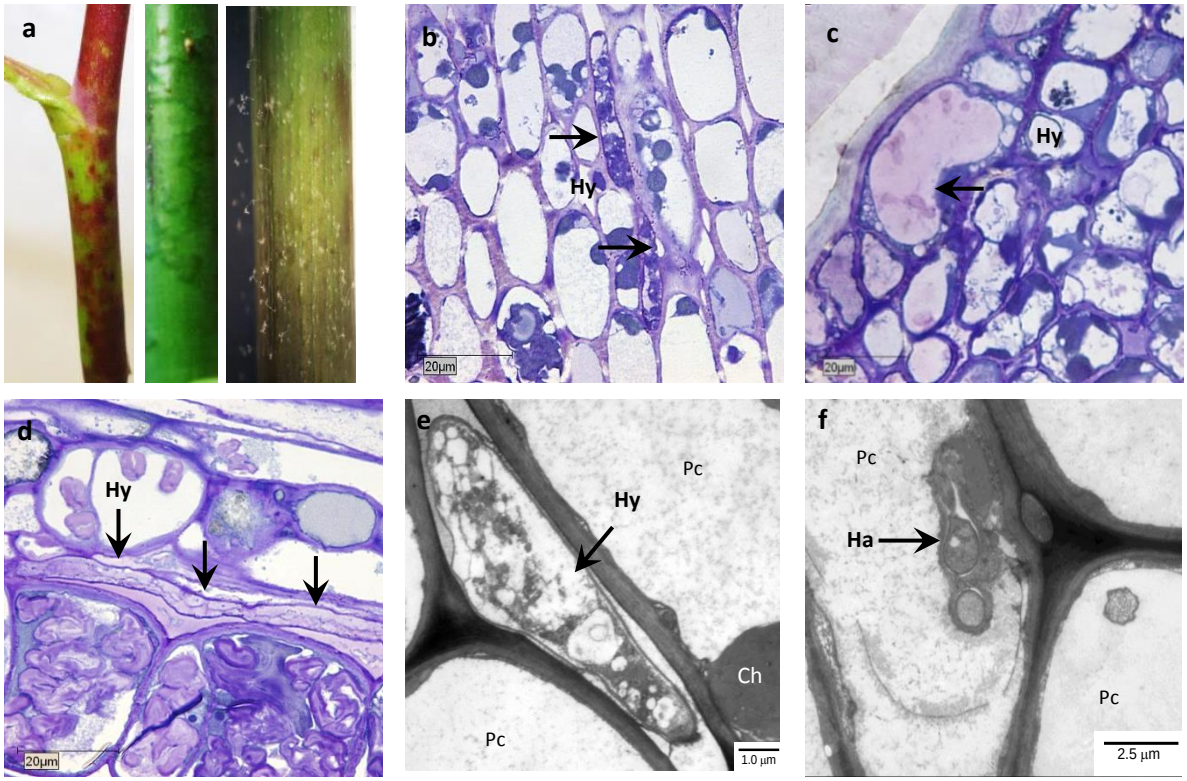

Figure 4.11 Macro and microscopical structures of *Peronospora sparsa* in stems of rose cv. Elle® after localized inoculations; structures of the pathogen in semi thin sections observed under light microscope (b to d) and transmission electron microscope (e, f): **a**, from left to right: chlorotic areas with coalescent purple spots, irregular spots with prominent green borders, sporulation on symptomatic young stems; **b**, hyphae confined to cortical tissue; **c**, thick hypha produced in sporulating stem with swollen green borders; **d**, longitudinal section of cortical tissue with hyphae expanded parallel to stem cells; **e**, intercellular hypha in cortical tissue. **f**, haustorium infecting a cortical stem cell. Ch, chloroplast; Hy, hypha; Ha, haustorium; Pc, plant cell.

4.4 Discussion

The ability of downy mildews to establish spreading infections have been reported for other species and is confirmed in this study for *P. sparsa* in rose. Populer (1981) defined the occurrence of systemic infection of downy mildews when colonization continues after the first symptoms appear. It was observed that *P. sparsa* spreads acropetally and basipetally in rose leaves and shoots. After localized inoculation, visual and histological evaluation of leaves, petioles and stems confirmed systemic infection of *P. sparsa* in rose tissue.

Although *P. sparsa* developed in a comparable way on young leaves of cv. Elle® and cv. Sweetness®, differences were observed in intermediate and mature leaves. The susceptibility of cv. Elle® was higher and therefore the spread of *P. sparsa* was faster in this cultivar. Differences between the spread of *P. sparsa* in rose cultivars were clearly

observed in intermediate and mature stages of maturity. The ability of *P. sparsa* to colonize new tissue was strongly affected by the maturity of the tissue. In young leaves, shorter latent periods and higher numbers of oospores in petioles and at the inoculation sites (apical leaflets) contrast with those of intermediate and mature leaves. These results confirm the importance of maturity of rose leaf tissue as a factor of resistance to the pathogenesis and spread of *P. sparsa*.

Symptomless invasion of the stem tissues of *Pisum sativum* by *P. viciae* resulted in systemic infection, indicating that some apical infection may originate from leaf lesions. In addition, removal of infected leaves in pea plants reduced systemic infection under high temperatures (Taylor et al., 1990). This result shows the importance of infected leaves in the colonization of new tissue, as observed with *P. sparsa* on rose leaves. Williamson et al. (1995) observed hyphae of *P. sparsa* (syn. *P. rubi*) entering the veins and petioles and spreading to cortical tissues of the stem of *Rubus* spp., although this infection extended only a few centimeters. In the present study *P. sparsa* spread in rose stems from one single site of infection. This constitutes an important observation since roses are vegetatively propagated woody perennials.

In histological observations of infected tissue, intercellular hyphae and haustoria of *P. sparsa* were observed in inoculated and infected neighboring leaflets, petioles and stems. Nevertheless, no infection was observed in inner cells of the vascular vessels and hyphae and haustoria were mainly observed penetrating bundle sheath cells. Hyphae of the pathogen were observed to be confined to the cortex. Similar results were observed by Xu and Pettitt (2004) in leaves and petiole sections from different sources where invasion of vascular tissue by *P. sparsa* was not present. Intercellular mycelium of *P. sparsa* was the structure responsible for the internal colonization of rose tissue. On the contrary, Xu and Pettitt (2004) observed that mycelia did not spread from infected leaves to stems as they observed new healthy leaves growing from previously infected nodes. In the current investigation, after localized inoculation, *P. sparsa* spread from lesions on the stems and apical leaflets to neighboring leaflets and stems.

In the present study, *P. sparsa* produced hyphae in the cortical tissue of petioles and stems. Similar findings were obtained by Aegerter et al. (2002), who observed intercellular mycelium of *P. sparsa* located between epidermal and cortex parenchyma and haustoria and oospores within the stem cortex of infected rose canes. By PCR and microscopy, these authors demonstrated the persistence of *P. sparsa* infection in stems, roots and the crown of rose plants. In addition, due to the less consistent occurrence of the pathogen in vascular tissues, they suggested that *P. sparsa* probably colonizes the crown by mycelial

growth through the stem cortex. Williamson et al. (1995) observed *P. sparsa* (syn. *P. rubi*) growing in a parallel arrangement through the cortex intercellular spaces of the host *Rubus* sp., and oospores were not found, thus corresponding with the findings of the current study. In contrast, Aegerter et al. (2002) did observe oospores in rose stems, probably due to the age of the evaluated tissue. Nevertheless, similar haustoria were observed in the cortical cells of the stems in both studies.

When *P. sparsa* sporulated in infected petioles and stems, some thick hyphae grew under the cuticle (Fig. 4.10b and 4.11c). Hyphae of *P. grisea* were observed growing at short distances from the hosts (Fraymouth, 1956). Nevertheless, more detailed observations on rose are required to see if *P. sparsa* grows extensively under the cuticle or in epidermal tissue. Due to the dense presence of hyphae of *P. sparsa* along the petiole, this part of the leaf comes to be the structure used by *P. sparsa* hyphae to spread across leaflets, from stems to leaves, and vice versa. Fraymouth (1956) pointed out that hyphae can cover important distances up or down the plant surrounding cortical cells. Indeed, the ability of the *Peronosporales* to adapt their shape to intercellular spaces was also mentioned by Fraymouth (1956). Likewise, by electron microscopy it was observed that *P. sparsa* produced hyphae in the narrow intercellular spaces of midrib, petiole and stem collenchyma, but this condition was not a limiting factor for its spread.

This study confirmed systemic infection of rose tissue by *P. sparsa* and allowed visualizing the structures of the pathogen that are present in the leaf tissue. The production of oospores on leaves and petioles by the pathogen as it spreads illustrates both the colonization strategy of *P. sparsa* and the contrasts observed between susceptible cultivars and maturity stages of leaf tissue. These findings complement earlier studies on *P. sparsa* in *Rose* sp.. Nevertheless, additional research in adult and old plants in commercial crops may enhance the knowledge obtained so far.

5. COMPARISON OF LEAF COLONIZATION OF ROSE CULTIVARS WITH DIFFERENT SUSCEPTIBILITY TO *Peronospora sparsa* USING THERMAL IMAGING

5.1 Introduction

Downy mildews constitute a particular group of pathogens, not only because of their morphology, but due to the fact that they are considered detrimental parasites in many important crops (Viennot-Bourging, 1981). Early detection of plant biotic stress is a relevant factor in current crop protection programs. Imaging techniques allow detection of stress situations before visual symptoms. Therefore, they are promising tools for crop yield management (Chaerle and Van der Straeten, 2001). Thermal and chlorophyll fluorescence are considered in this group. Thermal imaging detects temperature at the plant surface. Areas of high temperature reflect stomatal closure, and low temperatures reflect stomatal opening or tissue damage (Chaerle et al., 2002). By thermography, pathogen infection affecting stomata aperture can be rapidly visualized (Chaerle and Van der Straeten, 2001; Chaerle et al., 2004; Chaerle and Van der Straeten, 2000). Besides, leaf temperature can be altered due to damage of plant cuticle, degradation of cells, blocked water uptake or accumulation of plant defense compounds (Chaerle et al., 2004; Jones, 2004). Tissue damage is expected to cause a decrease in leaf surface temperature, since the content of damaged cells evaporates and locally cools the surface (Chaerle et al., 2001).

Infrared thermography has allowed visualizing the establishment of harpin-induced hypersensitive response (HR) by *Erwinia amylovora* in *Nicotiana sylvestris* leaves (Boccara et al., 2001). Before visual symptoms appeared, thermography has also permitted the monitoring of an increase in temperature after infection of resistant tobacco by tobacco mosaic virus (Chaerle et al., 2002). As thermal responses may vary, knowledge on the disease signatures of different plant–pathogen interactions could allow early identification of emerging biotic stresses in crops (Chaerle et al., 2004). In cucumber leaves, before visible symptoms of downy mildew caused by *Pseudoperonospora cubensis* appeared, the maximum temperature difference within thermograms allowed the discrimination between healthy and infected leaves (Lindenthal et al., 2005). Moreover, these results showed that infrared thermography can be successfully applied to pre-symptomatic detection of downy mildew attack in cucumber (Lindenthal et al., 2005; Oerke et al., 2006). The interaction between *Plasmopara viticola* and grapevine leaves was detected thermographically 3 or 4 days after inoculation, before any visual symptoms

occurred. In addition, downy mildew pathogenesis resulted in a considerable heterogeneity in spatial and temporal variation of leaf temperature (Stoll et al., 2008).

Some studies have reported latent infection of *P. sparsa* in *Rosa* sp.. The occurrence of the disease in symptomless tissues has been reported for other downy mildews. However, no research has been conducted to find alternative methods for early detection of *P. sparsa* in non-invasive inspections. Therefore, it is necessary to investigate the presymptomatic detection of diseased plants. The aims of this study were (i) to explore the possible use of IR thermography to detect infections of *P. sparsa* in rose leaves, (ii) to identify thermal responses of leaf tissue to pathogenesis and (iii) to assess the infection of downy mildew in different rose cultivars by thermography.

5.2 Materials and methods

5.2.1 Plant material

Plants of the grandiflora rose cv. Sweetness® (Jackson & Perkins, Hodges, South Carolina USA), the Hybrid tea rose cv. Elle® (Meilland International SA, Le Luc-en-Provence, France) and the floribunda rose cv. Frensham® grown under greenhouse conditions of 16 h photoperiod and day/night average temperatures of 23°C/18°C were used as source of plant material. Young leaves, susceptible to *Peronospora sparsa* infection were used in the study. Previous to the inoculation, leaves of these three cultivars were harvested and rinsed once with tap water and twice with distilled sterile water. Then, the leaves were placed with the adaxial side in contact with wet filter paper in Petri dishes (100% RH), in order to track the infection of *P. sparsa* over time.

5.2.2 Pathogen and inoculation

The isolate Ps 6 of *P. sparsa* kept under controlled conditions on rose leaflets was used as source of inoculum. Seven days after inoculation (dai), sporangia were collected in distilled sterile water and the density was adjusted to 1 x 10^5 sporangia per ml using a Fuchs-Rosental hemocytometer. As roses have imparipinnate compound leaves, only one leaflet was inoculated. Two 25 µl drops of the inoculum were placed in the center of the leaflet on the abaxial side and then distributed uniformly using a soft brush to cover a stripe of 0.5 cm. After inoculation the leaves were kept under 18°C/16°C day/night temperatures and 16 hours of light in a growth chamber.

5.2.3 Disease evaluation

Three days after inoculation (dai) and daily for twenty four days, microscopic and IR thermography evaluations were carried out on inoculated and non-inoculated leaves. The progress of the infection was evaluated by presence of sporulation of *P. sparsa* on rose leaves visualized under the stereo microscope (Leica S4E, Wetzlar, Germany). To record the presence of sporulation, the leaflets were labeled as follows: number one (1) corresponded to the apical leaflet; numbers two (2) and three (3) were the middle leaflets and numbers four (4) and five (5), the distal leaflets. Leaflet 3 was inoculated as described before. RBG images were taken to register the development of the disease.

5.2.4 Thermographic measurements

The inoculated and non-inoculated leaves were adapted to the conditions of the room (20±2°C, 60±5% RH) at least for 60 minutes before thermographic evaluations. As detached leaves adapt to the temperature of water they are floating on, they were placed on a paper towel for 10 seconds and then transferred to a humid chamber for 20 minutes to continue the drying process, thus avoiding the desiccation of the leaves and the dehydration of the pathogen. After this time, thermal images were taken at a distance of 30 cm from the leaves. Thermographic images were obtained using an infrared Stirling-cooled scanning camera VARIOSCAN 3201 ST (Jenoptic Laser, Jena, Germany) with a spectral sensitivity from 8 to 12 μm and 1.5 m radians of geometric resolution (240 × 360 pixels focal plane array and a 30° × 20° field of view lens with a minimum focus distance of approximately 20 cm). Thermal resolution was 0.03 K and accuracy of absolute temperature measurement was <±2 K.

5.2.5 Thermograms and statistical analysis

The thermographic images were analyzed using the software IRBIS® Plus version 2.2 (Infratec, Dresden, Germany). The outline of the leaflets was reframed using the polygon tool of the IRBIS® program to obtain the average temperature of inoculated and non-inoculated leaflets for each thermogram. Mean temperature differences (ΔT) between inoculated and non-inoculated leaflets were calculated in order to visualize the effect of the infection on leaf temperature over time. The statistical analyses were carried out using the Superior Performing Software System SPSS 21.0 (SPSS Inc., Chicago, IL, USA) conducting independent-sample *t*-test analyses for means comparison at a significance level of 95% (*t*-test, $P \leq 0.05$). All the experiments were performed at least two times.

5.3 Results

5.3.1 Presence of sporangia of Peronospora sparsa on leaf tissue

Differences between the three rose cultivars in terms of sporulation of *P. sparsa* were detected. The first sporangiophores with sporangia at the inoculation site were observed 5.8 dai (±1.0) in cv. Elle® and 7.0 dai (±1.0) in cv. Sweetness®. Slight sporulation of the pathogen on the whole leaflet surface was observed 8.8 dai (±0.5) in cv. Elle® and 8.0 dai in cv. Sweetness®. Leaflets covered by dense sporulation of *P. sparsa* were observed 10.5 dai (±1.0) and 10.8 dai in cv. Elle® and cv. Sweetness®, respectively. On leaves of cv. Frensham® no sporulation of the pathogen was observed. In cultivars Elle® and Sweetness®, the profuse sporulation of the pathogen was followed by presence of brown tissue at the inoculated site and later on in neighboring areas.

In cv. Elle®, sporulation of *P. sparsa* on leaflets 1 and 2, which are opposite to the inoculated leaflet (3), was observed 11 dai. In addition, sporangiophores and sporangia of the pathogen were produced on leaflets 4 and 5, 12 dai. In cv. Sweetness® sporulation of the pathogen on leaflet 1 was observed 15 dai, on leaflet 2 which is opposite to the inoculated leaflet (3) 11 dai and on leaflets 4 and 5, 13 dai.

5.3.2 Imaging of Peronospora sparsa infection of leaves

The thermograms showed high temperatures at the inoculation site as early as 3 dai in comparison to non-inoculated leaflets (Fig. 5.1). During this time, no changes in leaf tissue or presence of structures of the pathogen on the leaf surface of the three cultivars were detected visually. The temperatures of the warm areas of inoculated leaflets of cv. Elle® and cv. Sweetness® were significantly different 6 dai in comparison to non-inoculated leaflets. In the thermograms, the higher temperatures of inoculated leaflets as compared to non-inoculated ones were observed until 11 dai in cv. Elle® and until 13 dai in cv. Sweetness®. At the end of the evaluations (24 dai), a decline of leaf temperature of the inoculated leaflets could be observed in both cultivars (Fig. 5.2). The same leaf temperature response associated with the infection of the pathogen was visualized on the adaxial and abaxial sides of infected leaves. During the evaluations, no significant differences were detected in leaf temperature of inoculated leaflets in cv. Frensham®. Due to a natural detachment of leaflets of this cultivar, observations and imaging were done only for a period of 15 dai.

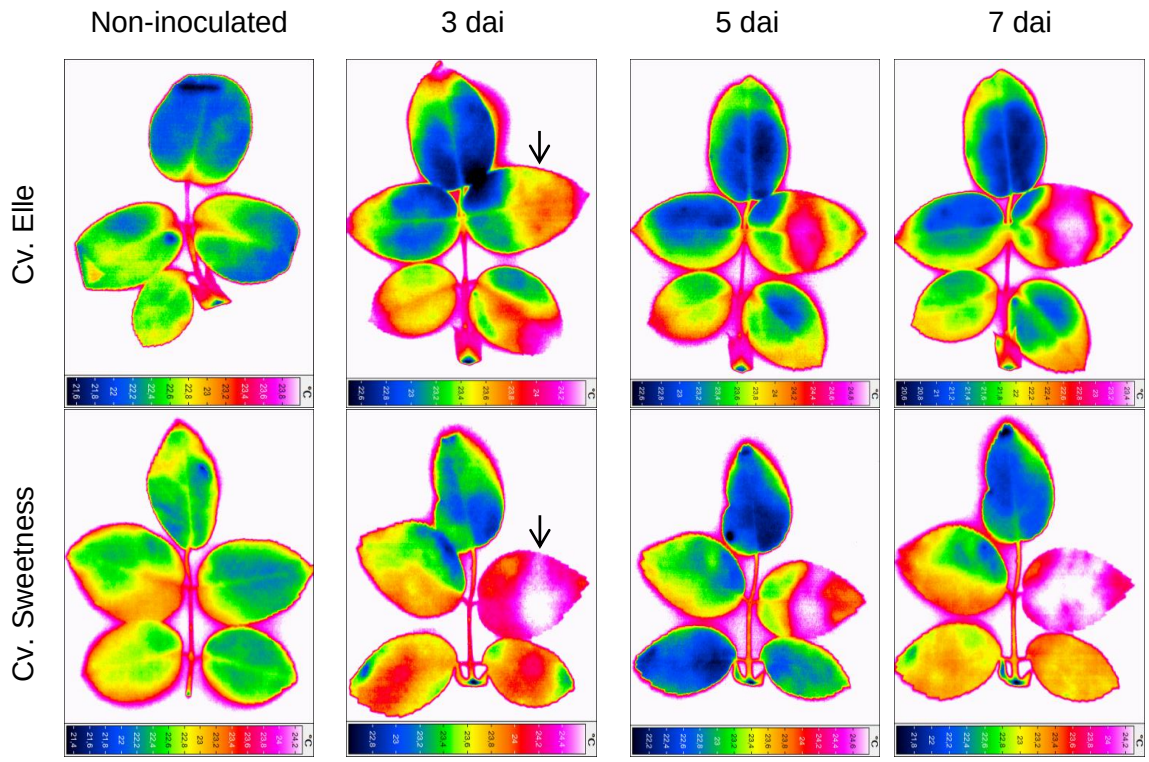

Figure 5.1 Dynamics of leaf temperature of two cultivars of rose in early stages of pathogenesis before the formation of sporangia 3 and 5 dai and with presence of first sporangia 7 dai, after localized inoculation of *Peronospora sparsa* on leaflet number 3 indicated by the arrows, visualized by IR thermography. Days after inoculation: dai.

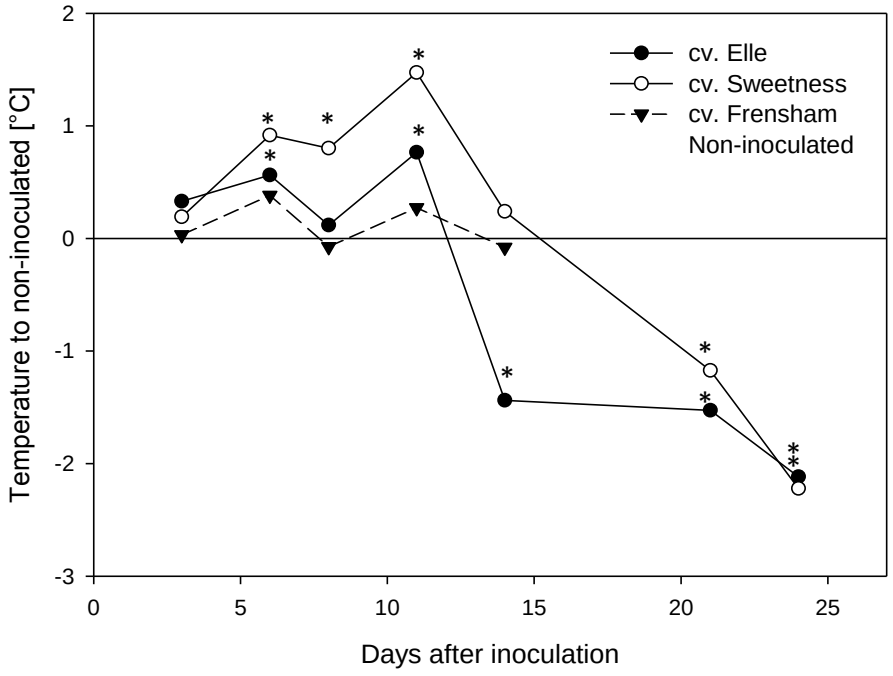

Figure 5.2 Effect of *Peronospora sparsa* infection on leaf temperature of three rose cultivars. Data show differences in temperature to non-inoculated. Asterisk indicates value significantly different from non-inoculated leaves (*t*-test, $P \leq 0.05$).

The leaf temperature dynamics of inoculated and neighboring leaflets (1, 2, 4 and 5) over time is presented in Fig. 5.3. Warm areas at the inoculation site 6 dai were followed by a decrease in the leaf temperature of the inoculated leaflet. Then, the temperature of neighboring leaflets declined 14 and 24 dai as the infection progressed. A strong leaf temperature decrease was observed in the leaflets surrounding the inoculated leaflet (3) in cv. Elle® 12 dai. Moreover, the thermograms taken 14 dai and later showed significantly low temperatures in all the leaflets of the leaf in comparison with non-inoculated ones (Fig. 5.4a). In cv. Sweetness® neighboring leaflets to leaflet 3 showed higher temperatures until 14 dai. Then, the thermograms showed a cooling process in all

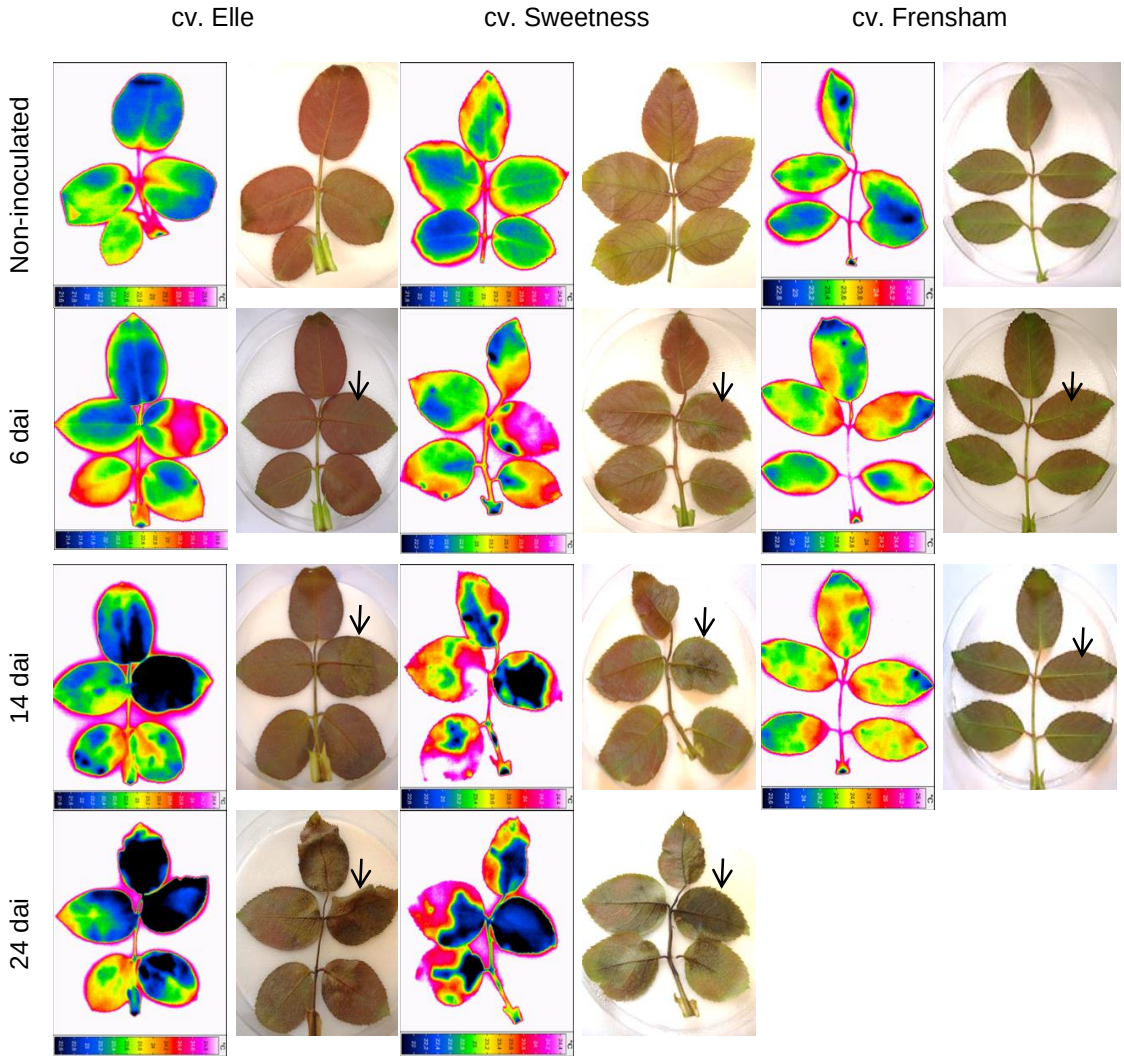

Figure 5.3 Development of *Peronospora sparsa* from localized inoculation on leaflet number 3, indicated by the arrows, in rose cvs. Elle®, Sweetness® and Frensham® visualized by IR thermography in different periods of time. Thermal images (left) and RGB images (right) depict the development of the infection at the site inoculation and the spread of the pathogen within the leaf. Days after inoculation: dai.

the other leaflets of the leaf (Fig. 5.4b). No statistical differences were detected in the leaf temperatures of cv. Frensham® when compared to the non-inoculated ones (Fig. 5.4c).

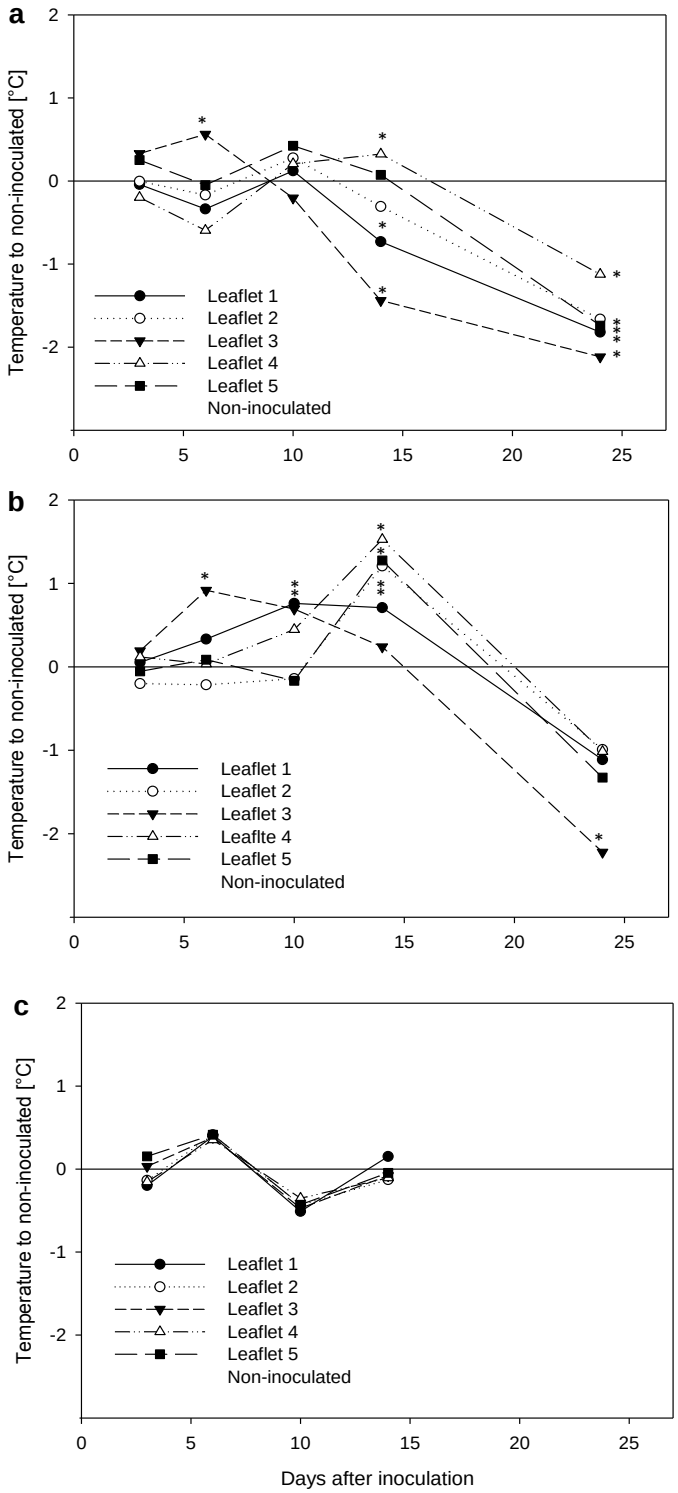

Figure 5.4 Effect of *Peronospora sparsa* infection on leaf temperature of three rose cultivars after localized inoculation on leaflet 3: **a**, cv. Elle®; **b**, cv. Sweetness®; and **c**, cv. Frensham®. Numbering of leaflets: leaflet 1, apical leaflet; 2 and 3: middle leaflets; 4 and 5, distal leaflets. Asterisk indicates value significantly different from non-inoculated leaves (*t*-test, $P \leq 0.05$).

5.4 Discussion

Changes in leaf temperature of infected rose leaves after localized inoculation of the pathogen were detected by IR thermography. Infection of *P. sparsa* in rose leaves was visualized three to four days earlier by thermography than by naked eye. Moreover, the variations in leaf temperature over time due to pathogenesis as visualized in the thermograms were closely related to the development of *P. sparsa* in leaf tissue. An increase of leaf temperature after the inoculation and a subsequent decline in advanced stages of the disease were observed in the susceptible cultivars evaluated. It can be concluded from the results that *P. sparsa* alters rose leaf temperature and the effect of the infection on thermal responses of the leaves is dynamic over time.

Colonization of leaf tissue by intercellular hyphae in early stages of the disease and production of sporangia seem to be the episodes of *P. sparsa* development that coincide with strong thermal changes of leaf surface. In the present study, the increase of leaf temperature at first stages of rose downy mildew infection is in accordance with the response of cucumber leaves to *Pseudoperonospora cubensis* infection in early stages of the disease (Lindenthal et al., 2005; Oerke et al., 2006). Effect on leaf temperature during pathogenesis has been reported in many host-pathogen interactions including *Venturia inaequalis* - apple (Kümmerlen et al., 1999; Oerke et al., 2011), *Cercospora* - sugar beet (Chaerle et al., 2004) and *Erwinia amilovora* - *Nicotiana sylvestris*. Chaerle et al. (2001) observed a cell-death-associated leaf temperature increase in bO transgenic tobacco plants prior to the appearance of localized leaf damage.

The profuse sporulation of *P. sparsa* on the leaf surface and the presence of brown tissue coincided with leaf temperature decreases. These two events occurring simultaneously in rose leaves may affect tissue structure and function. In consequence, during late stages of *P. sparsa* infection, water loss from leaf tissue may determine the cooling effect observed in late stages of the disease as has been reported by many authors. In downy mildew of cucumber and apple scab, a temperature drop in the infected tissue is caused by evaporation of leaf water as a consequence of damage of plant cuticle (Lindenthal et al., 2005; Oerke et al., 2006). Likewise, potato infection by *Phytophthora infestans* induced stomata to open more than normal under different light conditions (Farrel et al., 1969).

Oerke et al. (2011) observed thermographic differences in apple scab severity due to resistance of the leaves and aggressiveness of isolates of the pathogen. In the case of rose downy mildew, thermography confirmed differences among the three evaluated

cultivars in their susceptibility to *P. sparsa* infection. Thus, in the context of thermal sensing of rose cultivars, leaf temperature may be considered as an indicator of the success (or failure) of *P. sparsa* to infect leaf tissue and develop in it. When leaves had been infected, differences in thermal responses could be detected and varied in intensity and duration with the susceptibility of the cultivar. In cv. Frensham® no significant changes in leaf temperature were detected over time and no progress of the pathogen was observed 15 dai or later. In cv. Sweetness® and cv. Elle®, infection of *P. sparsa* was detected by thermography. Though the increase of leaf temperature in early stages of the disease followed by a decrease in leaf temperature occurred in both cultivars, differences between them were observed. The increase in the leaf temperature of the infected leaves as compared to that of non-inoculated ones was higher in cv. Sweetness® than in cv. Elle®. In addition, leaf response visualized as warm areas after *P. sparsa* infection took longer in cv. Sweetness®. Due to a fast spread of the pathogen in cv. Elle®, the inoculated leaflet rapidly displayed a leaf temperature decrease in the surrounding tissue. Cv. Elle® may be considered as a more conductive cultivar for *P. sparsa* infection in contrast to cv. Sweetness®. The obtained results reveal that infrared thermography is a suitable technique to detect *P. sparsa* infection in rose and to study this plant pathogen and its interaction with *Rosa* sp. from different approaches.

In this study, the detection of *P. sparsa* infection before presence of visual signs of the pathogen or changes in leaf tissue was possible using thermal imaging. Results indicated that the use of thermography may be a suitable alternative tool to detect downy mildew infection on rose leaves at early stages, to discriminate rose cultivars for their susceptibility to *P. sparsa* infection and to visualize the spread of the pathogen. However, as the study was conducted using a modified in vivo system, the technique has to be evaluated in plants and under production conditions.

6. THERMOGRAPHIC RESPONSE OF ROSE LEAVES DURING *Peronospora sparsa* PATHOGENESIS IN PLANTA

6.1 Introduction

Rose leaves infected by *Peronospora sparsa* (Berk.) develop purplish red to dark brown irregular spots and may turn chlorotic (Horst, 1983). Lesions are normally angular with well-defined margins follow by the mayor leaf vessels and they may become necrotic in later stages of the infection. Severe leaf drop is typical of the disease (Xu and Pettitt, 2003). Oospore formation has been found in leaves, stems and flowers but it seems to be sporadic (Francis, 1981; Xu and Pettitt, 2004).

The coenocytic mycelium of downy mildews shows indeterminate intercellular growth (Clark and Spencer-Phillips, 2004). Hyphae may vary in shape and size, absorb nutrients all over their surface and fill most of the intercellular space in the host tissue; haustoria penetrate the cells being basically filamentous in almost all species of *Peronospora* (Fraymouth, 1956). According to Fraymouth (1956) this mass of mycelium strongly interferes with the processes of the host plant. Invasive growth of downy mildews is well documented. Intercellular mycelia of *P. sparsa* isolated from rose extensively colonized leaf discs of tummelberry in short time (Breese et al., 1994). In a susceptible genotype of grapevine, *Plasmophara viticola* filled the intercostal areas of the leaves with mycelium three days after the inoculation (Unger et. al., 2007).

Downy mildews are typically confined to the leaf mesophyll or the stem cortex, but some species may be systemic and the mycelium ramifying throughout the host plant (Dick, 2002). For instance, *P. sparsa* (syn. *P. rubi*) systemically infected *Rubus* species (Wallis et al., 1989; Williamson et al., 1995) and *Peronospora viciae* systemically infected *Pisum sativum* in symptomless plants (Taylor et al., 1990). *Peronospora sparsa* may be transmitted as dormant mycelium in cuttings (Francis, 1983; Horst, 1983). The colonization of stem cortex tissue and the presence of *P. sparsa* in crowns and root tissue were confirmed by PCR and microscopical observation (Aegerter et al., 2002).

Sporulation of downy mildews occurs mainly in the dark and under high relative humidity usually on green tissue (Yarwood, 1943; Populer, 1981; Ingram, 1981). In rose, *P. sparsa* sporulates densely on the lower leaf surfaces and sporangia may be produced for long periods of time as long as high relative humidity and low temperature persist (Francis, 1983). Severe damage of the host coincides with sporulation because the pathogen

demands more nutrients from de host cells at this phase of the disease (Yarwood, 1941; Fraymouth, 1956; Clark and Spencer-Phillips, 2004).

Early detection of plant pathogens is relevant to improve disease control and to reduce yield losses (Stoll et al., 2008). Due to its sensitivity, infrared (IR) thermography is suitable for the detection of diseases that induce changes in transpiration and water status (Oerke and Steiner, 2010). Leaf temperature depends on many factors such as the effect of pathogens on stomatal conductivity, the damage of plant cuticle, the degradation of cells and the transport and accumulation of plant defense compounds, among others (Chaerle et al., 1999; Chaerle et al., 2004; Oerke et al., 2006). Effect on leaf temperature following plant pathogen infection has been reported in diverse host-pathogen interactions, e. g. *Fusarium oxysporum* f. sp. *cucumerinum* - cucumber (Wang et al., 2012), *Venturia inaequalis* - apple (Kümmerlen et al., 1999) and *Cercospora beticola* - sugar beet (Chaerle et al., 2004; Oerke et al., 2011). The development of pathogens in plant tissue indirectly affects leaf temperature, thus histological observation during pathogenesis may reveal alterations of plant tissue that can be sensed by thermal imaging. This is of particular interest in perennial plants hosting obligate parasites that may spread systemically and produce latent infections.

The potential of IR thermography for the study of plant diseases has been well reported (Chaerle et al., 2004; Lindenthal et al., 2005; Oerke et al., 2006; Oerke et al., 2011). Moreover, results obtained in other downy mildews using IR thermography have contributed interestingly to the knowledge of this devastating group of pathogens. Hence, the objectives of this study were (i) to evaluate the capability of IR thermography for presymptomatic detection of rose downy mildew, (ii) to characterize thermographically the symptoms of the disease in leaves, (iii) to monitor the spread of *P. sparsa* from localized inoculation, (iv) to identify leaf thermal response and structures of *P. sparsa* in leaf tissue and (v) to investigate thermal changes of leaves associated with sporulation of *P. sparsa.*

6.2 Materials and methods

6.2.1 Plant material

Plants of rose cv. Elle® Var. Meibderos (Meilland International SA, Le Luc-en-Provence, France), Hybrid tea rose planted in 10 L pots in a 3:1 mixture of soil and Profi-substrat Typ ED73 (Gebrüder Patzer GmbH & Co Sinntal-Jossa, Germany) were kept in glasshouse under 16 h photoperiod and average temperatures of 23°C/18°C (day/night). The plants

were watered with tap water and fertilized periodically according to requirements. Main stems of plants were cut to promote the development of young shoots and leaves for the inoculation due to their susceptibility to *P. sparsa* infection (Horst, 1983; Aegerter et al., 2002). Inoculation was carried out when most of the leaves were completely expanded but still juvenile.

6.2.2 Inoculum and inoculation

A suspension of sporangia was used as source of inoculum. The isolate Ps 3 of *P. sparsa* used was collected in a Colombian commercial rose crop during epidemics of the disease. Sporangia were produced on the leaflets in a growth chamber under 18°C/16°C (day/night) and 16 h photoperiod. Seven-day sporangia were collected in distilled sterile water using a soft brush. Then, the concentration was adjusted to 5.0×10^4 sporangia per ml using a Fuchs-Rosental hemocytometer. Leaves were inoculated on the abaxial side using a soft brush to localize the inoculum on a stripe of 0.5 cm in the middle of apical leaflets. Control leaves were mock inoculated with distilled sterile water in the same plants together with inoculated leaves. The plants were kept for 48 hours at 10°C under 100% RH in a growth chamber (Viessmann®, Saale, Germany) in the darkness to guarantee optimal conditions for pathogen infection. Then, the plants were transferred to 22°C/18°C day/night and 60±10% RH conditions with additional light source (Philips Son-T Agro-HPS 400W, Amsterdam, The Netherlands) to provide a 16 hour photoperiod. Water was supplied regularly to guarantee the suitable development of plants. Half of the plants were kept daily at ≥90% RH (HRH) during nighttime to promote sporulation of the pathogen; the rest of the plants were kept overnight under 60% RH (LRH).

In order to track the infection of the pathogen histologically, leaf discs of 20 mm of diameter of rose cv. Elle® were inoculated with the suspension of sporangia and placed into Petri dishes with wet filter paper (100% RH) and kept in growth chamber under the conditions mentioned above.

6.2.3 Disease assessment

Three days after inoculation (dai) and for 17 days, daily observations of inoculated and control plants were carried out to monitor the appearance of symptoms and their progress over time. The description of the lesions was done immediately before thermal

assessment. RBG images were taken daily to illustrate symptoms observed and their progress in time.

6.2.4 Thermographic measurements

Thermal images were obtained using an infrared Stirling-cooled scanning camera VARIOSCAN 3201 ST (Jenoptic Laser, Jena, Germany) with a spectral sensitivity from 8 to 12 µm and 1.5 m radians of geometric resolution (240 × 360 pixels focal plane array and a 30° × 20° field of view lens with a minimum focal distance of approximately 20 cm). Thermal resolution was 0.03 K and accuracy of absolute temperature measurement was <±2 K. As the disease induces leaf distortion and the angle between the leaf and the stem decreases as the infection progresses, control and inoculated leaves were hold horizontally extended during the recording of IR images using a frame with a 6 x 11 square grid of (1.7 cm^2 each) made of the synthetic polymer nylon. In agreement with preliminary evaluations, the system did not physically disrupt or alter the thermal status of the leaves. Moreover, it permitted air circulation around the leaf. The height of the system was modified at every measurement according to the position of leaves in the shoot. Thermal images of leaves were recorded at a distance of approximately 30 cm, without moving.

6.2.5 Analysis of thermograms

The thermographic images were analyzed using the software IRBIS® Plus version 2.2 (Infratec, Dresden, Germany). The outline of inoculated and control leaflets was reframed using the polygon tool of the IRBIS® program to obtain the average temperature of inoculated and control leaflets for each thermogram. The image analysis was focused on the apical and middle leaflets (L2 and L3). Thermal lesions detected in the thermograms were analyzed in detail by placing a series of five independent concentric 2.0 mm width rings in the center of the lesion. The profiles and linear transects of the leaves were analyzed in order to describe the heterogeneity of leaf temperature. Temperature differences (ΔT) between the mean temperature of the inoculated leaflets and the controls were calculated in order to visualize the effect of the infection on leaf temperature over time. Moreover, the maximum temperature difference (MTD) provided by the IRBIS® program was analyzed for selected areas in the thermogram of the leaves (Lindenthal et al., 2005; Oerke et al., 2006; Oerke et al., 2011; Wang et al., 2012). Environmental

temperature at the moment of image recording was measured in the surroundings of the leaves in each thermogram.

6.2.6 Microscopy

Infection of *P. sparsa* in rose leaves was monitored in samples taken from inoculated leaf discs every 24 hours over time of the study. The tissue was cleared in chloral hydrate (AppliChem) (2.5 g ml^{-1} water) (Bruzzese and Hasan, 1983; Jende, 2001) for seven days at room temperature (20 ± 3°C). Then, the tissue was stained in 0.01% acid fuchsin for 48 hours (Fluka) (Gerlach, 1977). Once stained and mounted, the material was observed using a photomicroscope (Leitz DMRB; Leica, Wetzlar, Germany) with the software Diskus 4.2 (Hilgers, Königswinter, Germany) and equipped with Nomarski-interference-contrast to evaluate cleared leaf tissue.

6.2.7 Statistical analysis

Data were statistically analyzed using the Superior Performing Software System SPSS 21.0 (SPSS Inc., Chicago, IL, USA) to conduct independent-sample *t*-tests (two-sample *t*-test) analyses for means comparison and standard analysis of variance at a significance level of 95% (*t*-test, $P \leq 0.05$) and (Tukey test, $P \leq 0.05$) respectively. The experiments were repeated at least 2 times.

6.3 Results

6.3.1 Development of symptoms and thermographic visualization

Subtle distortion of the leaf lamina and loss of brightness at the site of inoculation were the first symptoms observed 6 dai. Slight brown spots and leaf distortion became more evident through direct inspection 7 dai. The lesions coincided with typical symptoms reported for the disease 8 dai. The first sporulation of *P. sparsa* was observed 8 dai only on the abaxial side of HRH leaves. Angular dark brown spots were observed 9 dai on HRH leaves and 10 dai on LRH leaves; this type of lesion was more frequent under HRH than under LRH (89% and 63% respectively). On neighboring leaflets symptoms were observed 18 dai. No significant differences in days to the presence of slight and typical disease symptoms on apical and neighboring leaflets were detected between LRH and HRH leaves (Fig. 6.1).

The thermal pattern of the symptoms was diverse. Areas warmer than healthy tissue were associated with infection of *P. sparsa* without visual alterations and early symptoms such as slight leaf distortion, dull areas or a subtle change of tissue color. Cold spots were observed in early stages associated with soft brown lesions (Fig. 6.2). As the symptoms progressed, warm areas expanded, the leaf lamina became distorted and purple areas were visible. In strongly diseased leaflets or in advanced disease stages the presence of brown lesions was related to medium temperatures. In brown lesions the temperature decreased, but the overall temperature of leaflets was still significantly higher than that of healthy tissue. Temperatures remained high in the surroundings of the colonized area. In most of the cases the area showing thermal alterations was larger than the affected area as detected by naked eye (Fig. 6.2).

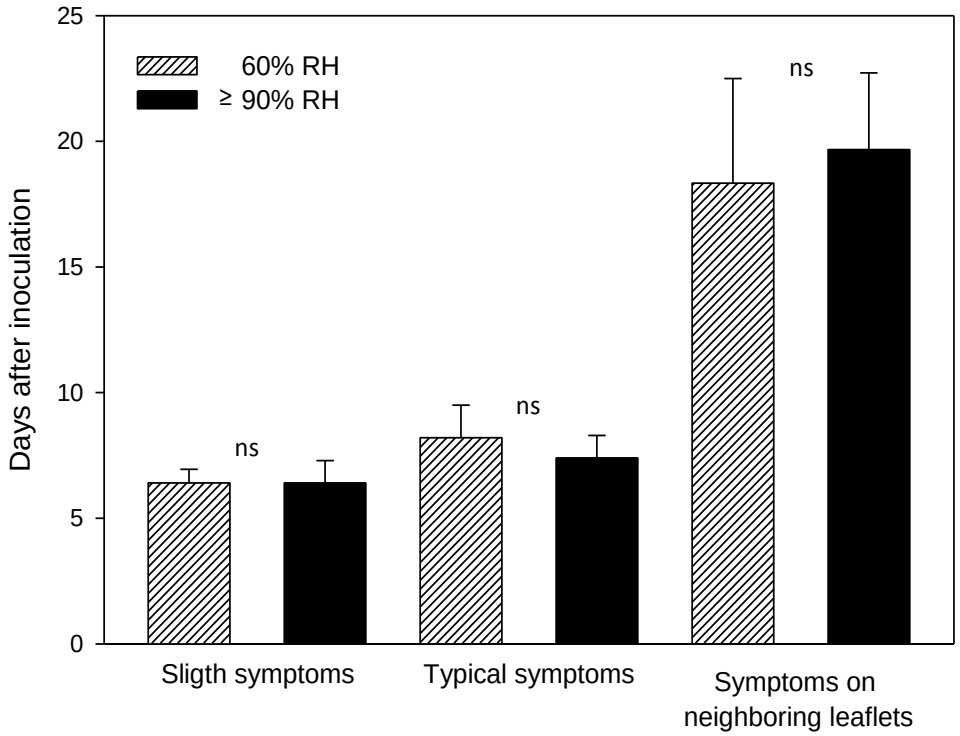

Figure 6.1 Development of downy mildew symptoms on rose cv. Elle® after localized inoculation of the pathogen and maintained under different nighttime conditions of relative humidity RH. Low relative humidity: 60% RH; high relative humidity: ≥90% RH. Error bars represent the standard deviation; ns, indicates values no significantly different (*t*-test, $P \leq 0.05$).

6.3.2 Effects of infection on leaf temperature

Leaves inoculated with *P. sparsa* showed an increase in leaf temperature at the sites of infection. The presence of the pathogen in leaf tissue was visualized in thermograms as

warmer areas delimited and distinguishable from healthy low temperature areas. Temperature increased significantly 6 dai and coincided with the appearance of the first disease symptoms. After this time, maximum temperature increase was significantly high and remained stable until the end of the evaluations under both nighttime relative humidity conditions. Nevertheless, in HRH leaves the maximum temperature decreased since 10 dai and thereafter, while LRH leaves showed only a slight decrease 13 dai. Under both RH conditions leaf temperature underwent a second increase at the last stage of the disease.

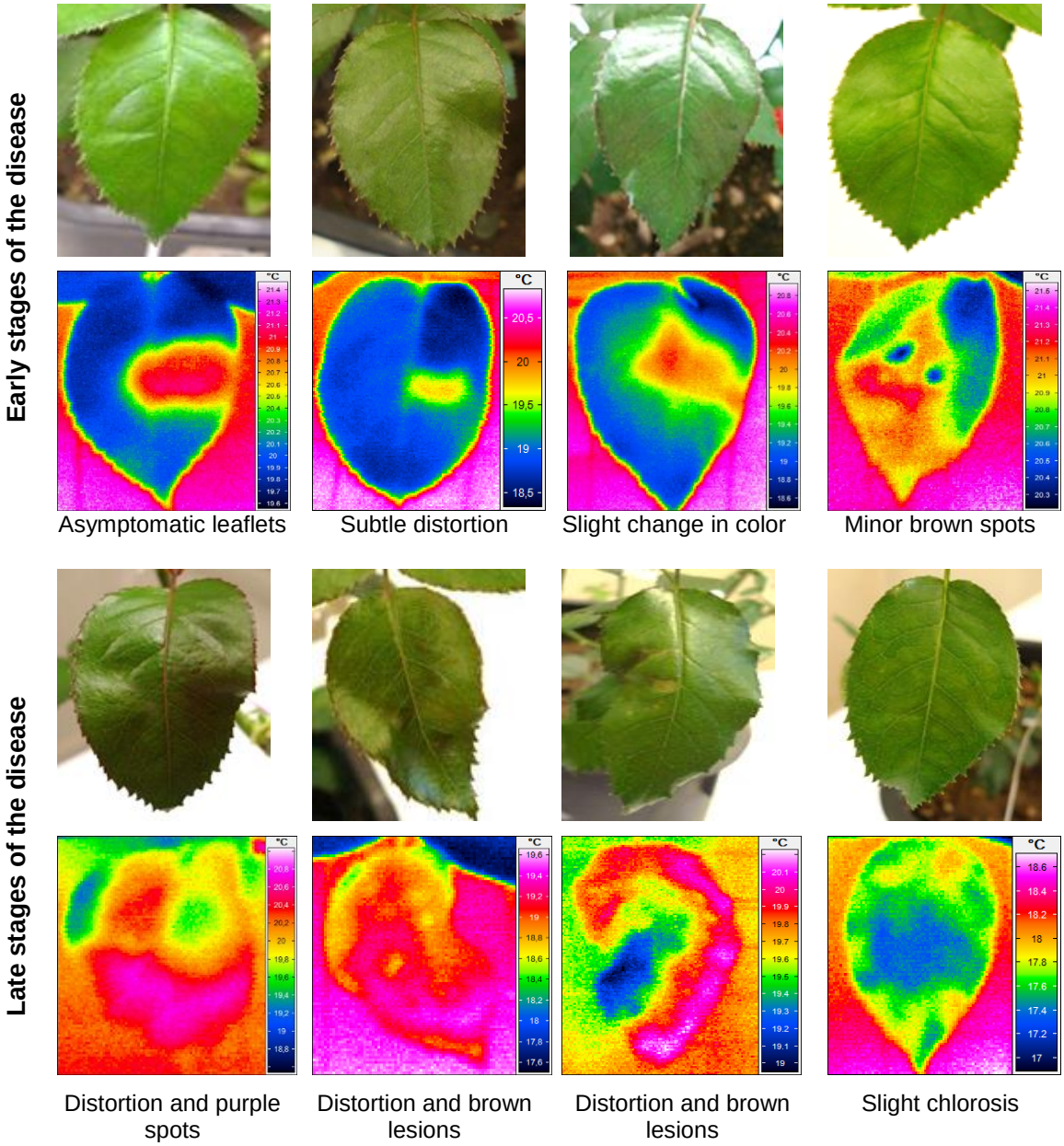

Figure 6.2 Effect of rose leaf cv. Elle® colonization by *Peronospora sparsa* on symptoms development in early and late stages of the disease, and its influence on leaf temperature. RGB (upper) and thermal (lower) images correspond to the same leaflet.

During most of the experiment, in HRH leaves the average temperature increase was significant when compared to that of control leaves, while in LRH leaves the increase was significant only 8 dai, coinciding with the presence of typical disease symptoms (Fig. 6.3).

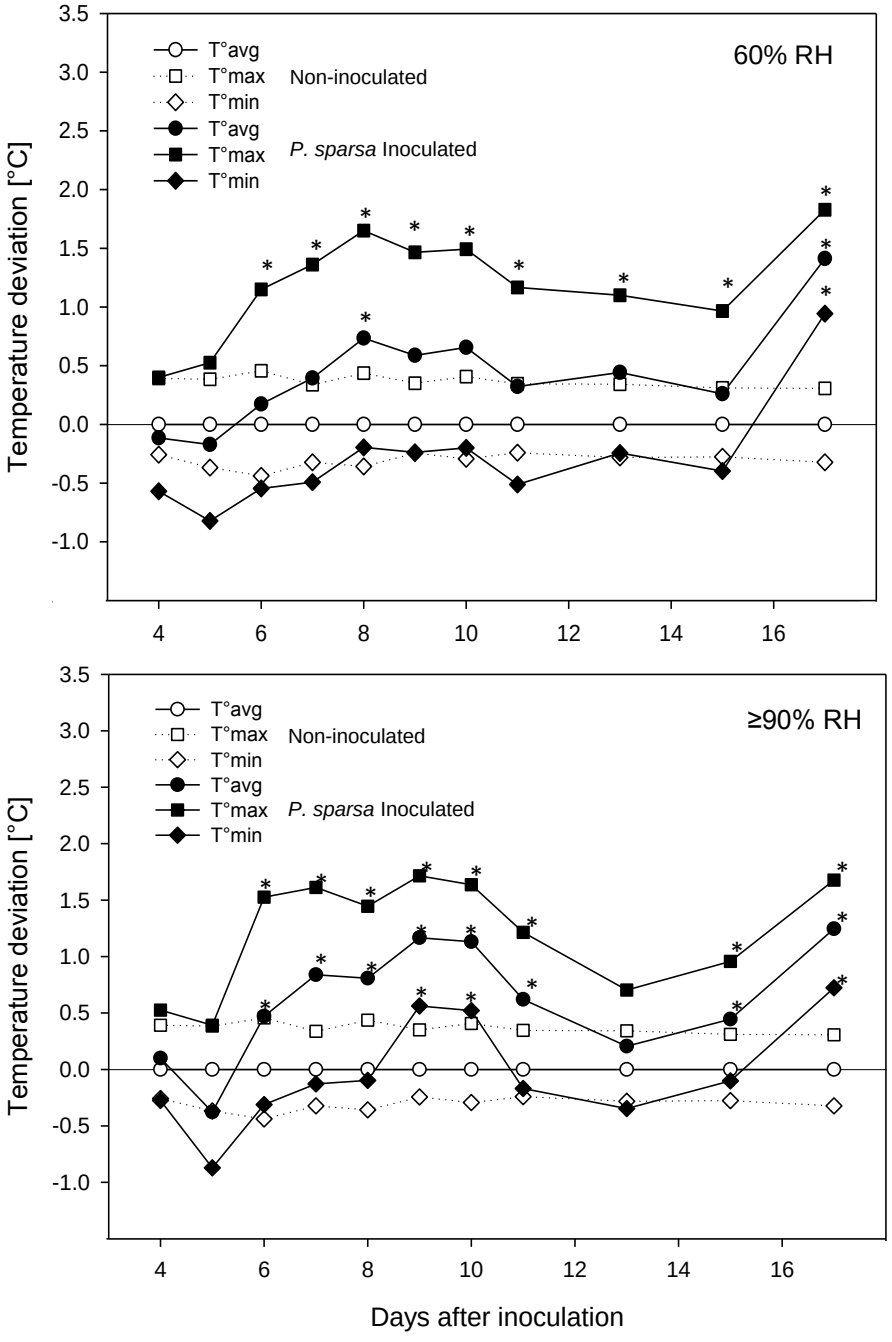

Figure 6.3 Effect of *Peronospora sparsa* infection on average, maximum and minimum temperature of apical leaflets of rose cv. Elle® after localized inoculation and different relative humidity conditions: **a**, plants maintained under 60% RH at night; **b**, plants maintained under ≥90% RH at night. Values represent differences to temperature values of control leaves. T°avg, average temperature; T°max, maximum temperature; T°min, minimum temperature. Asterisk represents value significantly different from non-inoculated leaves (n = 5*; t*-test, $P \leq 0.05$).

A decrease in leaf temperature was noticed with the presence of brown tissue and the sporulation of the pathogen on densely infected tissue in later stages of the disease. In HRH leaves warm areas expanded fast and turned to medium temperature areas 11 dai. The strong increase in leaf temperature observed 17 dai coincided with the presence of desiccate infected tissue in both conditions

Seven and 8 dai, visual assessment of thermograms of the infected tissues demonstrated significant differences between leaf areas with thermal changes when compared to healthy tissue. HRH leaves were more severely affected and displayed stronger thermal responses than LHR leaves, especially in early stages of the disease (Fig. 6.4).

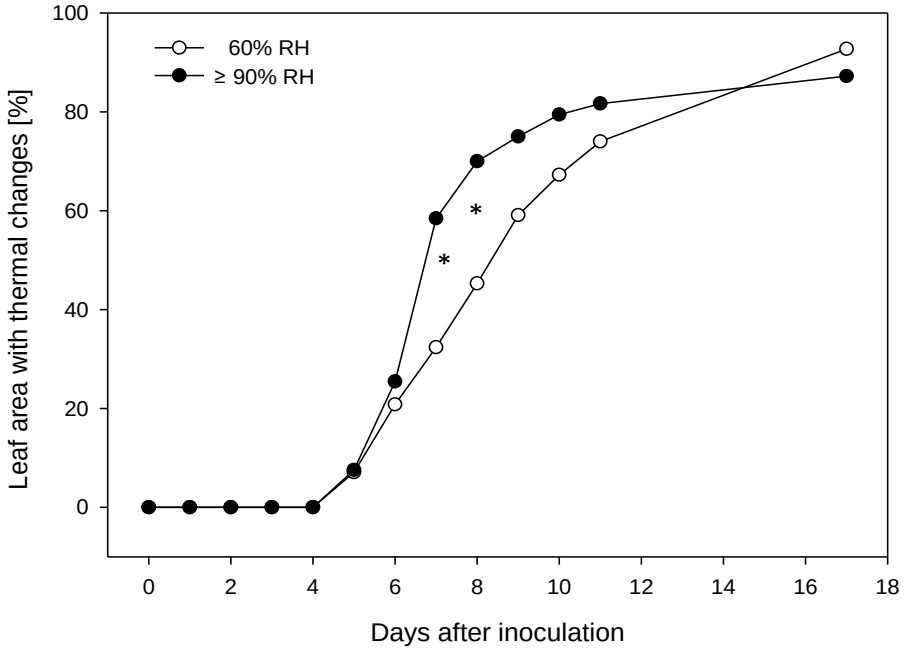

Figure 6.4 Effect of *Peronospora sparsa* infection on thermal changes visualized in thermograms of rose leaves cv. Elle® after localized inoculation and incubated under nighttime relative humidity suitable (≥90% RH) and non-suitable (60% RH) for sporulation. Asterisk represents values significantly different (*t*-test, $P \leq 0.05$). Relative humidity: RH.

6.3.3 Effect of pathogenesis on maximum temperature difference (MTD)

Maximum temperature difference increased significantly 4 dai under both conditions. However, the strongest effect was observed in LRH leaves. The MTD of inoculated leaves increased progressively until reaching maximum values 6 and 7 dai when the first disease symptoms appeared. LRH and HRH leaves were found to be significantly different 9 and 10 dai, when the MTD of LRH leaves was significantly higher than that of HRH. In both

conditions of nighttime humidity, MTD increased in the first stages of the disease and decreased in later stages. This effect began 8 dai for HRH leaves and 11 dai for LRH leaves (Fig. 6.5). In HRH leaves warm areas expanded from the site of infection rapidly and changed to medium temperature regions due to the presence of brown lesions at the site of initial infection and sporulation of *P. sparsa*. These more homogeneous temperature patterns were reflected in decreased MTDs. Since *P. sparsa* just spread without sporulation in LRH leaves, the contrast between healthy and infected tissue lasted longer and resulted in higher MTD values over time.

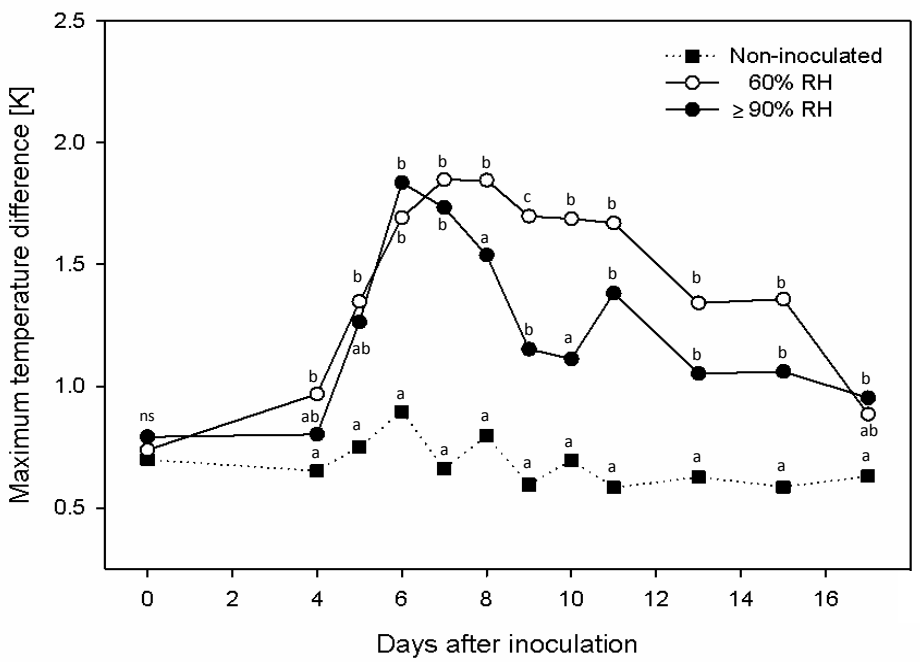

Figure 6.5 Influence of *Peronospora sparsa* infection on maximum temperature difference of leaves of rose cv. Elle® after localized inoculation and incubated under different nighttime relative humidity conditions: 60% and ≥90% RH. Values followed by the same letter are not significantly different (Tukey test, $P \leq 0.05$). Relative humidity: RH.

6.3.4 Detection of infection and spread of Peronospora sparsa

IR thermography detected downy mildew infections in rose leaves one day before the presence of first symptoms and three days before typical disease symptoms occurred. No significant differences were detected between LRH and HRH leaves in the time to manifest visible symptoms of the disease. The spread of the pathogen within inoculated leaflets and to other leaflets could be observed. Symptoms on neighboring leaflets (L2 and/or L3) were observed 17 dai in 63.6% and in 55.6% of the inoculated LRH and HRH leaves, respectively. Detection of *P. sparsa* in neighboring leaflets took place 4 to 6 days before visual symptoms occurred (Fig. 6.6). The MTD of neighboring leaflets remained stable until 10 dai when MTD increased slightly under both RH conditions, the values

being significantly different from those of non-inoculated leaves as early as 10 and 11 dai, when HRH leaves registered elevated values of this parameter (Fig. 6.7). Thermography showed how the colonization of neighboring leaflets by *P. sparsa* initially revealed some differences between them, but they all became densely colonized in the following days.

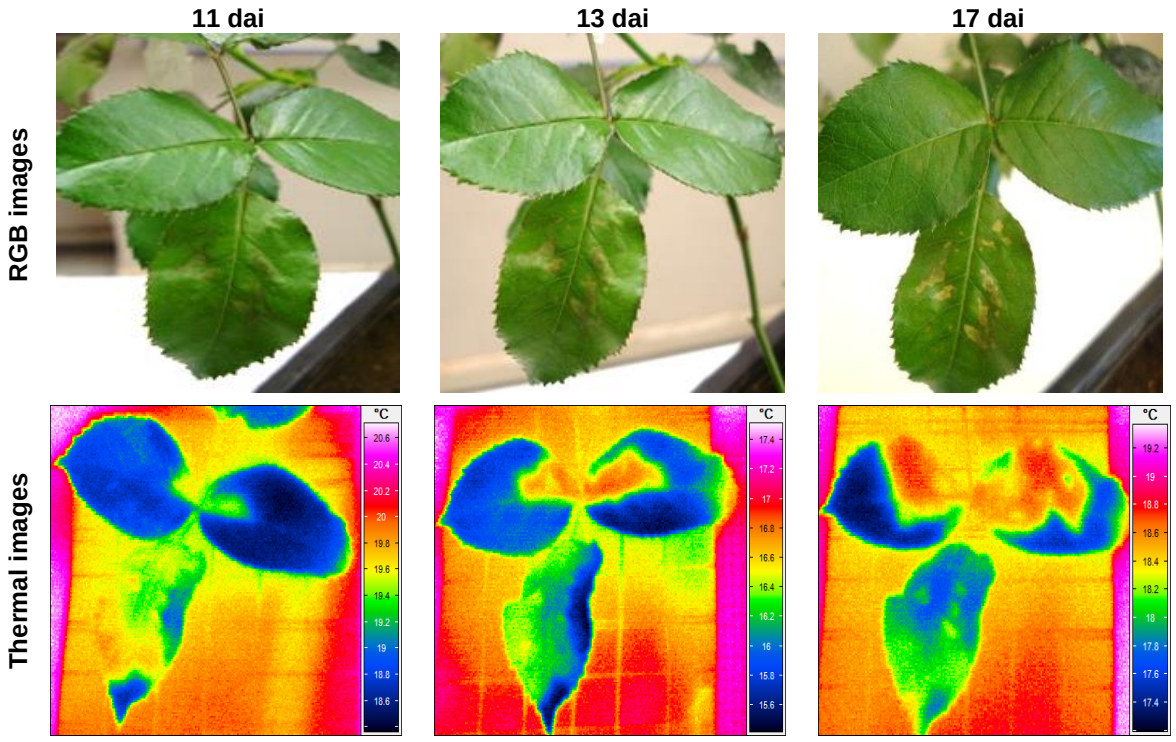

Figure 6.6 Spread of *Peronospora sparsa* in rose cv. Elle® leaves from localized inoculations on apical leaflets to neighboring leaflets visualized by IR thermography 11, 13 and 17 dai. RGB and thermal images correspond to the same leaf. Days after inoculation: dai.

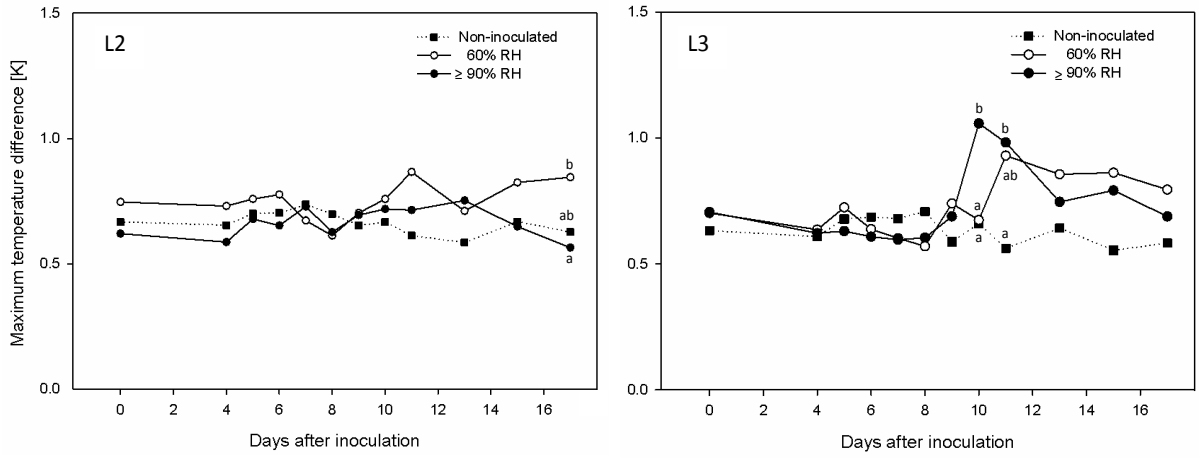

Figure 6.7 Influence of *Peronospora sparsa* infection on maximum temperature difference of neighboring leaflet L2 and L3 of rose cv. Elle® after localized inoculation on apical leaflets. Inoculated leaves under 60% RH or under ≥90% RH. Values followed by the same letter are not significantly different (Tukey test, $P \leq 0.05$).

6.3.5 Spatial distribution and dynamics of leaf temperature associated with downy mildew development

The frequency of low temperatures was high for healthy leaf tissue and showed a Gaussian distribution. For infected leaves the frequency of pixels of the image with high temperature increased progressively and resulted in a bimodal distribution 10 dai (Fig. 6.8). The presence of brown lesions or sporulation of *P. sparsa* was associated with the occurrence of medium temperatures at the initial site of infection (Fig. 6.8a, b). Complete colonization of the leaf by *P. sparsa* resulted in a rather high, uniform temperature throughout the leaf. In HRH leaves, the proportion of tissue with high temperature increased faster than in LRH leaves (Fig. 6.8a, b). Linear profiles along the middle vein and crossing the site of infection showed a sharp increase of temperature as the pathogen colonized tissue from the middle to the apical and distal ends of leaflets. In later stages the difference in temperature along the transects became smaller. Linear transects demonstrated that the spread of *P. sparsa* was bidirectional, but still showing some preferences toward petioles, which as colonized by *P .sparsa,* are used for the spread to neighboring leaflets (Fig. 6.8).

6.3.6 Development of the pathogen and thermal dynamics at the inoculation site

Changes in leaf temperature were related to the development of *P. sparsa.* Initially warm areas coincided with the presence of hyphae and haustoria that expanded intercellularly to neighboring cells and proximal tissue layers after the infection. Then, the inoculated area was densely colonized. The intercellular growth of the pathogen was associated with the heterogeneous temperature pattern (Fig. 6.9). In early disease stages a high dissimilarity between warm infected tissue and cold healthy tissue was reflected in increases of MTD. When the whole leaf had been colonized, uniform high temperatures resulted in medium MTD values (Fig. 6.5). The fast expansion of the initially warm area demonstrated the ability of *P. sparsa* to spread rapidly and aggressively in rose leaves. Strongly infected tissues showed medium temperatures, with dense occurrence of hyphae in substomatal cavities, sporulation through stomata and presence of oospores in the leaves (Fig. 6.9). In LRH leaves, the heterogeneity of leaf temperatures remained for longer time because the mycelia of *P. sparsa* mainly spread in leaf tissue and sporulation was inhibited. Dense intercellular hyphae, sporulation and oospores were associated with a slight decrease of leaf temperature of brown leaf tissue (Fig. 6.9).

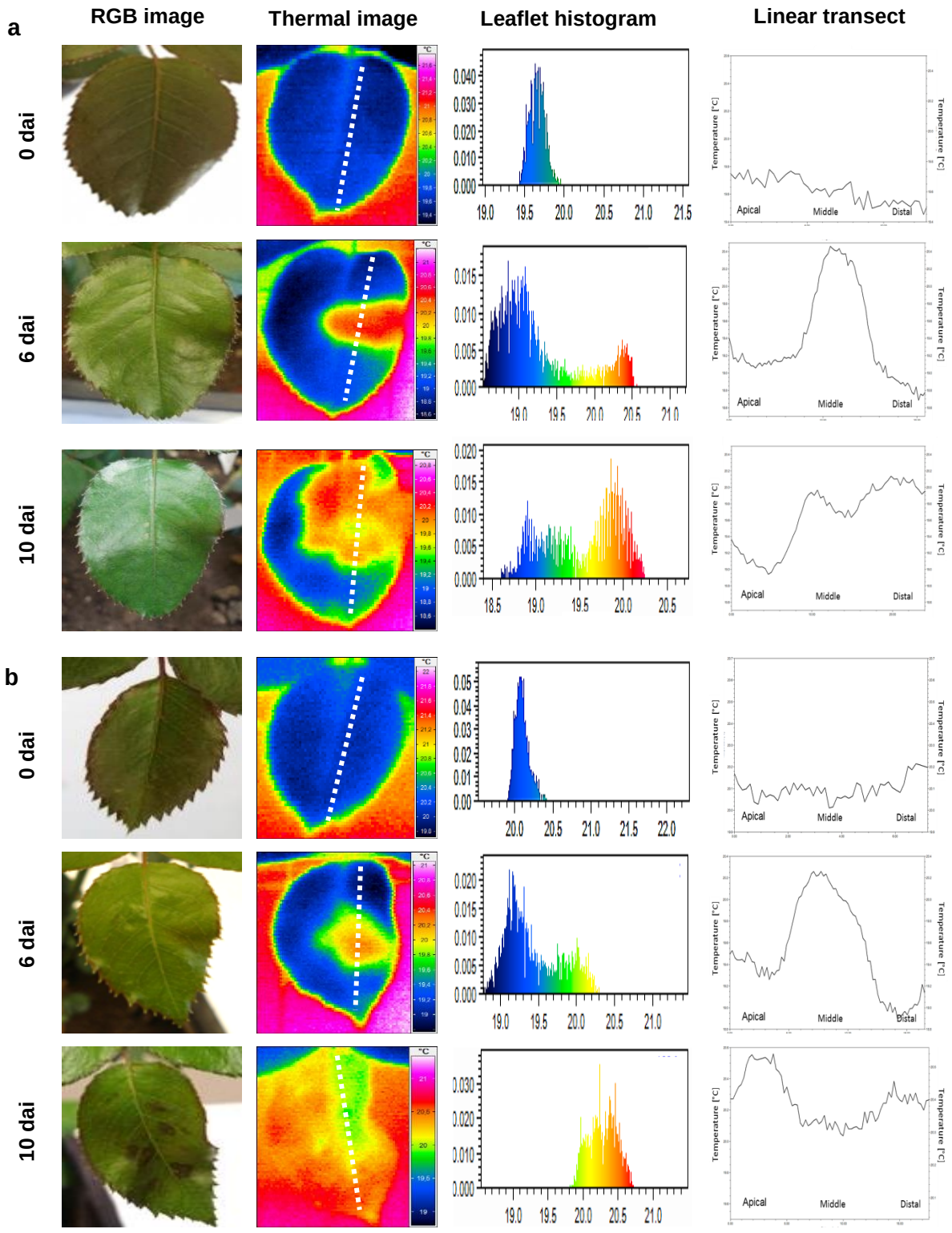

Figure 6.8 Influence of *Peronospora sparsa* on spatial distribution of temperature changes of rose leaves cv. Elle® after localized inoculations and two nighttime relative humidity conditions HR: **a**, 60% RH; **b**, ≥90% RH. Leaflet histogram: frequency of temperature of leaflets; linear transect: thermal changes along the dotted line in thermal images.

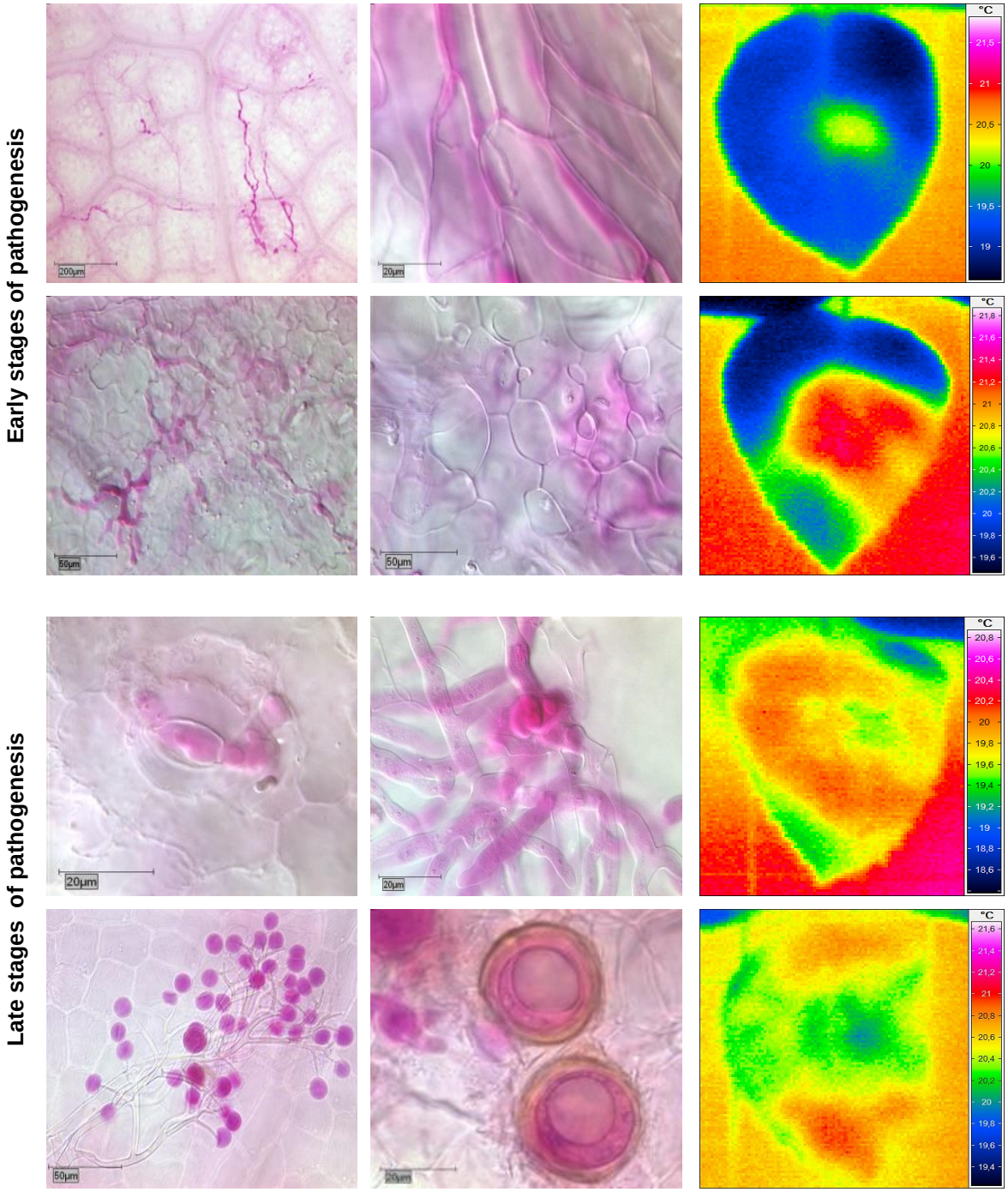

Figure 6.9 Development of *Peronospora sparsa* in rose cv. Elle® and thermal responses of the leaf tissue to the infection visualized by IR thermography. Early stages of pathogenesis: presence of intercellular hyphae spreading in leaf tissue and presence of haustoria; late stages of pathogenesis: dense mycelia, haustoria in all tissue layers, sporangia produced through leaf stomata (≥90% RH) and oospores in brown tissue.

The temperature of the five independent concentric areas located close to the core of the infection was higher than that of healthy tissue in the same leaf (Fig. 6.10). The results of the close-up thermographic view of *P. sparsa* spreading in a delimited tissue area of 12

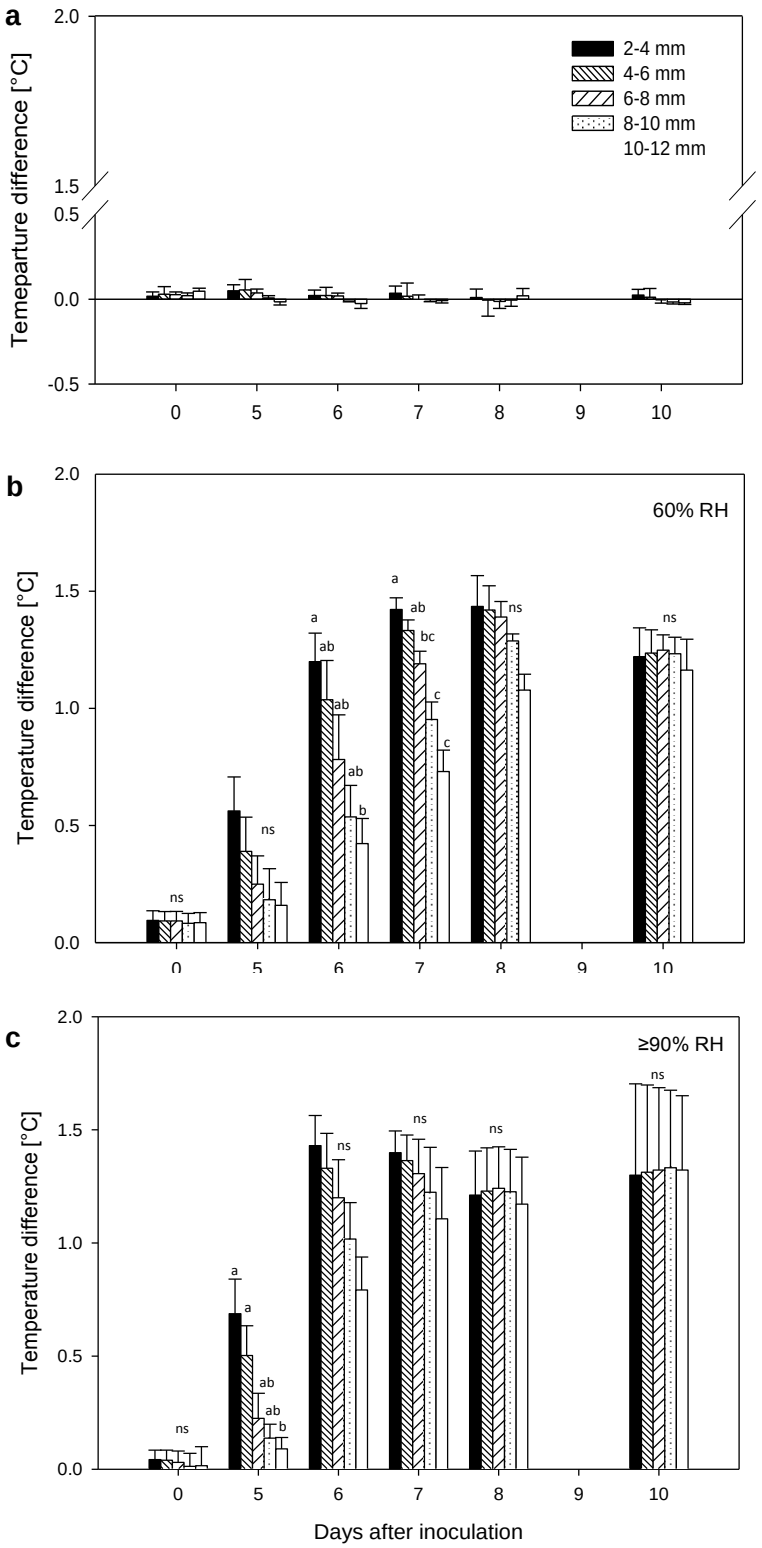

Figure 6.10 Influence of *Peronospora sparsa* colonization on rose leaf temperature difference to healthy tissue at the inoculation site, discriminated into five independent concentric leaf areas of plants incubated under two conditions of nighttime relative humidity RH: **a**, non-inoculated; **b**, inoculated leaves under 60% RH; **c**, inoculated leaves under ≥90% RH. Values followed by the same letter are not significantly different (Tukey test, $P \leq 0.05$). Error bars represent the standard error.

mm in HRH and LRH leaves showed how 5 dai, the pathogen might have colonized an area of approximately 4 mm, which exceeds 10 mm one day later.

Leaf temperature was high close to the center of the lesion and low in the external areas not different from healthy tissue. Within a few days the temperature of neighboring areas increased as *P. sparsa* spread into this tissue. Close to the primary site of infection in HRH leaves, the temperature difference was 0.7°C 5 dai and it increased to 1.4°C 6 dai. In turn, LRH leaves reached 0.6°C 5 dai and 1.4°C 7 dai. Significant differences between areas were detected 6 and 7 dai in LRH leaves and 5 dai in HRH leaves. These results showed how the rapid radial progress of *P. sparsa* infection in rose leaf tissue was faster for HRH than for LRH leaves. The slight temperature decrease observed 8 dai in HRH and 10 dai in LRH coincided with the presence of brown tissue or sporulating areas along the evaluated regions.

6.4 Discussion

IR thermography was suitable for presymptomatic detection of rose downy mildew. Presence of *P. sparsa* in leaf tissue was detected one or two days before early disease symptoms. Though symptoms in leaves were diverse, particular temperature responses associated with symptoms could be detected. Minor and major changes in leaf tissue were detected by thermal imaging. Temperature increases were visualized in infected asymptomatic and diseased leaflets with subtle alterations like dull tissue, changes in color or slight leaf distortion. Increased leaf temperature was also detected in desiccated areas or leaflets at later stages. Medium temperature regions in thermograms coincided with tissue areas showing brown angular lesion. Densely colonized leaflets with brown lesions or sporulating tissue were also visualized as areas with slightly decreased temperature. These results showed the sensitivity of thermal imaging to subtle changes in leaf tissue.

Detection of other downy mildews by thermography before visible symptoms has been reported in cucumber infected by *Pseudoperonospora cubensis* (Lindenthal et al., 2005; Oerke et al., 2006) and grapevine infected by *Plasmopara viticola* (Stoll et al., 2008a). In cucumber and grapevine, as well as in rose, infection increased leaf temperature of the host plants before disease symptoms were detected. Nevertheless, there are differences in the thermal responses of leaf tissue over time. Cucumber leaves infected by *P. cubensis* developed water soaked flecks in early stages of the disease, which resulted in a strong decrease of leaf temperature, which increased with the presence of necrotic

tissue (Lindenthal et al., 2005; Oerke et al., 2006). In *P. sparsa* - *Rosa* sp., the infection significantly increased leaf temperature during pathogenesis, although the increase was lower when brown tissue was observed. Although damaged and desiccated tissue has been observed in *P. cubensis* and *P. sparsa* pathogenesis, these events took place at different times. Both pathogens being obligate biotrophs, differences in pathogenesis and thermal effects would be due to the host plant, the biology of the pathogen or the relation between the pathogen and the plant tissue.

Thermal leaf patterns associated with *P. sparsa* infections were dynamic in time and space and were closely related to the development of the pathogen. *P. sparsa* colonized leaf tissue by intercellular hyphae penetrating rose cells with filiform haustoria. The presence of these structures was associated with increased leaf temperature in the first phases of the primary infection and during colonization of new leaf tissue in neighboring and more distant areas of the leaf. Densely colonized tissue, sporulation and oospore formation, together with tissue damage, resulted in a decline of the high temperature values observed at the beginning of the process. In final stages of the disease, desiccated tissue caused an increase of temperature again.

Many factors may induce changes in leaf temperature after infection by plant pathogens (Chaerle et al., 1999; Oerke et al., 2006; Oerke and Steiner, 2010). For *P. cubensis* in cucumber, Lindenthal et al. (2005) related the cooling effect observed in thermograms to an uncontrollable water loss resulting from altered membrane integrity. In grapevine, *P. viticola* caused significant water losses due to stomatal deregulation in early disease stages (Allègre et al., 2007). In rose downy mildew, a similar effect might occur related to tissue damage and decreases of leaf temperature. The results in rose indicate that the process in infected leaf areas, visualized as a leaf temperature increase followed by a subsequent decrease, may continue in new leaf areas as the pathogen colonizes healthy tissue or new infections take place. Variable leaf temperature patterns have also been reported in different plant-pathogen studies using thermography (Lindenthal et al., 2005; Chaerle et al., 2004).

In rose downy mildew MTD increased in infected leaves 4 dai, two days before early symptoms, thus appearing as a suitable factor to discriminate healthy from infected areas even in later stages of the disease. MTD in cucumber downy mildew has been correlated with disease severity (Oerke et al., 2006). In grapevine infected by *P. viticola*, MTD of inoculated leaves was higher than that of controls earlier than visual symptoms appeared (Stoll et al., 2008). As suggested by Oerke and Steiner (2010), MTD is a sensitive parameter for early detection of plant pathogens. MTD was an indicated parameter for the

thermographic study of *Fusarium oxysporum* f. sp. *cucumerinum*, a soil-borne pathogen of cucumber (Wang et al., 2012). In addition, in the current study, MTD values of infected leaves showed differences between RH conditions through their effects on *P. sparsa* development in leaf tissue. This suggests the significance of MTD not only as a parameter to differentiate healthy and diseased tissue but also to establish differences in pathogenesis due to diverse factors.

The spread of *P. sparsa* from localized sites of infection in leaf tissue was confirmed by thermal imaging. Linear transects of infected leaves depicted the bidirectional spread of *P. sparsa* in leaflets, in some cases with preferences toward the leaf petiole. The spread of *P. sparsa* in the plants in terms of colonization of new leaf tissue and infection of distant parts of the leaf was visualized by thermal imaging. Populer (1981) defined the occurrence of systemic infection of downy mildews when colonization continues after the first symptoms appear. IR thermography was suitable to confirm systemic infection by *P. sparsa* in rose. Detection of *P. sparsa* infection in asymptomatic tissue is possible by IR thermography. Thus, measuring changes in leaf temperature becomes an alternative to track the pathogen in leaf tissue. Since latent infections play an important role in timely detection and management of the disease (Aegerter et al., 2002), these results may help to improve the detection of the disease at initial stages in rose crops.

The incubation periods of downy mildews caused by *Bremia lactucca* and *P. viticola* have been reported to be shorter at high relative humidity than at low relative humidity. Said shorter periods were correlated to faster mycelial growth in leaf tissue (Populer, 1981). Though early and typical disease symptoms appeared in HRH leaves faster than in LRH leaves, the differences were not significant but more important contrasts were observed during later stages of the disease. The relative humidity treatments affected the production of sporangia and influenced the development of the disease, as well as the thermal response of the leaves. In HRH leaves, *P. sparsa* spread faster from inoculated areas and more severe symptoms like presence of brown lesions were produced faster than in LRH leaves. Higher temperature increases in early stages and earlier MTD decreases were the main thermal changes in HRH leaves. These responses coincided with the sporulation of *P. sparsa* on leaf tissue, which may have induced thermal changes in leaf surfaces faster than in non-sporulating leaves. Interestingly, IR thermography detected differences between RH condition and its effect on downy mildew development. Populer (1981) pointed out that downy mildews are able to sporulate repeatedly for several successive nights on the same lesion. In addition, Yarwood (1941) mentioned that host injury in onions infected by *P. destuctor* may be due to the sporulation process.

Sporulation on rose leaflets increased tissue damage over time and influenced thermal responses.

Localized inoculation resulted in low inoculum pressure and initially limited infected tissue areas. Under these conditions, IR thermography detected infection before any disease symptoms were visible. The sensitivity of the technique allowed the characterization of rose leaf thermal responses associated with symptoms of the disease and particular stages of pathogenesis over time. These results clearly show the potential of IR to study the *P. sparsa* - *Rose* sp. interaction and the possible use of thermal imaging as a tool to track downy mildew infections in whole plants.

7. VISUALIZATION OF THERMAL RESPONSES OF ROSE PLANTS TO DOWNY MILDEW INFECTIONS

7.1 Introduction

Downy mildew caused by *Peronospora sparsa* may affect all types of roses including cut flowers, garden roses, potted miniature roses and roses used as ground covers (Chase, 2013). Symptoms caused by *Peronospora sparsa* are found on leaves, stems, peduncles, calices, and petals; the infection is commonly limited to young apexes (Aegerter et al., 2002). Downy mildews are considered one of the most devastating plant diseases. *Peronospora destructor* can cause up to 55% reductions in the dry weight of onion leaves (Yarwood, 1941); in cucumbers under severe epidemics of *Pseudoperonospora cubensis* yield loss could be between 80 to 90% (Lebeda, 1991). Besides significant crop losses, downy mildews participate with approximately 17% of the world fungicides market (Gisi, 2002). Though downy mildew is a destructive disease in susceptible rose cultivars, reports about crop losses are scarce. During the past 20 years rose downy mildew has become a serious problem causing significant losses to rose growers in the USA (Chase and Daughtrey, 2013). Suárez (1999) reported losses due to the disease around US $2,910 per hectare at the Bogota Plateau, Colombia.

Plant inspection is not suitable for early detection of destructive diseases like rose downy mildew and timely implementation of control measures. Non-invasive sensing techniques like infrared thermography have been reported to have a high potential for monitoring plant-pathogen interactions. Imaging techniques as reflectance measurements, fluorescence or temperature of leaves have been used for monitoring the physiological reaction of plants to pathogen attacks by several authors, e.g. Omasa et al. (1983), Chaerle and Van der Straeten (2000); Riera et al. (2005); Lindenthal et al. (2005); Oerke et al. (2011). Provided that transpiration of water through stomata cools the leaves, stomatal closure results in an increase of leaf temperature. On these grounds, leaf temperature measuring technology constitutes a promising alternative to study biotic factors causing stress in plants (Grant et al., 2006). Transpiration alterations may be used as cue for interpreting the development of plant diseases affecting stomatal aperture and functionality of cuticle integrity (Oerke and Steiner, 2010). Since stomata have a critical role in foliar pathogenesis and there is a negative correlation between evaporation rate and leaf temperature, thermal imaging is a suitable technique to detect spatial and temporal changes in stomatal aperture in plant–pathogen interaction (Inoue et al., 1990).

IR thermography has been successfully applied to visualize several plant diseases. *Erwinia amylovora* harpin-induced hypersensitive response (HR) in *Nicotiana sylvestris* leaves was detected by thermography (Boccara et al., 2001). Before visual symptoms appeared, thermography allowed monitoring an increase in temperature after infection of resistant tobacco by TMV (Chaerle et al., 2002). Digital visualization of temperature response of cucumber leaves enabled non-invasive detection of *Fusarium oxysporum* f. sp. *cucumerinum* infection and to study its effects on the water status of plants (Wang et al., 2012). Chaerle et al. (2004) pointed out that the knowledge of disease signatures for different plant–pathogen interactions could allow early identification of developing biotic stresses in crops. Results for downy mildew caused by *Pseudoperonospora cubensis* showed that IR thermography can be successfully applied to pre-symptomatic detection of the disease in cucumber (Lindenthal et al., 2005; Oerke et al., 2006). The interaction between *Plasmopara viticola* and grapevine leaves was detected by thermography 3 or 4 days after inoculation, before visual symptoms occurred and the pathogenesis resulted in a heterogeneous spatial and temporal variation of leaf temperature (Stoll et al., 2008).

Up to now, the detection of rose downy mildew is based on close inspection of plants to identify affected areas under greenhouse conditions. This method is time consuming, expensive and not suitable for detection of initial disease symptoms. In spite of this, only limited research has been conducted to identify alternative methods for the early detection of *P. sparsa*. Moreover, the physiological effects of *P. sparsa* infection on rose plants have not been studied to date. Thus the aims of this study were (i) to investigate the potential of thermography for early detection of rose downy mildew, (ii) to characterize thermal effects of rose plants infected by *P. sparsa* and (iii) to assess the effect of pathogen infection on stomatal aperture of rose leaves.

7.2 Materials and methods

7.2.1 Plant material

Adult plants of rose cv. Elle® Var. Meibderos (Meilland International SA, Le Luc-en-Provence, France), a Hybrid tea, were used in the study. The plants were planted in 10 L pots containing a 3:1 mixture of soil and Profi-substrat Typ ED73 (Gebrüder Patzer GmbH & Co Sinntal-Jossa, Germany) and grown in glasshouse under 16 h photoperiod, average temperatures of 23°C/18°C (day/night). Environmental conditions were controlled by the system INT800 (Kriwan GmbH, Forchtenberg, Germany). The plants were periodically watered with tap water and fertilized according to requirements. Main stems of 30 plants

were cut on axillary buds at the same time to have a uniform development of shoots; after six weeks, one to three shoots per plant were produced and then used for the study. Young shoots characterized by a reddish color of the leaves were selected for the inoculation due to their susceptibility to *P. sparsa* infections (Aegerter et al., 2002). Twenty plants were selected based on shoot development uniformity, half of which were inoculated and the other half treated as control plants.

7.2.2 Inoculum and inoculation

A suspension of sporangia of *P. sparsa* (Berk.) was used as source of inoculum. Sporangia produced on rose leaflets 7 dai at 18°C/16°C (day/night) and 16 h photoperiod were collected in distilled sterile water using a soft brush. Then, the desired concentration of sporangia was adjusted using a Fuchs-Rosental hemocytometer. The inoculation was carried out with a suspension of 2.5 x 10^4 sporangia per ml. The plants were inoculated on the abaxial and adaxial sides of the leaves, spraying the inoculum with a hand sprayer and applying 2.0 ml of suspension per plant. The control plants were sprayed with distilled sterile water. Inoculated and non-inoculated plants were kept under darkness for 48 hours at 10°C and 100% RH in a growth chamber (Viessmann®, Saale, Germany) to ensure pathogen infection. Then, the plants were transferred to 22°C/18°C day/night temperature and 60±10% RH conditions with an additional light source (Philips Son-T Agro - HPS 400W, Amsterdam, The Netherlands) to provide 16 hours of photoperiod. Water was supplied regularly to guarantee the suitable development of plants.

7.2.3 Disease assessment

Three days after inoculation (dai), daily evaluations of the inoculated and non-inoculated plants were carried out for 15 days to establish the presence and progress of the disease over time. Though all the leaves of the stem were young, they were divided in two levels according to their development, for data analysis purposes. The lower leaves were fully developed, extended and composed of a minimum of five leaflets at the moment of inoculation. The second level included leaves of the upper shoot which were not fully developed and extended at inoculation and most of them composed of three leaflets. The leaves of each shoot were numbered and daily inspected for the presence of the disease. Disease symptoms were scored according to the scale presented in Table 1. A disease index (DI) was calculated per stem as follows: $DI = [(0 \times n) + (1 \times n) + (2 \times n) + (3 \times n) + (4 \times n) + (5 \times n)] \div \sum n$. Where numbers show the categories presented in Table 7.1 and n represents the number of leaves observed under each category. In addition, at the end of

the evaluation (15 dai), floral buds of inoculated and non-inoculated shoots were assessed according to the scale presented in Table 7.1. During the evaluation, samples of different symptoms were collected to induce sporulation and confirm the presence of *P. sparsa* under the stereoscope. RBG images were recorded to illustrate the symptoms and their progress over time.

Table 7.1 Description of symptoms of downy mildew caused by *Peronospora sparsa* on rose plants cv. Elle® on leaves and floral buds grouped in grades used to score symptoms observed in plants after the inoculation.

Grade	Description of symptoms	
	Leaves	**Flower buds**
0	No symptoms	No symptoms
1	Dull leaflets, soft chlorotic spots and slightly disturbed leaves	Brown purple spots on sepals. Buds may look developed, but abnormal in size and shape. Early flat aperture
2	Disturbed leaves, strong chlorotic spots and/or brown purple color of angular shape	Small floral bud, brown color and developed peduncle
3	Highly disturbed leaves, strong and expanded brown spots, shrivelled leaves and desiccated areas or leaf borders	Very small floral bud brown color, bud and peduncle not developed; mommified
4	Strong brown spots, important desiccated leaf area >60%, drop of leaflets	_____
5	Strong spots, leaf completely desiccated, detached or absent	_____

7.2.4 Thermographic measurements

Thermographic images were obtained using an infrared Stirling-cooled scanning camera VARIOSCAN 3201 ST (Jenoptic Laser, Jena, Germany) with a spectral sensitivity of 8 to 12 µm and 1.5 m radians of geometric resolution (240 × 360 pixels focal plane array and a 30° × 20° field of view lens with a minimum focal distance of approximately 20 cm). Thermal resolution was 0.03 K and accuracy of absolute temperature measurement was <±2 K. Thermal images were taken at a distance of 100 cm between the camera and the plant material. Thermography images were analyzed using the software IRBIS® Plus version 2.2 (Infratec, Dresden, Germany). Circles of 5.0 mm diameter available as tool of

the IRBIS® program were used to obtain the average temperatures of inoculated and non-inoculated leaflets for each thermogram recorded over the period of evaluation. For this purpose, five circles were placed along each stem on five leaflets selected at random. The same procedure was followed for the lower and upper leaves of the stems. The differences (ΔT) between the mean temperatures of inoculated and non-inoculated leaflets were calculated in order to visualize the effect of *P. sparsa* infection on leaf temperature over time. In addition, the maximum temperature difference (MTD) or the difference between the maximum and minimum temperatures of the leaves, which is provided by the IRBIS® program for selected areas in the thermogram was analyzed (Lindenthal et al., 2005; Oerke et al., 2006; Oerke et al., 2011; Wang et al., 2012). To establish the environmental temperature at the moment of recording the images, five circles of 5.0 mm diameter of the IRBIS® program were placed at random in the surroundings of the stem. Due to uniformity within plants and within shoots in the development of the disease, the shoot was considered as the observation unit.

7.2.5 Assessment of stomatal aperture

Young leaf discs of rose cv. Elle® were inoculated with a suspension of 5 x10^4 sporangia per ml and kept in Petri dishes under 18°C/16°C day/night temperatures and 16 hours of light in a growth chamber. Stomatal aperture of inoculated and non-inoculated leaves was evaluated by taking imprints of the abaxial side of inoculated and non-inoculated leaf discs with nail polish, which was peeled off with transparent adhesive tape and then fixed on glass slides for subsequent evaluation (Lindenthal et. al., 2005). The samples were evaluated 24 hours after inoculation (hai) and every five days until completing three samplings (15 days), plus one additional sampling 17 dai. The width of stomatal aperture was measured using a photomicroscope (Leitz DMRB; Leica, Wetzlar, Germany) and the software Diskus 4.2 (Hilgers, Königswinter, Germany). The average of stomatal aperture was calculated using 50 stomata from five replicates.

7.2.6 Microscopy

Direct observations of leaf discs were carried out regularly using a stereo microscope (Leica S4E, Wetzlar, Germany) to visualize the formation of sporangia on the abaxial side of leaves. For histological observations, infected plant material was periodically extracted. Samples of 20 mm^2 were fixed with 2% paraformaldehyde and 2% glutaraldehyde in a 0.2 M sodium cacodylate buffer (Karnovsky, 1965). The samples were dehydrated in graded ethanol (AppliChem) water bi-distilled series (15, 30, 50, 70, 90 and 100%), washed two

times (10 minutes each) in propylene oxoide 99.5% (ALDRICH) and embedded in Spurr overnight (Spurr, 1969). Semi-thin sections (500 nm) were cut using a 45° glass knife in an ultra-microtome (Reichert Ultracut E; Leyca Microsystem, Nussloch, Germany) and then stained in 1% toluidine blue (AppliChem) following the protocol modified from Gerlach (1977). The specimens were observed under bright-field using a photomicroscope (Leitz DMRB; Leica, Wetzlar, Germany) with the software Diskus 4.2 (Hilgers, Königswinter, Germany).

7.2.7 Assessment of plant defoliation and stem growth

The length of the stems of inoculated and non-inoculated plants was measured immediately before inoculation and 15 days after to estimate the effect of the disease on the development of rose shoots. Furthermore, the influence of *P. sparsa* infection on leaf abscission was assessed on inoculated and non-inoculated plants 15 dai by calculating the percentage of nodes bearing firmly attached leaves on every stem.

7.2.8 Statistical analysis

Data were analyzed statistically using the Superior Performing Software System SPSS 21.0 (SPSS Inc., Chicago, IL, USA) to conduct independent-sample *t*-tests (two-sample *t*-test) analyses for means comparison and standard analysis of variance at a significance level of 95% (*t*-test: $P \leq 0.05$; Tukey test: $P \leq 0.05$, respectively). Graphics of the Pearson coefficient (*r*) were obtained using the program SigmaPlot 11.0 (Systat Software Inc., California, USA). All the experiments were performed at least two times.

7.3 Results

7.3.1 Development of symptoms

The first symptoms of downy mildew were observed 5 dai on upper and lower leaves. Dull leaflets, chlorotic spots and slight leaf distortion were the initial changes visually detected on infected leaves (Fig. 7.1a and b). Brown and chlorotic spots appeared 6 dai, shrivelled leaves were noticed 7 dai and severely disturbed leaves with extended brown-purple lesions were observed 8 dai (Fig. 7.1c and d). Leaf drop, desiccate leaf tissue, severe brown spots on the leaflets (Fig. 7.1e and f) and presence of purple spots on sepals of the bud flower were the main alterations observed 9 dai. Then, a marked drop of affected

leaves, brown and poorly developed floral buds (Fig. 7.1k and i) and a significant decline of diseased plants were observed. Subsequently (12 dai) angular purple-yellow leaf

Figure 7.1 Symptoms of downy mildew caused by *Peronospora sparsa* on leaves, stems and floral buds of rose plants cv. Elle®: **a**, slight chlorotic brown spots 5 dai; **b**, well defined chlorotic spots and slight disturbed leaves 5 dai; **c**, severely affected leaves 6 dai; **d**, brown angular spots 7 dai; **e**, shriveled leaves 9 dai; **f**, chlorotic and purple spots of angular shape 10 dai; **g**, expanded asymptomatic apical leaflet of upper leaf 10 dai; **h,** symptomatic area next to a asymptomatic area of upper leaf 12 dai; **i**, symptoms on stems 12 dai: right, dark brown areas white color and waxy center and left, chlorotic irregular spots with bulky appearance; **j**, affected bud flower grade 1, showing early opening and abnormal shape 15 dai; **k**, brown floral bud grade 2, 15 dai; **l**, bud flower poorly developed, dark brown color grade 3, 15 dai.

lesions were observed; brown spots with white waxy center appeared on the upper stems close to the floral peduncle. Moreover, chlorotic areas with slightly purple flecks and irregular spots with bulky appearance and green borders became visible (Fig. 7.1i). This last symptom had not been reported to be associated with *P. sparsa* infections in rose stems. After this time, no additional changes were noticed in infected plants; no symptoms or alterations were observed in non-inoculated plants.

Development of symptoms on upper and low leaves differed. Upper leaves were not completely expanded at the time of inoculation and consequently, were not uniformly inoculated. Typical symptoms developed in upper leaves in first stages of the disease but later, lesions were limited by the growth of non-infected leaf areas. Therefore, the new tissue remained healthy (Fig 7.1g and h).

7.3.2 Progress of the disease and effects on leaf temperature

Changes in leaf temperature of inoculated plants were detected as early as 3 dai in lower leaves. The average and maximum temperatures of inoculated plants were statistically higher than temperatures of non-inoculated plants, while minimum temperatures remained stable (Fig. 7.2). The leaf temperature increase of inoculated plants detected by IR thermography occurred two days before visual symptoms of disease were detected (Fig. 7.3). The severity of leaf symptoms increased over time and leaf spots and lamina distortion were followed by desiccate tissue and further drop of leaves (Fig. 7.4). The average, maximum and minimum temperatures of infected plants were statistically higher than those of non-inoculated plants by 1.5°C 7 dai and by 2.0°C 10 dai. The increase of leaf temperature of inoculated plants became smaller 10 dai. Nevertheless, the values were statistically higher than temperatures of non-inoculated plants (Fig. 7.2). Leaves of non-inoculated plants had similar temperatures throughout the experiment (Fig. 7.5). Disease severity and leaf temperature increased simultaneously and were positive correlated ($P \leq 0.05$) (Fig. 7.6).

At first stages, the disease index (DI) showed a similar trend in lower and upper leaves. Statistical differences were detected 8 dai when upper leaves had lower disease severity (Fig. 7.4). Five days after inoculation, average, minimum and maximum leaf temperatures of upper leaves were higher ($P \leq 0.05$) than those of non-inoculated leaves. Six days after inoculation, this temperature difference was almost 0.8°C, but it declined progressively until the end of the experiment, though it continued to be statistically significant (Fig. 7.2).

On upper leaves DI increased moderately 8 dai because those leaflets which had not been totally exposed to inoculation were hardly infected and, therefore, exhibited uniform low temperature areas like the healthy tissues. The lesions were minor, leaves grew up and leaf drop was rare. For the upper leaves the relationship between DI and average, minimum and maximum temperature of inoculated leaves was not significant ($P \geq 0.05$), (Fig. 7.6).

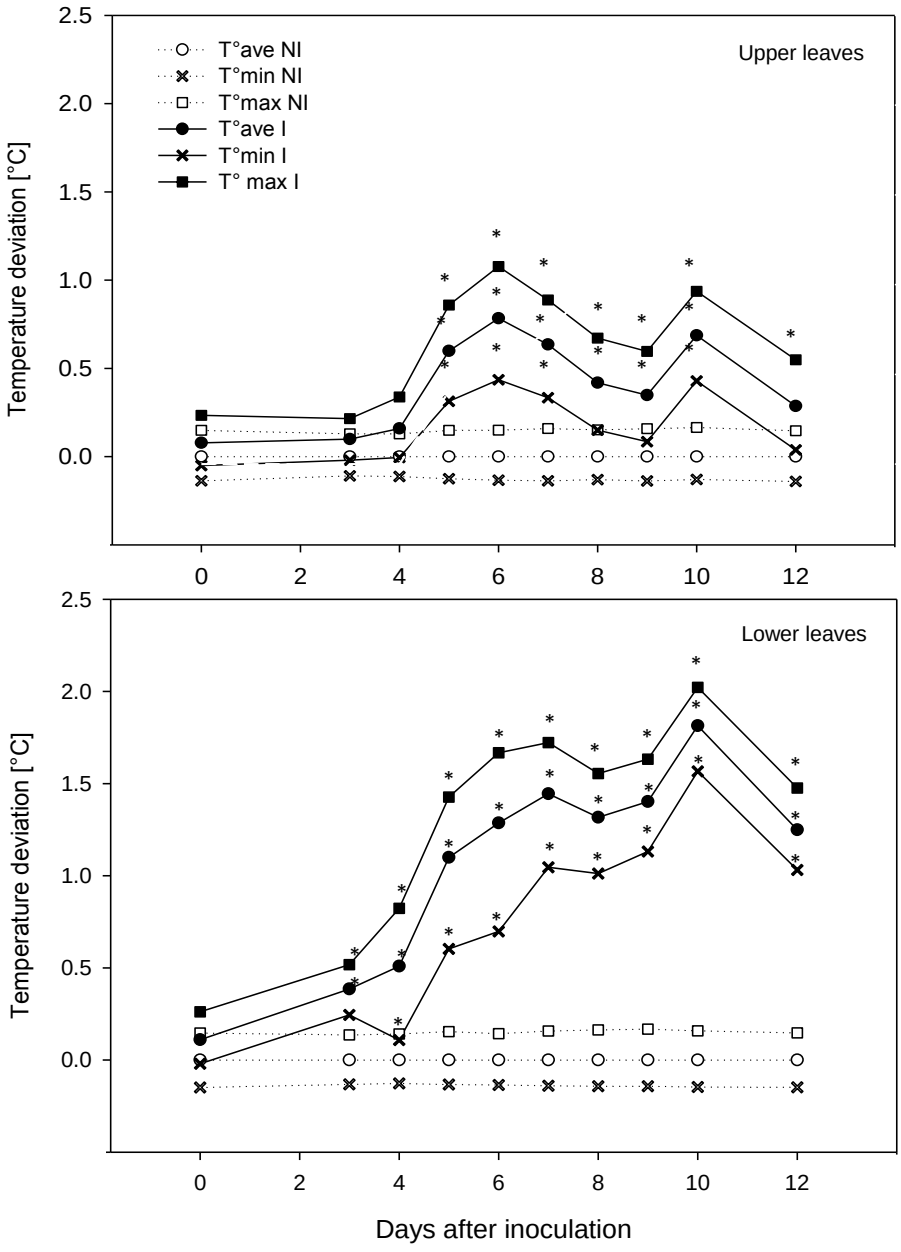

Figure 7.2 Effect of *Peronospora sparsa* infection on average, maximum and minimum temperature of low and upper leaves of rose cv. Elle®. Values represent differences in temperature related to average temperature of non-inoculated leaves. Inoculated: I; Non-inoculated: NI. Asterisk represents value significantly different from non-inoculated leaves (n =11*; t*-test, $P \leq 0.05$).

7.3.3 Effect of Peronospora sparsa infection on maximum temperature difference

The MTD of inoculated leaves increased significantly over that of non-inoculated leaves 4 dai, one day before the presence of initial visual symptoms such as dull leaves, chlorotic spots and slight distortion of foliar lamina. The highest MTD value (0.98 K) was registered 6 dai and was related to an increase in leaf distortion and the presence of brown angular spots on leaves. MTD of lower leaves of inoculated plants was significantly higher than that of non-inoculated plants until the end of the experiment (Fig. 7.7). In early stages of symptom development, the thermal profile was heterogeneous. Infected leaf areas corresponding to warm regions contrasted with the low temperature areas of healthy tissue. In contrast, non-inoculated leaves were characterized by homogeneous low temperature and low MTD, which varied slightly (0.24-0.30 K) over time. Seven days after inoculation, MTD decreased progressively and coincided with the expansion of lesions, increase of distorted leaf areas and presence of desiccated tissue. In the thermograms these symptoms were visualized as uniform warm areas with reduced temperature heterogeneity (Fig. 7.8).

On the upper leaves, MTD increased slightly 4 dai. Associated with presence of the first disease symptoms, it was found to be significantly different from non-inoculated leaves 5 dai. The highest MTD (0.64 K) was observed 6 dai, when the symptoms became more severe. Then, it decreased slightly and remained constant over time, showing no relevant changes in established leaf lesions. The presence of new healthy tissue and complete expansion of leaves were visualized in thermograms as areas with uniform low temperature.

7.3.4 Influence of Peronospora sparsa infection on stomata aperture

The stomatal opening of infected leaves indicated that infection by *P. sparsa* affected the stomatal aperture of rose leaves and differences with non-inoculated leaves were significant in all evaluations 1, 5, 10, 15 and 17 dai (Fig. 7.9). Stomatal aperture of infected leaves was lower than in non-inoculated 1 and 5 dai. Then, an abnormal wider aperture of stomata of inoculated leaves was observed 13, 15 and 17 dai and it coincided with the presence of advanced stages of *P. sparsa* infection, characterized by dense sporulation and brown leaf tissue (Fig. 7.10).

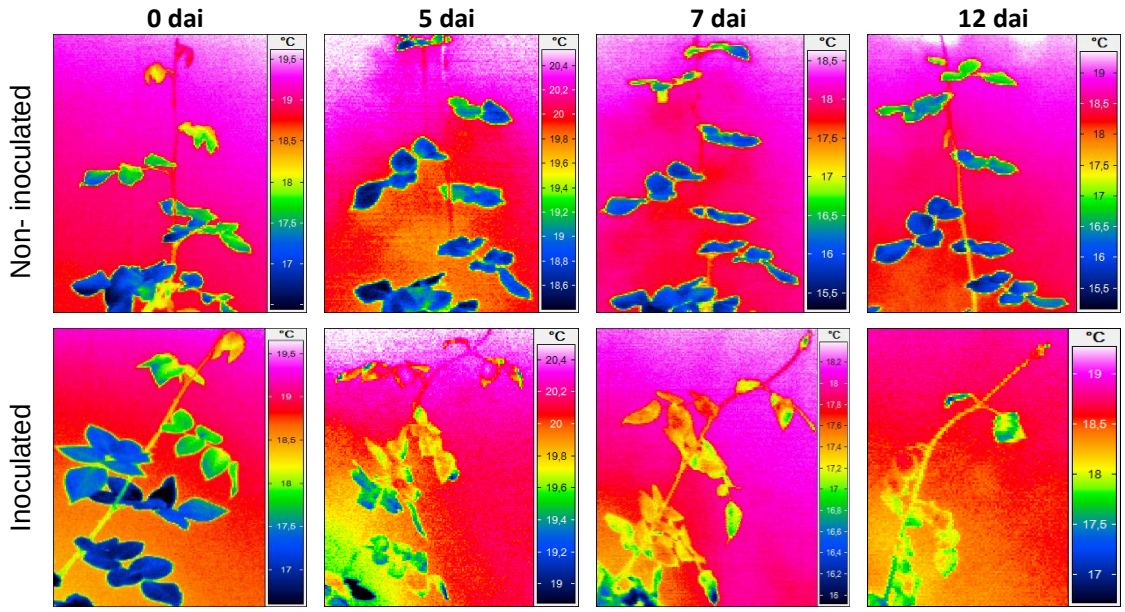

Figure 7.3 Effect of *Peronospora sparsa* on leaf temperature of rose cv. Elle® during pathogenesis visualized by IR thermography 0, 5, 7 and 12 days after inoculation (dai).

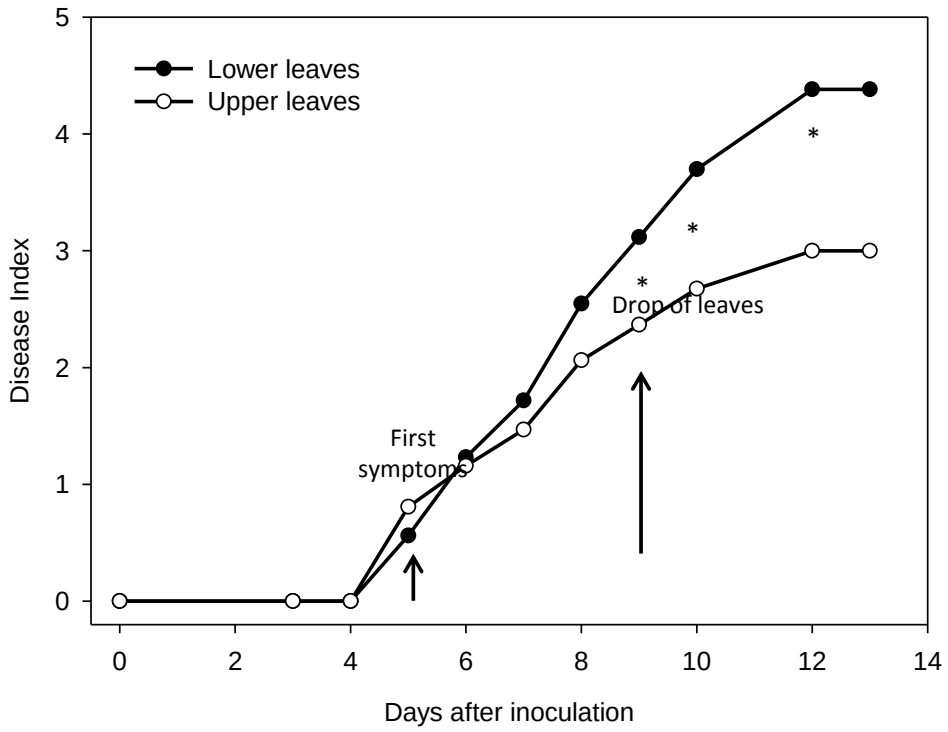

Figure 7.4 Progress of downy mildew caused by *Peronospora sparsa* in rose cv. Elle® as the disease index of lower and upper leaves. The time of visualization of first symptoms and drop of leaves are shown with the arrows. Asterisk represents values significantly different between leaf levels (n=18*; t*-test, $P \leq 0.05$).

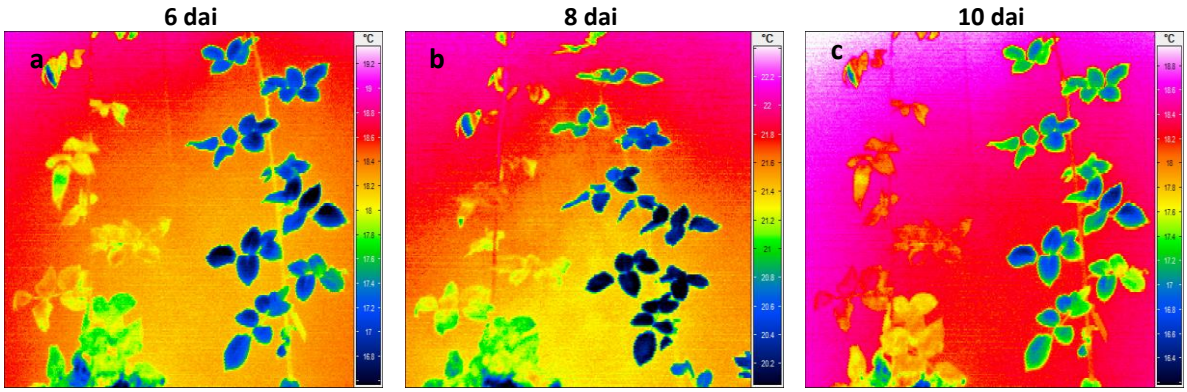

Figure 7.5 Effect of *Peronospora sparsa* on leaf temperature of rose cv. Elle® during pathogenesis visualized by IR thermography. Inoculated plant (left) and non-inoculated plant (right). Days after inoculation: dai.

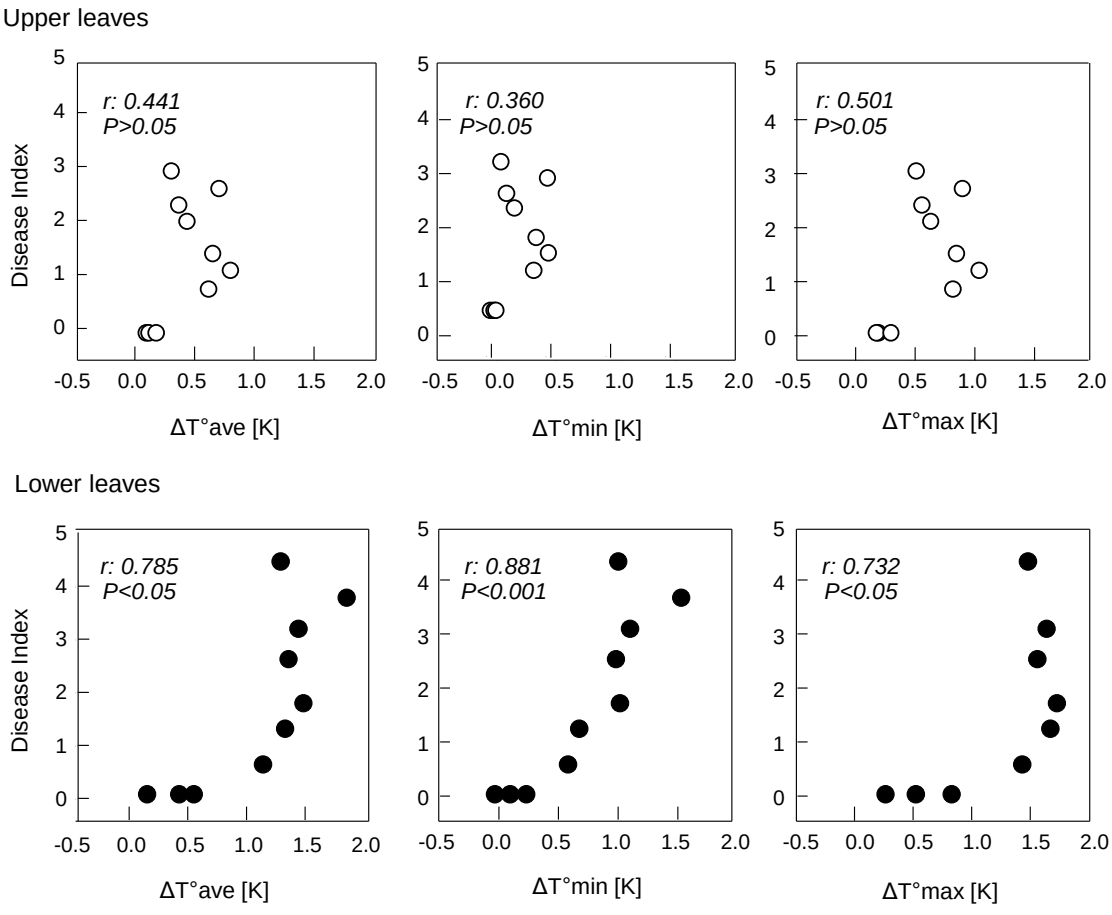

Figure 7.6 Relationship between disease index and temperature deviation of inoculated plants from 0 to 12 days after inoculation. Pearson´s product-moment correlation coefficient *r* for each pair of variables is presented. Pairs of variables with positive *r* and *P* values below 0.05 tend to increase together. T°ave, average temperature; T°min minimum temperature; T°max, maximum temperature.

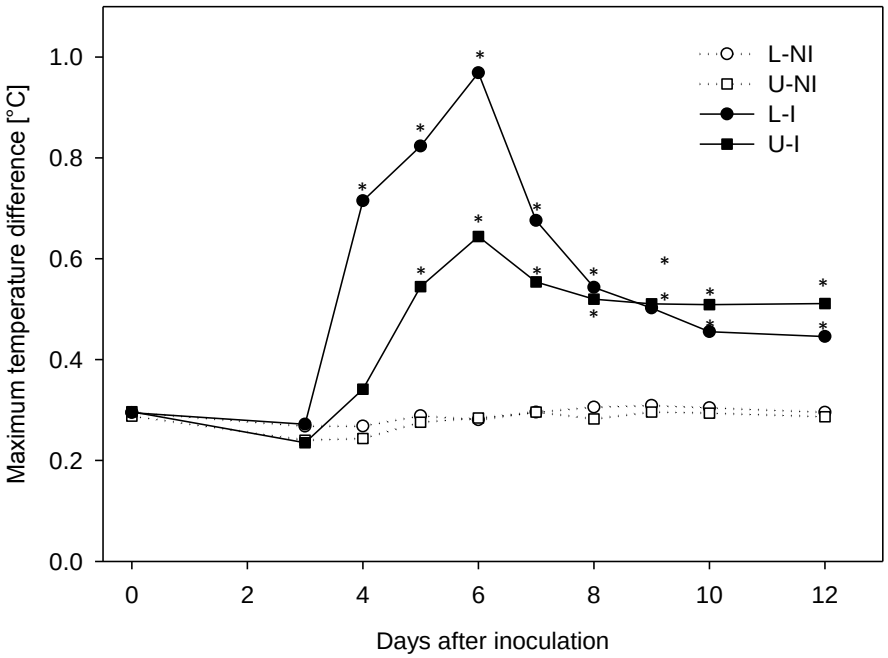

Figure 7.7 Influence of *Peronospora sparsa* infection on maximum temperature difference MTD of lower and upper leaves of rose cv. Elle®. Values indicate the difference between the maximum and minimum temperature of inoculated and non-inoculated leaves. L, lower leaves; I, inoculated; NI non-inoculated; U, upper leaves. Asterisk represents value significantly different from non-inoculated leaves. Lower leaves and upper leaves were compered separately (n = 11*; t*-test, $P \leq 0.05$).

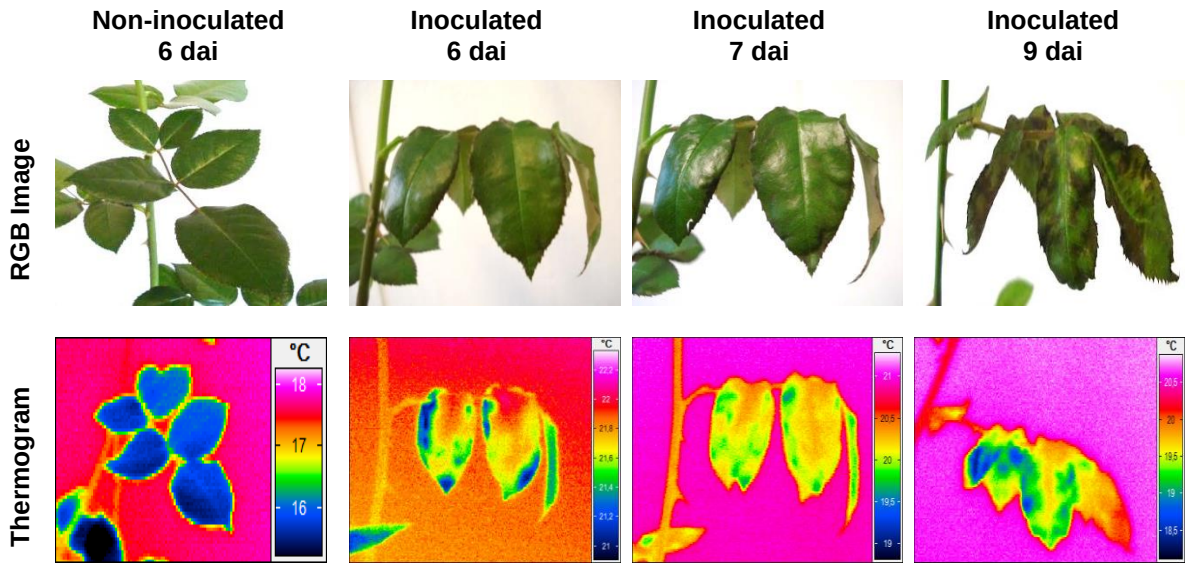

Figure 7.8 Dynamics of downy mildew infection on leaves of rose cv. Elle® and effect of the infection on leaf temperature during pathogenesis visualized by thermal imaging 6 to 9 days after inoculation (dai).

7.3.5 Structures of Peronospora sparsa in plant tissue

The formation of the first sporangiophores was observed through stomata 5 dai. Masses of sporangiophores and first oospores were observed 7 dai. Profuse sporulation of the pathogen and production of oospores was followed by presence of brown tissue 11 dai (Fig. 7.10a, d). In vertical sections, hyphae were observed in all tissue layers, especially in spongy parenchyma, including substomatal cavities where they were densely aggregated (Fig. 7.10e-f) simultaneously with intensive sporulation of the pathogen.

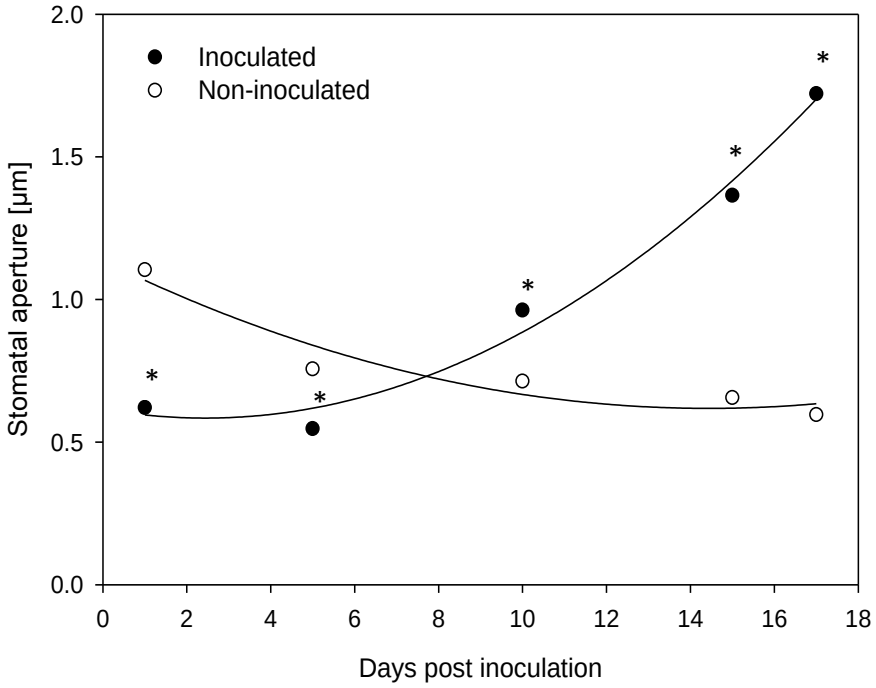

Figure 7.9 Stomatal aperture of rose leaves cv. Elle® infected and non-infected by *Peronospora sparsa* during pathogenesis. Asterisk indicates values significantly different (*t*-test, $P \leq 0.05$).

Vertical sections of symptomatic plant material showed leaf mesophyll densely colonized by hyphae and cells penetrated by haustoria; hyphae and haustoria were also visualized in cortical tissue of petioles and stems. Histological observations of stems with chlorotic irregular spots and prominent green borders confirmed the presence of *P. sparsa* in cortical tissue. Under low relative humidity (60±10% RH), sporangia were not observed neither on symptomatic leaves nor petioles or stems. Strong sporulation was observed on symptomatic leaves and petioles 24 hours after incubation under 100% RH and 72 hours later on stems under the same conditions.

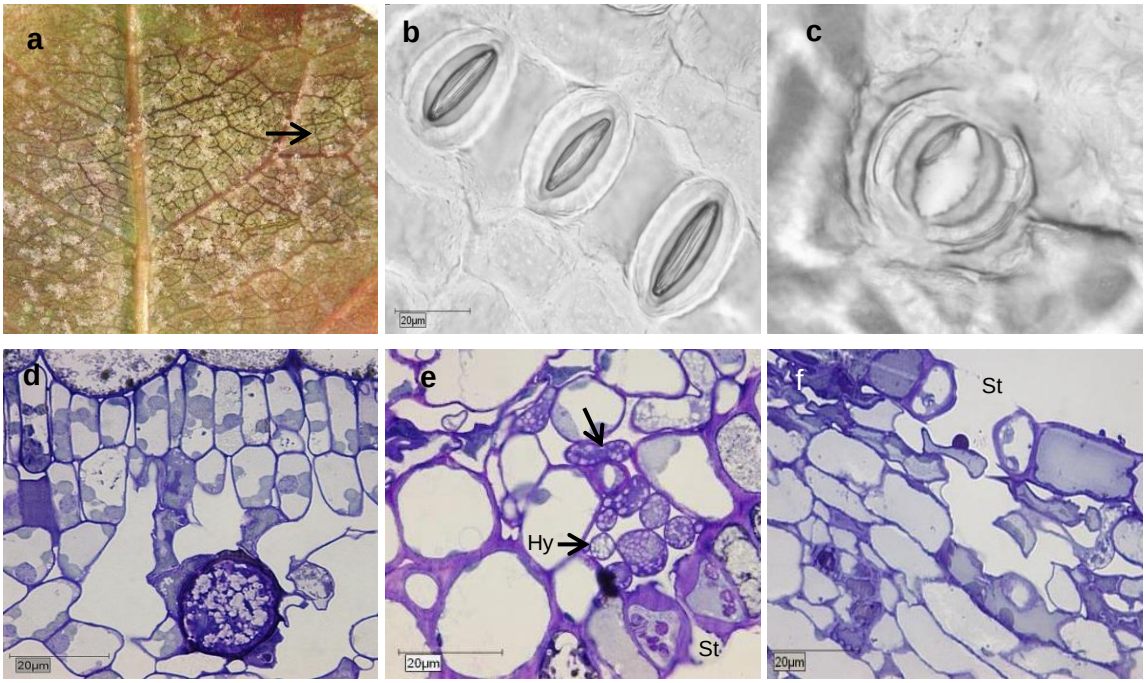

Figure 7.10 Macroscopic and microscopic visualization of *Peronospora sparsa* in leaves of rose cv. Elle®: **a**, profuse sporulation and presence of brown tissue 11 dai; **b**, stomata of non-inoculated leaves 12 dai; **c**, stomata abnormally open in disrupted tissue 12 dai; **d**, oospore in mesophyll tissue 11 dai; **e**, Hyphae of *P. sparsa* in substomatal cavity 8 dai; **f**, leaf tissue with stoma abnormally open. Hy, hyphae; St, stoma.

7.3.6 Influence of downy mildew on plant development

Drop of infected leaves occurred four days after first symptoms of the disease. In infected plants only 38% of the leaves remained attached to the stems 15 dai, most of them in the upper part, in contrast to 100% of non-inoculated plants (Fig. 7.11a). Increase in stem length 15 dai was significantly higher in non-inoculated plants than in inoculated plants. The length of the stems of healthy plants exceed by almost 100% that of the stems of inoculated plants (Fig. 7.11b). Only 11% of the floral buds produced on inoculated plants showed normal size, shape and color in comparison to those of non-inoculated plants. Disease symptoms of floral buds varied from light alterations on sepals, through atypical development to complete distortion. Short peduncles were produced in some cases and floral buds produced an atypical flower shape that showed early aperture (Fig. 7.11c).

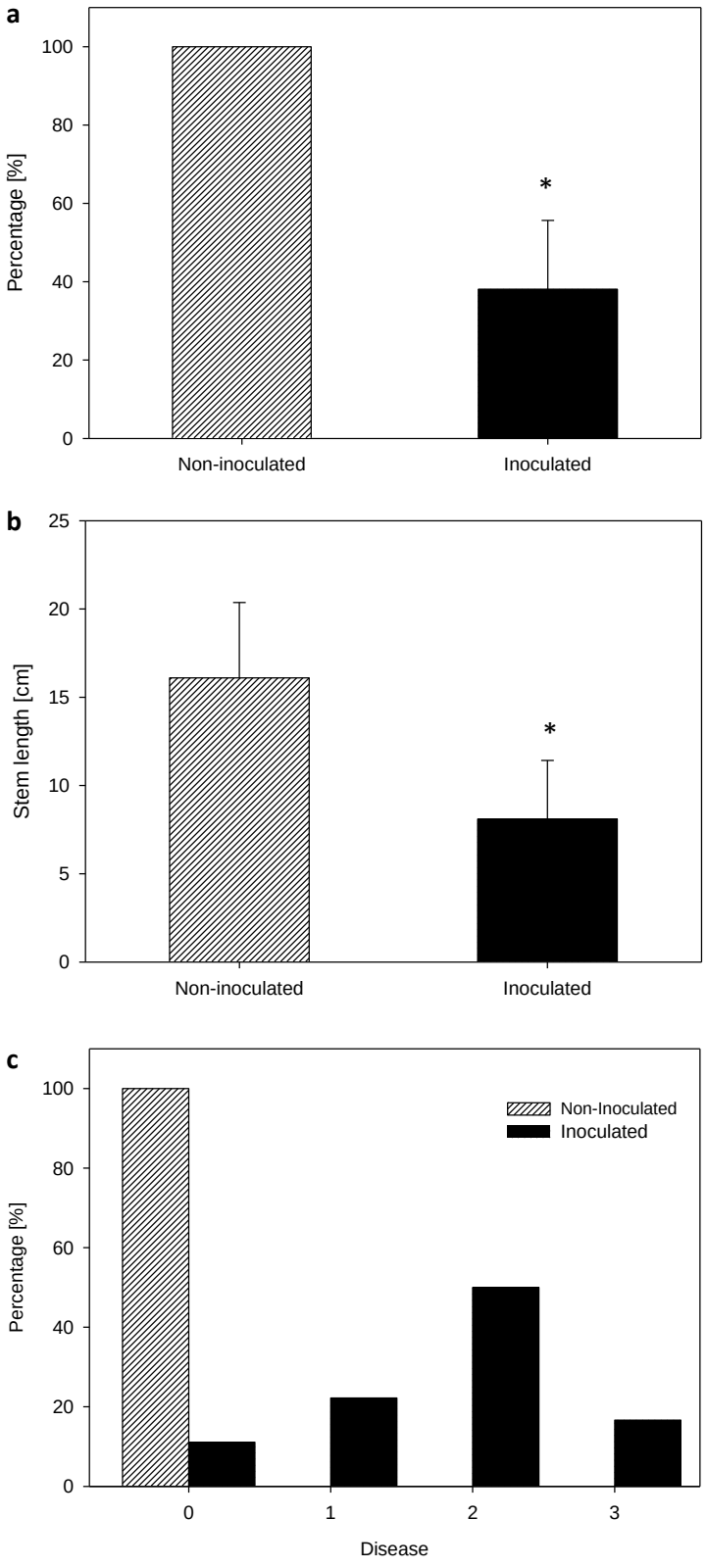

Figure 7.11 Effect of *Peronospora sparsa* infection on development rose cv. Elle®: **a**, drop of leaves in percentage of nodes per stem of inoculated and non-inoculated plants with leaves firmly attached 15 days after treatment; **b**, increase of stems length of inoculated and non-inoculated plants 15 days after treatment; **c**, effect of *P. sparsa* infection on floral bud development. Values represent the distribution of floral buds in four grades of disease. Asterisk represents value significantly different from non-inoculated (n= 18*; t*-test, $P \leq 0.05$). Error bars represent the standard deviation.

7.4 Discussion

The results clearly showed the devastating effects of *P. sparsa* infection and its important role in the quality of the stems and bud flowers. The strong influence of the disease may be explained by reduced photosynthesis and, hence, plant development. Shtienberg (1992) concluded that photosynthesis decreased linearly with increments and disease severity of several foliar pathogens, including downy mildews. Certainly, Fraymouth (1956) and Ingram (1981) reported that downy mildews impair photosynthesis, especially close to sporulation.

Despite the rapid development of visible disease symptoms, IR thermography detected *P. sparsa* infection two days earlier. Rose downy mildew was detected by naked eye 5 dai. The infection was clearly visualized in thermograms 4 dai, when MTD of infected leaves increased due to a more heterogeneous leaf temperature as compared to that of non-inoculated leaves. Reports of early detection of plant pathogens by IR thermography are numerous (Chaerle et al., 2004; Stoll et al., 2008a; Oerke et al., 2011). For downy mildews, Lindenthal et al. (2005) recorded thermal changes of the infected tissue one day before the appearance of disease symptoms of *P. cubensis*. Stoll et al. (2008) also detected *Plasmopara viticola* infection before the appearance of visual symptoms in grapevine.

The patterns of leaf temperature were closely related to *P. sparsa* development. Temperature increase started 3 dai well before the presence of dull leaflets and continued with the rapid colonization of leaf tissue and the severity of the symptoms. Maximum temperatures occurred with the presence of desiccate tissue and heavy drop of leaves. A similar increase in temperature of necrotized leaf areas with subsequent desiccation of dead tissue was observed by Lindenthal et al. (2005) in *P. cubensis*-cucumber interaction. In later stages of rose downy mildew, the remained leaves showed a decrease in leaf temperature associated with brown lesions, severely disturbed leaves and densely colonized tissue.

Leaf temperature depends, among other factors, on the effect of the pathogen on stomatal conductivity, damage of plant cuticle, degradation of cells or transport and accumulation of plant defense compounds (Chaerle et al., 1999; Oerke et al., 2006; Chaerle et al., 2004). Leaf temperature increase after inoculation has been reported in diverse plant-pathogen interactions (Nilsson, 1991; Oerke and Steiner, 2010), and in some of them a reduction of

stomatal aperture resulting from infection has been observed (Grimmer et al., 2012). In the case of downy mildews, thermal responses were mainly associated with an early decrease of leaf temperature promoted by evaporation of leaf water as a consequence of plant cuticle damage and abnormal aperture of leaf stomata (Lindenthal et al., 2005; Oerke et al., 2006). In later stages of the disease, leaf temperature increased due to the desiccation of dead tissue. In contrast, *P. sparsa* constantly increased the overall temperature of rose leaves since early stages of infection and this reaction was related to stomatal closure and a decrease of leaf temperature occurred only in later disease stages. Similar findings associated with early leaf temperature increases in rose downy mildew have been reported for irrigated grapevine and *Plasmopara viticola* (Stoll et. al., 2008a). Downy mildew in pearl millet caused by *Sclerospora graminicola* similarly induced stomata closure and thus decreased transpiration rate and water loss (Kumar and Gour, 1992). These results show that different profiles of thermal responses in downy mildew infections may occur.

The results indicate that *P. sparsa* affected rose stomata aperture in connection with infection progress in leaf tissue. After inoculation, stomata remained closed and abnormal opening was observed 8 dai together with extensive leaf colonization, hyphae in stomatal cavities and sporulation. Later, the maximum stomatal aperture occurred in brown tissue, with dense sporulation and the presence of oospores in spongy parenchyma. This condition affected the structure of the tissue and limited the normal functioning of stomata. Consequently, the leaves lost water from the affected tissue and the temperature decreased. Chaerle et al., (2001) pointed out that a decrease in leaf surface temperature may be due to tissue damage since the contents of bruised cells evaporate and locally cool the surface until the wound dried. The relation between abnormal stomata aperture and histological observations of *P. viticola* was reported by Allègre et al., (2007). These authors observed that the abnormally open stomata of grapevine increased water loss after infection. Substomatal cavities filled with the pathogen showed the corresponding stomata opening wider than those with empty cavities, and it was concluded that stomatal aperture depended on the spread of the pathogen under the stomata. Similar abnormal stomatal openings associated with loss of membrane integrity due to the pathogen were observed by Lindenthal et al. (2005) in downy mildew of cucumber and by Farrel et al. (1969) in potato infections by *Phytophthora infestans*. Though sporulation of *P. sparsa* was not observed in plants under the experimental conditions, the profuse sporulation on leaves shortly after keeping symptomatic leaves under 100% RH indicated that all symptomatic leaves were densely colonized.

Oerke and Steiner (2010) mentioned that diseases that affect stomata regulation may produce modifications in transpiration before and after the initial symptoms and some pathologies affecting cuticular transpiration when the tissue is severely affected. In some plant–pathogen interactions, reduction of transpiration is caused by defoliation, obstruction of stomata and conducting tissue (Bassanezi et al., 2002; Chaerle et al., 2001; Spotts, 1979). The findings of this study suggest that the rose plant´s response to downy mildew infection increased leaf temperature after infection and was related to closure of stomata. The first subtle symptom of rose downy mildew, which corresponded to dull leaflets that looked weighty in comparison to healthy ones, may reveal an initial reaction of infected leaves. A possible reason may be attributed to an increase in permeability of the cuticle and epidermal cells caused by direct penetration of sporangia that may induce stomata closure. Then, as lesions developed, severely infected areas became dry, followed by leaf desiccation and subsequent drop. These reactions could suggest a decrease in leaf transpiration visualized as higher temperature due to stomata closure. Indeed, diverse studies have demonstrated a negative linear correlation between transpiration rate and leaf temperature (Inoue et al., 1990; Merlot et. al., 2002; Lindenthal et al., 2005). Besides, in early studies of downy mildew, Fraymouth (1956) mentioned that distortion and curling of the leaves of certain plants could be due to the drying out and shrivelling of the lower surface of the leaf. The rapid increase in volume of the hyphae as they grow under the lower epidermis toward the stomata has the effect of raising the epidermis and completely disrupting the leaf.

Though pathosystems are diverse and leaf temperatures of cucumber plants infected by *F. oxysporum* f. sp. *cucumerinum* recorded by Wang et al. (2012) were enormously higher (3.0-8.0°C approx.) in contrast to temperatures observed in rose leaves infected by *P. sparsa*, it is worth noting that the tendency of maximum, average and minimum temperatures was similar in both studies. This likeness may suggest that diseases associated with increases of leaf temperature after infection could have common plant response factors, even in different plant-pathogen interactions. Strong increases in leaf temperature corresponded to lower transpiration rates and stomatal conductance levels, together with a positive correlation between leaf temperature and levels of ABA (Wang et al., 2012).

Stomatal closure may be caused by damage of the photosynthetic apparatus (Meyer et al., 2001; Grimmer, 2012). Compounds that accumulate during pathogenesis such as salicylic acid, nitric oxide (NO), phenolic compounds and plant hormones like auxin and abscisic acid (ABA), together with oxidative stress may also induce stomatal closure

(Chaerle et al., 1999; Wang et al., 2004; Grimmer et al., 2012). Nevertheless, it has been demonstrated that ABA is the main factor accounting for this reaction (Jones and Mansfield, 1970; Pegg, 1976; Wang et al., 2012) and plays a fundamental role in plant response to water stress (Wang et al., 2004; Grimmer et al., 2012). The stomata closure induced by the infection of *P. sparsa* may be related to ABA. In rose, loss of leaf turgor was observed in severely affected leaves but there was no stem or flower bud wilting. The possible role of ABA might be also related to the impairment of development of floral buds and drop of leaves of inoculated plants. Pegg (1976) mentioned that stunting is a feature of diseases especially those involving systemic colonization of the host which occurs in colonized and non-colonized tissue associated with increased ABA levels. Along with this, it is worth mentioning that systemic colonization by *P. sparsa* in rose has been observed (results not shown). Moreover, ABA plays an important role in abscission (Andicott and Lyon, 1969) and drop of infected leaves is common in natural infections of *P. sparsa*. Further studies are required to investigate the hypothesis of the role of ABA in stomatal closure after *P. sparsa* infections and to identify other factors involved in plant response.

Early detection of *P. sparsa* infection was possible using thermal imaging. Sensing to discriminate infected from healthy plants was effective two days before inspection by naked eye. The results clearly indicate that *P. sparsa* infection in roses promoted stomatal closure and increased plant temperature. However further studies have to be conducted to elucidate the plant responses observed. IR-thermography proved to be a suitable tool to detect downy mildew infection in roses early in pathogenesis. Nevertheless, the technique has to be evaluated under conditions of commercial production.

8. GENERAL DISCUSSION

Downy mildew caused by *Peronospora sparsa* is a serious problem in nurseries and commercial cut rose crops in various countries. Despite of this importance, reports concerning the impact of the disease are rather limited. In this study, the development of symptoms and the progress of the disease were evaluated. In addition, leaf abscission, stem length and the percentage of abnormal floral buds harvested from inoculated plants were quantified on *P. sparsa* infected plants. The results showed the strong effect of the disease on the development of a susceptible rose cultivar.

Colombian isolates of *P. sparsa* from cut rose crops at the Bogota Plateau showed similar aggressiveness regardless of the location or cultivar of origin. Varila (2005) observed a homogeneous response of *P. sparsa* isolates to the temperature. Based on these results and the low genetic diversity found for Colombian isolates (Ferrucho, 2005; Ayala et al., 2008), chemical control and sanitary practices of disease management would have contributed to the selection of a homogeneous population of the pathogen, as Ferrucho (2005) suggested. In addition, the introduction of the pathogen in commercial plantations within the plant material, which is highly probable (Aegerter et al., 2002), may have contributed to this situation. Differences in the aggressiveness of *P. sparsa* may be expected when samples from different countries are studied. On the contrary, the results allow inferring that a new set of samples from Colombian crops would probably show similar development patterns.

Histological investigations revealed a vertical and a horizontal colonization of rose leaves by *P. sparsa*. In the vertical progress of the infection, epidermal cells of the opposite layer to the inoculated surface were colonized 96 hai. Horizontally, after the direct adaxial leaf penetration, hyphae grew under the upper cuticle profusely. *P. sparsa* confirmed its capacity to produce sporangiophores through this tissue layer and oospores under the adaxial leaf cuticle. In a more internal level, horizontal colonization of the tissue occurred by intercellular hyphae and the leaf lamina was colonized 120 hai. These results confirm that the intercellular space is highly important for long distance colonization by the pathogen. Microscopical observations coincided with results presented by Fraymouth (1956) for other downy mildews. The results give a hint to comprehend the extensive growth of the pathogen in susceptible rose tissue and the severity of disease symptoms.

The obtained results complement previous studies conducted by Xu and Pettitt (2004) and Gomez and Filgueira (2012) among others and provide new findings about the biology of

P. sparsa: (i) first visualization of ultrastructures and their interaction with rose tissue, (ii) description of adaxial leaf infection, (iii) observation of intercellular hyphae spreading from the site of infection and leaf petioles conducting the pathogen from leaves to stems and vice-versa, (iv) visualization of hyphae growing in parallel to leaf veins along the cortical tissue of petioles and stem cortex and rarely observed in xylem and phloem and (v) evaluation of the capacity of production of oospores in leaf tissue of different cultivars and leaf ages. In addition, this investigation demonstrated the ability of the pathogen to systemically invade plant tissue. Micro- and macroscopical observation showed the invasive development of *P. sparsa* especially in young tissue.

In this study, presymptomatic detection of the disease was possible by IR thermography. The thermographic detection of the infection before macroscopic symptoms was successfully observed, as well in *Pseudoperonospora cubensis* in cucumber, and in *Plasmopara viticola* of grapevine (Lindenthal et al., 2005; Oerke et al., 2006, Stoll et al., 2008). The effect of pathogen infection on leaf temperature reflects leaf transpiration during pathogenesis (Oerke et al., 2006). *P. sparsa* infection induced an increase of leaf surface temperature that declined in late disease stages due to tissue damage and dense colonization that promoted leaf transpiration or water loss. In the current study, IR thermography not only allowed differentiating infected rose leaflets, leaves and plants from healthy ones, but also made it possible to discriminate cultivars based on their susceptibility to *P. sparsa*. Moreover, using thermal sensing the asymptomatic spread of the pathogen was visualized. The results obtained by IR thermography concerning the cultivars susceptibility and spread of the pathogen coincided with those obtained in the biological and histological investigation of the infection.

The growth of *P. sparsa* tending to spread quickly and invade intercellular tissue layers was demonstrated. By thermal sensing, infections of *P. sparsa* were visualized before the macroscopical detection of the disease. Due to the sensitivity of IR thermography, subtle changes in leaf temperature resulting from the pathogenic activity of *P. sparsa* were observed in the present study. Therefore IR thermography has proven to have a remarkable potential as a non-invasive method of detection. This is particularly important since few alternatives had been explored for the presymptomatic detection of downy mildew, a destructive disease of difficult control. Based on the obtained results, thermal imaging appears as a promising tool to be used in risk assessment programs of rose crops, in the framework of a more sustainable management of ornamental production.

1

9. SUMMARY

The infection and spread of *Peronospora sparsa* on *Rosa* sp. was investigated from different approaches: visual, thermographic, light and electron microscopical studies were conducted. The main conclusions were as following:

- *Peronospora sparsa* isolates from different commercial crops at the Bogota Plateau did not vary significantly in the biological parameters assessed. Although scattered differences were detected in a few isolates, the assessed variables altogether showed that the aggressiveness of the isolates on cvs. Elle® and Sweetness® was similar. Cultivar and geographical origin of the isolates had no effect on the aggressiveness of the isolates.

- The latent period of the evaluated isolates was 6.0 days in cv. Elle® and cv. Sweetness®. The AUDPC (Area Under Disease Progress Curve) of incidence of sporulation, the sporulation index, the amount of sporangia and the number of oospores in leaf tissue were significantly higher in cv. Elle® than in cv. Sweetness®.

- An effect of the leaf side on infection, development and sporangia production of *P. sparsa* in rose was observed. The pathogen penetrated and sporulated on the adaxial and abaxial leaf surface. However, the abaxial surface, more than the adaxial one, favored the pathogen penetration, and fast and profuse sporangia production.

- After inoculation, mesophyll cells were densely penetrated with filiform haustoria, which were observed in other tissues like the epidermis or the bundle sheath cells. Exhibiting a neck like constriction, haustoria penetrated into the cells surrounded by the intact host membrane. *P. sparsa* entered leaf cells always as haustoria, structures like intracellular hyphae not being observed. By electron microscopy no collapsed cells were observed even under heavy infection (7dai).

- Different histological techniques described the invasive growth of *P. sparsa* in rose leaves. Five days after inoculation the whole leaf lamina was colonized and hyphal growth was not limited by leaf veins. Intercellular hyphae growing outside the bundle sheath cells of secondary and tertiary veins penetrated only into bundle sheath cells but not further into cells of xylem or phloem parenchyma. During the colonization process, thick fasciated hyphae were observed growing parallel to leaf veins and penetrating cortical cell tissue with long filiform haustoria. Hyphae and haustoria were

also found in the small intercellular spaces of collenchyma in midribs and petioles, as well as in the stem cortex.

- Visual and histological evaluations confirmed the ability of downy mildew to establish systemic infection in rose tissue. *P. sparsa* spreads acro and basipetally in rose leaves. Intercellular mycelium growth was responsible for the long distance colonization of the tissue. After localized inoculation, *P. sparsa* spread from apical to neighboring leaflets in 60% of the cases and to the stems in 20% of them. Spread to upper leaf insertions occurred in 50% of symptomatic stems. Disease symptoms on inoculated apical leaflets, neighboring leaflets and stems of cv. Elle® were observed in average 10, 22 and 28 dai, respectively. Symptoms on inoculated stems appeared 18 dai and spread to higher leaf insertions 34 dai.

- The pathogen used petioles to spread between leaflets in the leaf and between stem tissue and leaves. Sporangiophores of *P. sparsa* were observed on middle and distal leaflets one or two days after they were observed on the previous petiole segment. Oospores were densely produced in leaf areas where profuse sporulation occurred.

- Leaf age influenced infection, development and spread of *P. sparsa*. Shorter latent periods, higher number of oospores in leaves and petioles were observed in young leaves in contrast to intermediate and mature leaves. On intermediate leaves, first hyphae and profuse colonization of the tissue were observed 52 h later than in young leaves; in mature leaves, few hyphae occurred 120 h later than in young leaves. Sporangia on young leaves were observed as far as 70 mm from the inoculation site 15 dai and around 50 mm on intermediate leaves by the same period of time. *P. sparsa* spread in a comparable way on young leaves of cv. Elle® and cv. Sweetness®. Differences were observed in intermediate and mature leaves.

- IR thermography detected presymptomatic rose downy mildew infections. With this technique the presence of *P. sparsa* in leaf tissue was visualized one or two days before early disease symptoms. Using thermal imaging it was possible to discriminate infected parts of tissues before symptoms became visible. MTD (Maximum Temperature Difference) was a suitable parameter to differentiate between healthy and diseased tissue. In early stages of the disease, MTD increased due to a more heterogeneous temperature pattern of the leaf as compared to that of non-inoculated leaves and decreased as the pathogen spread.

- *P. sparsa* infection altered leaf surface temperature in rose. This effect was related to the influence of *P. sparsa* infection on stomatal function. In first stages of the infection, *P. sparsa* promoted stomatal closure, which resulted in leaf temperature increase of 1.5°C with respect to healthy tissue. Abnormal stomatal opening was observed in later disease stages caused by tissue damage and dense sporulation through the stomata. Due to the consequently loss of water from the leaves, temperature declined to medium values of 0.5°C above those of healthy tissue.

- In early stages of infection the center of lesions visualized by thermography was around 1.4°C warmer than healthy tissue (6 and 7 dai). Thermal imaging showed the fast radial progress of *P. sparsa* from the initial infection site.

- Thermography confirmed the spread of *P. sparsa* from localized sites of infection. Linear transects of infected leaves depicted the bidirectional spread of *P. sparsa*, in some cases with preference toward the leaf petiole. By IR thermography the infection of non-inoculated asymptomatic areas of the leaf could detected.

- The histological development of *P. sparsa* coincided with changes in leaf temperature visualized by thermal imaging. Presence of intercellular hyphae and haustoria penetrating the cells coincided with increased leaf temperature in the first phases of colonization at the inoculation site and in more distant areas as *P. sparsa* spread. Densely colonized and damaged tissue, sporulation and the formation of oospores coincided with temperature decline.

- MTD permitted to establish differences in pathogenesis due to relative humidity conditions. Under high relative humidity, which promoted sporulation, *P. sparsa* spread faster in leaf tissue. Sporulation on leaflets increased tissue damage and thermal responses of the leaf surface were induced faster than in non-sporulating leaves under low RH.

- Although leaf symptoms were diverse, particular temperature responses associated with tissue alterations could be visualized by IR thermography: increased temperatures, as compared to those of healthy tissue, were detected in first disease symptoms, asymptomatic but infected leaves and dry leaf tissue. Medium leaf temperature coincided with brown angular lesions, densely colonized leaflets and profuse sporulating tissue.

- By thermal sensing of rose cultivars inoculated with *P. sparsa* it was possible to discriminate between susceptible and tolerant cultivars. The thermal changes observed during pathogenesis (time and intensity) made it possible to differentiate between the susceptibility of cultivars. The results coincided with the susceptibility of the cultivars observed in the biological and histological studies.

- *P. sparsa* infection caused severe effects in rose plants and affected the quality of the leaves, stems and flower buds. After the first symptoms (5 dai), a strong change leading to severely affected plants occurred by 7 dai. The disease caused significantly shorter stems, drop of 62% of the leaves and 89% of potential flowers did not develop or showed abnormalities in size or shape 15 dai.

REFERENCES

Aegerter, B.J., Nuñez, J.J., and Davis, R.M. 2002. Detection and management of downy mildew in rose rootstock. Plant Dis. 86:1336-1368.

Aegerter, B.J., Nuñez, J.J., and Davis, R.M. 2003. Environmental factors affecting rose downy mildew and development of a forecasting model for a nursery production system. Plant Dis. 87:732-738.

Ahmad, I., Khalid, M.S., Khan, M.A., and Saleem, M. 2011. Morpho-physiological comparison of cut rose cultivars grown in two production systems. Pak. J. Bot. 43:2885-2890.

Alfieri, S.A. 1968. Downy mildew of rose caused by *Peronospora sparsa* Berk. Florida Department of Agriculture Division of Plant Industry. Plant Pathology Circular No. 66.

Allègre, M., Daire, X., Héloir, M.-C., Trouvelot, S., Mercier, L., and Adrian, M. 2007. Stomatal deregulation in *Plasmopara viticola*-infected grapevine leaves. New Phytol. 173:832–40.

Anderson, J.B., and Kohn, L.M. 1995. Clonality in soilborne, plant - pathogenic fungi. Annu. Rev. Phytopathol. 33:369-391.

Andicott, B.F.T., and Lyon, J.L. 1969. Physiology of absicic acid. Annu. Rev. Plant. Physiol. 20:139-164.

Arbeláez, G. 1999. El mildeo velloso del rosal ocasionado por *Peronospora sparsa* Berkeley. Revista Acopaflor. 6:37-39.

Ayala, M., Argel, L.E., and Marín, M. 2008. Genetic diversity of *Peronospora sparsa* (Peronosporaceae) on rose crops from Colombia. Acta Biologica Colombiana 13:79-94.

Bassanezi, R.B., Amorim, L., Bergamin, F.A., and Berger, R.D. 2002. Gas exchange and emission of chlorophyll fluorescence during the monocycle of rust, angular leaf spot and anthracnose on bean leaves as a function of their trophic characteristics. J. Phytopathol. 47:37–47.

Blom T.J., and Tsujita, M.J. 2003. Cut rose production. Pages 594-600 in: Encyclopedia of Rose Science. A. Roberts, T. Debener and S. Gudin, (eds.). Academic Press, London, UK.

Boccara, M., Boue, C., De Paepe R., and Boccara, A.C. 2001. Early events in plant hypersensitive response leaves revealed by IR thermography, Proc.SPIE 4434, 183. http://dx.doi.org/10.1117/12.446675.

Bock, C.H., Poole, G.H., Parker, P.E., and Gottwald, T.R. 2010. Plant disease severity estimated visually, by digital photography and image analysis, and by hyperspectral imaging. Crit. Rev. Plant Sci. 29:59–107.

Bonarriva, J. 2003. Industry and trade summary - cut flowers. United States International Trade Commission, USITC Publication 3580. Washington, DC. 34 p. *Available at:* http://www.usitc.gov/publications/332/pub3580.pdf [Accessed July 25, 2013].

Bout, A., Boll, R., Mailleret, L., and Poncet, C. 2010. Realistic global scouting for pests and diseases on cut rose crops. J. Econ. Entomol. 103:2242–2248.

Brandenberger L.P., Correll, J.C., Morelock, T.E., and McNew, R.W. 1994. Characterization of resistance of spinach to white rust (*Albugo occidentlis*) and downy mildew (*Peronospora farinosa* f. sp. *spinaciae*). Phytopathol. 84:331-37.

Breese, W.A., Shattock, R.C., Williamson, B., and Hackett, C. 1994. *In vitro* spore germination and infection of cultivars of *Rubus* and *Rosa* by downy mildews from both hosts. Ann. App. Biol. 125:73–85.

Bruzzese, E., and Hasan, S. 1983. A whole leaf clearing and staining technique for host specificity studies of rust fungi. Plant Pathol. 32:335-338.

Cairns, T. 2003. Horticultural classification schemes. Pages 117-124 in: Encyclopedia of Rose Science. A. Roberts, T. Debener and S. Gudin, (eds.). Academic Press, London, UK.

Campbell, C.L., and L.V. Madden. 1990. Introduction to plant disease epidemiology. John Wiley and Sons, New York, NY. USA. 532 p.

Chaanin, A. 2003. Selection strategies for cut roses. Pages 33-41 in: Encyclopedia of Rose Science. A. Roberts, T. Debener and S. Gudin, (eds.). Academic Press, London, UK.

Chaerle, L., Van Caeneghem, W., Messens, E., Lambers, H., Van Montagu, M., and Van der Straeten, D. 1999. Presymptomatic visualization of plant-virus interactions by thermography. Nature Biotechnology 17:813–6.

Chaerle L., and Van der Straeten, D. 2000. Imaging techniques and the early detection of plant stress. Trends Plant Sci. 5:495–501.

Chaerle L., De Boever F., Van Montagu M., and Van der Straeten, D. 2001. Thermographic visualization of cell death in tobacco and *Arabidopsis*. Plant Cell Environ. 24:5-25.

Chaerle, L., Vande Ven, M., Valcke, R., and Van der Straeten, D. 2002. Visualization of early stress responses in plant leaves. Thermosense XXIV, Proc. SPIE 4710, p. 417-423.

Chaerle, L., Hagenbeek, D., De Bruyne, E., Valcke, R., and Van der Straeten, D. 2004. Thermal and chlorophyll-fluorescence imaging distinguish plant-pathogen interactions at an early stage. Plant Cell Physiol. 45:887-896.

Chaerle, L., Leinonen, I., Jones, H. G., and Van der Straeten, D. 2007. Monitoring and screening plant populations with combined thermal and chlorophyll fluorescence imaging. J. Exp. Bot. 58:773–784.

Chase, A.R., and Daughtrey, L.M. 2013. Rose downy mildew review. Available at: http://www.gpnmag.com/rose-downy-mildew-review. [Accessed July 30, 2013].

Chase A.R. 2013. Available at: http://www.chaseagriculturalconsultingllc.com/resources/pdfs/articlesPdf/48ROSEDISEASESANDTHEIRCONTROL.pdf. [Accessed July 28, 2013].

Clark, J.S.C., and P.T.N. Spencer-Phillips. 2004. The compatible interactions in downy mildew. Pages 1–34 in: Advances in Downy Mildew Research, Vol. 2. P.T.N. Spencer-Phillips and M.J. Jeger (eds.). Kluwer Academic Publishers, Dortdrecht, The Netherlands.

Coates, M.E., and Beynon, J.L. 2010. *Hyaloperonospora Arabidopsidis* as a pathogen model. Annu. Rev. Phytopathol. 48:329–45.

Cohen, Y., Eyal, H., Hanania, J., and Malik, Z. 1989. Ultrastructures of *Pseudoperonospora cubensis* in muskmelon genotypes susceptible and resistant to downy mildew. Physiol. Mol. Plant P. 34:27–40.

Debener, T., and Linde, M. 2009. Exploring Complex Ornamental Genomes: The rose as a model plant. Crit. Rev. Plant Sci. 28:267–280.

De Vries, D.P., and Dubois L.A.M. 1996. Rose Breeding: past, present, prospects. Acta. Hortic. 424: 241-248.

De Vries, D.P. 2003. Selection strategies for pot roses. Pages 41-48 in: Encyclopedia of Rose Science. A. Roberts, T. Debener and S. Gudin, (eds.). Academic Press, London, UK.

Dick, M.W. 2002. Towards an understanding of the evolution of the downy mildew. Pages 1–57 in: Advances in Downy Mildew Research. P.T.N. Spencer- Phillips, U. Gisi and A. Lebeda (eds.). Kluwer Academic Publisher, Dortdrecht, The Netherlands.

Drewes-Alvarez, R. 2003. Black Spot. Pages 148-153 in: Encyclopedia of Rose Science. A. Roberts, T. Debener and S. Gudin, (eds.). Academic Press, London, UK.

Dunleavy, J.M. 1981. Downy mildews of soybean. Pages 515-529 in: The Downy Mildews. D.M. Spencer (ed.). Academic Press, London, UK.

Evans, A. 2009. Rose imports. Floraculture Intl. 19:42-43.

Farrel, G.M., Preece, T.F., and Wren, M. 1969. Effects of infection by *Phytophthora infestans* (Mont.) de Bary in the stomata of potato leaves. Ann. Appl. Biol. 63:265-275.

Ferrucho, R. L. 2005. Diagnóstico molecular y variabilidad genética de *Peronospora sparsa* Berkeley en cultivos de rosa (*Rosa* sp.) bajo invernadero. Master thesis, Universidad Nacional de Colombia - Bogotá. 74 p.

Francis, S.M. 1981. *Peronospora sparsa.* Commonwealth Mycologycal Institute Descriptions of Pathogenic Fungi and Bacteria. N°690. CIM, Kew, Surrey, England.

Fraymouth, J. 1956. Haustoria of the *Peronoporales*. Transactions British Mycological Society 39:50-109.

Gachomo, E.W. 2004. Studies of the life cycle of *Diplocarpon rosae* Wolf on roses and the effectiveness of fungicides on pathogenesis. Doctoral thesis Faculty of Agricultural Science, University of Bonn. 147 p.

Gerlach, D. 1977. Botanische Mikrotechnik, eine Einführung. Georg Thieme Verlag Stutgart. 311 p.

Giraldo, S.L., García, C. and Restrepo, F. 2002. Effect of light and temperature on sporangia germination and on the sporulation of *Peronospora sparsa* Berkeley on rose cultivar Charlotte. Agronomia Colombiana 20:31-37.

Gisi, U. 2002. Chemical control of downy mildew. Pages 110–159 in: Advances in Downy Mildew Research. P.T.N. Spencer- Phillips, U. Gisi and A. Lebeda (eds.). Kluwer Academic Publishers, Dortdrecht, The Netherlands.

Gomez, S.Y., and Filgueira, J.J. 2012. Monitoring the infective process of the downy mildew causal agent within micropropagated rose plants. Agronomia Colombiana 30:214-221.

Gonzales, C., and Sarmiento, V. 2013. Boletín Económico. Asociación Colombiana de Exportadores de Flores Asocolflores. Bogotá, Colombia. Available at: http://www.asocolflores.org/ [Accessed August 29, 2013].

Grant, O.M., Chaves, M.M., and Jones, H.G. 2006. Optimizing thermal imaging as a technique for detecting stomatal closure induced by drought stress under greenhouse conditions. Physiol. Plantarum 127:507–518.

Grimmer, M.K., Foulkes, M.J., and Paveley, N.D. 2012. Foliar pathogenesis and plant water relations: a review. J. Exp. Bot. doi:10.1093/jxb/ers143 p. 2-11.

Gullino, M.L., and Garibaldi, A. 1996. Diseases of rose: evolution of a problem and new approaches for their control. Acta Hortic. 424:195-201.

Gulya, T.J., Sackston, W.E., Viranyi, F., Masirevic, S. and Rashid K.Y. 1991. New races of the sunflower downy mildew pathogen (*Plasmopara halstedii*) in Europe and North and South America. J. Phytopathol. 132: 303–311.

Hall, H.K., and Gardner, Ch. 1982. Oospores of *Peronospora sparsa* Berk.on *Rubus* species. New Zealand Journal of Experimental Agriculture. 10:429-432.

Hildebrand P.D., and Sutton, J.C. 1985. Environmental water in relation to *Peronospora destructor* and related pathogens. Can. J. Plant Pathol. 7:323-330.

Horst, K. 1983. Compendium of rose diseases. The American Phytopathological Society, St. Paul, USA. 50 p.

Hu, X. 2001. Growth and productivity of cut roses as related to the rootstock. Ph.D. Thesis, Wageningen University, The Netherlands. 90 p.

Hummer, K.E., and Janick, J. 2009. Rosaceae: taxonomy, economic importance, genomics. Pages 1-17 in: Genetics and genomics of Rosaceae. Folta and S.E. Gardiner (eds.). Springer Science+Business Media. LLC 2009. Available at: http://www.springerlink.com/index/10.1007/978-0-387-77491-6 [Accessed August 22, 2013].

IDEAM, 2005. Atlas climatologico de Colombia. Instituto de Hidrología, Meteorología y Estudios Ambientales. Bogota, Colombia. Available at: https://documentacion.ideam.gov.co/openbiblio/Bvirtual/019711/019711.htm [Accessed September 19, 2013].

Ingram, D.S. 1981. Physiology and bioquemistry of host-parasite interaction. Pages 143-163 in: The Downy Mildews. D.M. Spencer (ed.). Academic Press, London.

Inoue, Y., Kimball, B.A., Jackson R.D., Pinter P.J., and Reginato R.J. 1990. Remote estimation of leaf transpiration rate and stomatal resistance based on infrared thermometry. Agr. Forest Meteorol. 51:21–33.

Irish, B. M., Correll, J. C., Koike, S. T., and Morelock, T. E. 2007.Three new races of the spinach downy mildew pathogen identified by a modified set of spinach differentials. Plant Dis. 91:1392-1396.

Jende, G. 2001. Die Zellwand des Oomyceten *Phytophthora infestans* als Wirkort von Fungiziden. Disertation, der Hohen Landwirtschaftlichen Fakultät der Rheinischen Friedrich-Wilhelms-Universität zu Bonn. 114 p.

Jones, H.G. 2004. Application of thermal imaging and infrared sensing in plant physiology and ecophysiology. Adv. Bot. Res. 41:107–163.

Jones, R.J., and Mansfield, T.A. 1970. Suppression of stomatal opening in leaves treated with abscisic acid. J. Exp. Bot. 21:714–719.

Kamoun, S., Huitema, E., and Vleeshouwers, V. 1999. Resistance to oomycetes: a general role for the hypersensitive response? Trends Plant Sci. 4:196–200.

Karlik, J.F., and Tjosvold S.A. 2003. Integrated pest management. Pages 466-473 in: Encyclopedia of Rose Science. A. Roberts, T. Debener and S. Gudin, (eds.). Academic Press, London, UK.

Karnovsky, M.J. 1965. A formaldehyde-glutaraldehydehyde fixative of high osmolarity for use in electron microscopy. J. Cell Biol. 27:137-138.

Kumar, A., and Gour, H.N. 1992. Downy mildew of pearl millet: I. Leaf diffusive resistance and transpiration. Biochemie und Physiologie der Pflanzen 88:39–43.

Kümmerlen, B., Dauwe, S., Schmundt, D., and Schurr, U. 1999. Termography to measure water relations of plant leaves. Pages 636-672 in: Handbook of Computer Vision and Application. B. Jähne (ed.). Academic Press, London, UK.

Lebeda, A. 1991. Resistance in muskmelons to Czechoslovak isolates of *Pseudoperonospora cubensis* from cucumbers. Scien. Hortic.-Amsterdam. 45:255–260.

Lebeda, A., and Reinink, K. 1991. Variation in the early development of *Bremia lactucae* on lettuce cultivars with different levels of field resistance. Plant Pathol. 40:232-237.

Lenk, S., Chaerle, L., Pfündel, E.E., Langsdorf, G., Hagenbeek, D., and Lichtenthaler, H. K. 2007. Multispectral fluorescence and reflectance imaging at the leaf level and its possible applications. J. Exp. Bot. 58:807–14.

Linde, M., and Shishkoff, N. 2003. Powdery Mildew. Pages 158-165 in: Encyclopedia of Rose Science. A. Roberts, T. Debener and S. Gudin, (eds.). Academic Press, London, UK.

Lindenthal, M., Steiner, U., Dehne, H.-W., and Oerke, E.-C. 2005. Effect of downy mildew development on transpiration of cucumber leaves visualized by digital infrared thermography. Phytopathology 95:233-240.

Lindqvist, H., Koponen, H., and Valconen, J.P.T. 1998. *Peronospora sparsa* on cultivated *Rubus articus* and its detection by PCR based on ITS sequences. Plant Dis. 82:1304-1311.

Lindqvist-kreuze, H., Koponen, H., and Valkonen, J.P.T. 2002. Variability of *Peronospora sparsa* (syn. *P. rubi*) in Finland as measured by amplified fragment length polymorphism. Eur. J. Plant. Pathol. 108:327-335.

Lu,Y.J., Schornack, S., Spallek, T., Geldner, N., Chory, J., Schellmann, S., Schumacher, K., Kamoun, S., and Robatzek, S. 2012. Patterns of plant subcellular responses to successful oomycete infections reveal differences in host cell reprogramming and endocytic trafficking. Cell. Microbiol. 14:682–697.

Mahlein, A.-K., Steiner, U., Dehne, H.-W., and Oerke, E.-C. 2010. Spectral signatures of sugar beet leaves for the detection and differentiation of diseases. Precision Agric. 11:413-431.

Mahlein, A.-K., Oerke, E.-C., Steiner, U., and Dehne, H.-W. 2012. Recent advances in sensing plant diseases for precision crop protection. Eur. J. Plant Pathol. 133:197–209.

McDonald, B.A., and Linde, C. 2002. The population genetics of plant pathogens and breeding strategies for durable resistance. Euphytica 124:163-180.

Meyer, S., Rizza, F., and Genty, B. 2001. Inhibition of photosynthesis by *Colletotrichum lindemuthianum* in bean leaves determined by chlorophyll. Plant Cell. Environ. 24:947–955.

Merlot S., Mustilli A.C., Genty, B., North, H., Lefebvre, V., Sotta, B., Vavasseur, A., and Giraudat, J. 2002. Use of infrared thermal imaging to isolate *Arabidopsis* mutants defective in stomatal regulation. Plant Journal 30:601–609.

Misko, L.A., and Postnikova, N.L. 1989. Histopathology of rose infected by *Peronospora sparsa* Berk. Mikologiya I Fitopatologiya 23: 84-90.

Nilsson, H.E. 1991. Hand-held radiometry and IR-thermography of plant diseases in field plot experiments. Int. J. Remote. Sens. 12:545–557.

Nutter, F., van Rij, N., Eggenberger, S.K., and Holah, N. 2010. Spatial and temporal dynamics of plant pathogens. Pages 27–50 in E.-C. Oerke, R. Gerhards, G. Menz, and R. A. Sikora (eds.). Precision crop protection -the challenge and use of heterogeneity. Springer, London, UK.

Oerke, E.-C., Steiner, U., Dehne, H.W., and Lindenthal, M. 2006. Thermal imaging of cucumber leaves affected by downy mildew and environmental conditions. J. Exp. Bot. 57:2121–2132.

Oerke, E.-C., and Steriner, U. 2010. Potential of digital termography for disease control. Pages 168-183 in: Precision Crop Protection - the Challenge and Use of Heterogeneity. E.-C. Oerke, R. Gerhards, G. Menz, and R.A. Sikora (eds.). Springer, London, UK.

Oerke, E.-C., Fröhling, P., and Steriner, U. 2011. Thermographic assessment of scab disease on apple leaves. Precision Agric. 12:699-715.

Omasa, K., Hashimoto, Y., and Aiga, I. 1983. Observation of stomatal movements of intact plants using an image instrumentation system with a light microscope. Plant Cell Physiol. 24:281–288.

Osbourn, A. 1996. Saponins and plant defence: a soap story. Trends Plant Sci.1:4–9.

Parlevliet, J.E. 1979. Components of resistance that reduce the rate of epidemic development. Ann. Rev. Phytopathol. 17:203-22.

Parrado, C.A., Bojacá, C.R., Schrevens, E. 2011. Exploring more sustainable technological alternatives for the greenhouse cut flowers industry in Colombia. Acta Hortic. 893:1125-1132.

Pemberton, H.B. 2003. Pot rose production. Pages 587-593 in: Encyclopedia of Rose Science. A. Roberts, T. Debener and S. Gudin, (eds.). Academic Press, London, UK.

Pegg, G.F. 1976. Endogenous inhibitors in healthy and diseased plants. Pages: 608-631. in: Physiologycal plant pathology. R. Heitefuss and P.H. Willams (eds.) Springer, Berlin, Germany. 890 p.

Populer, C. 1981. Epidemiology of downy mildews. Pages 57-101 in: The Downy Mildews. D.M. Spencer (ed.). Academic Press, London, UK.

Restrepo, F., and Lee. R.A. 2007. Analysis of climate parameters during the incubation period of rose downy mildew *Peronospora sparsa* in Colombia. Pages 65–72 in: Advances in Downy Mildew Research. A, Lebeda and P.T.N Spencer- Phillips (eds.). Palacký Iniversity in Olomuc and JOLA, v.o.s. in Kostelec na Hané. Czcech Republic.

Restrepo, F. 2004. Recolección de información sobre las necesidades de investigación en el mildeo velloso del rosa, *Peronospora sparsa,* por parte de los floricultores de la Sabana de Bogotá. Asocolflores, unpublised report. Bogotá, Colombia.

POT - Plan de Desarrollo y Ordenamiento Territorial, Municipio de Tenjo. 2000. Secretaria de Planeación de Cundinamarca. Bogotá, Colombia. Available at: http://www.planeacion.cundinamarca.gov.co/BancoMedios/Documentos%20PDF/sig_doc_2000%20tenjo%20Aspecto%20biof%C3%ADsico%20No%201.pdf [Accessed September 27, 2013].

Reuveni, R., M. Tuzung, S., Cole, J.S., Siegel, M.R., and Kuc, J. 1986. The effects of plant age and leaf position on the susceptibility of tobacco blue mold caused by *Peronospora tabacina.* Phytopathology 76:455-458.

Reuveni, M. 1998. Relationships between leaf age, β-1,3-glucanase activity and resistance to downy mildew in grapevines. Phytopathology 146:125-130.

Riera, M., Valon, C., Fenzi, F., Giraudat, J., and Leung, J. 2005. The genetics of adaptive responses to drought stress: abscisic acid-dependent and abscisic acid-independent signaling components. Physiol. Plant 123:111–119.

Sakr, N. 2011. Relationship between virulence and aggressiveness in *Plasmopara halstedii* (sunflower downy mildew). Archives of phytopathology and plant protection. 44:1585-1594.

Satou, M., Nishi, K., Kubota, M., Michiko Fukami, M., Hideaki Tsuji, H., Van Ettekoven, K. 2006. Appearance of race Pfs: 5 of spinach downy mildew fungus, *Peronospora farinosa* f. sp. *spinaciae*, in Japan. J. Gen. Plant Pathol. 72:193-194.

Schulz, D.F., and Debener, T. 2007. Screening for resistance to downy mildew and its early detection in roses. Acta Hort. 751:189-198.

Schulz, D.F., Linde, M., Blechert, O. and Debener, T. 2009. Evaluation of genus *Rosa* germplasm for resistance to blacks, downy mildew and powdery mildew. Europ. J. Hort. Sci., 74:1-9.

Schulz, D.F., and Debener, T. 2010. Downy mildew in roses: strategies for control. Acta Hort. 870:163–170.

Schwinn, F.J. 1981. Chemical control of downy mildews of ornamentals. Pages 305-320 in: The Downy Mildews. D.M. Spencer (ed.). Academic Press, London, UK.

Scott and Healy, 1991. Enterprise guide for southern Maryland: producing cut flowers-general field crop management. Fact sheet 468. Meryland Coperative Extension, University of Meryland. Merylad, USA. Available at: http://georgesonbg.org/PDFs/Peonies/91.Aker.pdf [Accessed October 01, 2013].

Shattock, R.C. 2003. Rust. Pages 165-169 in: Encyclopedia of Rose Science. A. Roberts, T. Debener and S. Gudin, (eds.). Academic Press, London, UK.

Shtienberg, D. 1992. Effects of foliar diseases on gas exchange processes: A comparative study. Phytopatology 82:760-765.

Slusarenko, A. J., and Schlaich, N. L. 2003. Downy mildew of *Arabidopsis thaliana* caused by *Hyaloperonospora parasitica* (formerly *Peronospora parasitica*). Mol. Plant Pathol. 4:159–70.

Soto, L.C., and Filgueira, J.J. 2009. Effect of photoperiod and light intensity on the sporulation of *Peronospora sparsa* Berkeley under controlled environmental conditions. Agronomia Colombiana 27:245-251.

Spotts, R.A., and Ferree, D.C. 1979. Photosynthesis, transpiration, and water potential of apple leaves infected by *Venturia inaequalis*. Phytopathology 69:717–719.

Spurr, A.R. 1969. A low-viscosity epoxy resin embedding medium for electron microscopy. Journal of Ultrastructure Research 26:31-34.

Stahl, M. 1973. Einige Beobachtungen über den ,,Falschen Mehltau" bei Rosen. Nachrichtenbl. Deutsch. Pflanzenschutzd. 25:161-162.

Stoll, M., Schultz, H.M., Baecker, G., and Berkelmann-Loehnertz, B. 2008. Early pathogen detection under different water status and the assessment of spray application in vineyards through the use of thermal imagery. Precision Agric. 9:407–417.

Stoll, M., Schultz, Schultz, H.R., and Berkelmann-Loehnertz, B. 2008a. Thermal sensitivity of grapevine leaves affected by *Plasmopara viticola* and water stress. Vitis 47:133–134.

Suárez, J.R. 1999. Problemática actual del mildeo velloso en rosa. In: VIII Congreso Acopaflor - Asocolflores. Bogota, Colombia.

Sudhagar, M., and Phil, M. 2013. Production and marketing of cut flower (rose and gerbera). International Journal of Business and Management Invention 2:15–25.

Thines, M., and Kamoun, S. 2010. Oomycete-plant coevolution: recent advances and future prospects. Curr. Opin. Plant Biol. 13:427–33.

Taylor, P.N., Lewis, B.G., and Mattews, P. 1990. Factors affecting systemic infection of *Pisum sativum* by *Peronospora viciae.* Mycol. Res. 94:179-181.

Tate, K.G. 1981. Etiology of dryberry disease in New Zealand. N.Z.J. Exp. Agric. 9:371-376.

Unger, S., Büche, C., Boso, S., and Kassemeyer, H.-H. 2007. The course of colonization of two different *Vitis* genotypes by *Plasmopara viticola* indicates compatible and incompatible host-pathogen interactions. Phytopathology 97:780–6.

Urban, J., Lebeda, A., and Pejchar, M. 2007. Deferential sensitivity to fungicides in Czech populations of cucumber downy mildew *Pseudoperonospora cubensis*. Pages 251–255 in: Advances in Downy Mildew Research, A. Lebeda and P. T.N. Spencer-Phillips (eds.). Palacký Iniversity in Olomuc and JOLA, v.o.s. in Kostelec na Hané. Czcech Republic.

Vadivambal, R., and Jayas, D.S. 2011. Applications of thermal imaging in agriculture and food industry—a review. Food Bioprocess Tech. 4:186-199.

Vance, C.P., Kirk, T.K., Sherwood, R.T. 1980. Lignification as a mechanism of disease resistance. Ann. Rev. Phytopathol. 18:259–288.

Varila, D. 2005. Evaluación de la respuesta a la temperatura de siete de *Peronospora sparsa* provenientes de cultivos comerciales de rosa de la Sabana de Bogotá. Facultad de Agronomía, Universidad Nacional de Colombia –Bogotá.

Viennot-Bourging, G. 1981. History and importance of downy mildews. Pages 1-14 in: The Downy Mildews. D.M. Spencer (ed.). Academic Press, London, UK.

Wallis, W.A., Shattock, R.C., and Williamson, B. 1989. Downy mildew *Peronospora rubi* on micropropagated *Rubus*. Acta Hortic. 262: 227-230.

Wang, M., Ling, N., Dong, X., Zhu, Y., Shen, Q., and Guo, S. 2012. Thermographic visualization of leaf response in cucumber plants infected with the soil-borne pathogen *Fusarium oxysporum* f. sp. *cucumerinum*. Plant Physiol. Bioch. 61:153–61.

Wang, Y., Holroyd, G., Hetherington, A.M., and Ng, C.K.-Y. 2004. Seeing “cool” and “hot”-infrared thermography as a tool for non-invasive, high-throughput screening of *Arabidopsis* guard cell signaling mutants. J. Exp. Bot. 55:1187–93.

West, S. J., Bravo, C., Oberti, R., Moshou, D., Ramon, H., and McCartney, H.A. 2010. Detection of fungal diseases optically and pathogen inoculum by air sampling. Pages 135–150 in: Precision crop protection—the challenge and use of heterogeneity. E.-C. Oerke, R. Gerhards, G. Menz, and R.A. Sikora (eds.). Springer, Dordrecht, The Netherlands.

Wellan, M. 2009. So many roses . . . so little time. American Rose Society. Available at: http://msucares.com/lawn/garden/flowers/perennial/roses/so-many-roses.pdf [Accessed August 27, 2013].

Wheeler, B.E.J. 1981. Downy mildews of ornamentals. Pages 461-451 in: The Downy Mildews. D.M. Spencer (ed.). Academic Press, London, UK.

Williamson, B., Bresse, W.A., and Shattock, R.C. 1995. A histological study of downy mildew *Peronospora rubi* infection of leaves, flowers and developing fruits of tummelberry and other *Rubus* spp. Mycol. Res. 99:1311-1316.

Wisniewzca-Grzeszkiewicz, H. and Wojdyla, A.T. 1996. Evaluation of rose cultivars to fungal diseases susceptibility. Acta. Hortic. 424: 233-236.

Wissemann, V. 2006. Beauty and the bastards, intensive hybridization controls the evolution of wild roses. B.I.F. Futura 21:158–163.

Xu X.-M., and Pettitt, T. 2003. Rose downy mildew. Pages 154-158 in: Encyclopedia of Rose Science. A. Roberts, T. Debener and S. Gudin, (eds.). Academic Press, London, UK.

Xu X.-M., and Pettitt, T. 2004. Overwintering of rose downy mildew. Pages 99–106 in: Advances in Downy Mildew Research, Vol. 2. 2004. P.T.N. Spencer- Phillips and M.J. Jeger (eds.). Kluwer, Dortdrecht, The Netherlands.

Yan, Z. 2005. Towards efficient improvement of greenhouse grown roses: genetic analysis of vigour and powdery mildew resistance. Ph.D. Thesis, Wageningen University, The Netherlands. p. 90.

Yarwood, C.E. 1943. Onion downy mildew infections. Hilgardia 11:595-691.

Yarwood, C.E. 1941. Sporulation injury associated with downy mildew infections. Phytopathology 31:741-748.

1

Appendix 1. Sampling sites of symptomatic leaves infected by *Peronospora sparsa* in commercial rose crops at the Bogota Plateau.

	Isolate						
	Ps 1	**Ps 2**	**Ps 3**	**Ps 5**	**Ps 6**	**Ps 7**	**Ps 8**
Location[1]	Madrid	Facatativa	Facatativa	Torca	El Rosal	Cota	Suesca
Cultivar	Akito®	Samba Pa Ti®	Latin Beauty®	High Magic®	Espérance®	Vendela®	Daphne®
Breeder	Tantau	Kordes roses	De Ruiter	Pressman	De Ruiter	Tantau	Nirp
Color	White	Peach	Orange	Orange	White	White	Orange
Age of the plants	10 years	2 years	6 years	2.8 years	4.5 years	4 years	6 years
cv. Susceptibility[2]	High	High	High	High	High	High	High
Chemical control[3] (A.I)	Chlorothalonil Cymoxanil Fenamidone Folpet Fluopicolide Propamocarb	Fosetyl-Al Mancozeb Propamocarb	Dimetomorph Fenamidone Fosetyl-Al Mancozeb Mefamoxam	Dimetomorph Fenamidone Fosetyl-Al Iprovalicarb Mancozeb Propamocarb	Cymoxanil Dimetomorph Fenamidone Propamocarb	Cymoxanil Dimetomorph Fenamidone Fluopicolide, Folpet Fosetyl-Al Iprovalicarb Propamocarb Propineb	Chlorothalonil Fenamidone Fosetyl-Al Metalaxyl-M Propamocarb

[1]Location of the crop at the Bogota Plateau.

[2] Susceptibility of the sampled cultivar to *Peronospora sparsa* according to the grower experience: high, media, low.

[3] Active ingredients (A.I.) used in chemical control of the disease with fungicides.

Aknowledgements

The development of this PhD thesis was made possible by the support and assistance of people and institutions who generously contributed to this personal and professional project.

I wish to express my gratitude to Prof. Dr. Heinz-W. Dehne for giving me the opportunity to develop my research proposal and for his support during its development.

I am especially grateful to Dr. Ulrike Steiner for her support and guidance and for her valuable contributions during the talks and discussions. Her opportune comments and suggestions helped me to develop my research.

I would like to thank Dr. Erich-Christian Oerke, for his guidance and useful discussions of results, which left me always valuable academic lessons. He was always willing to talk when I needed his advice during the development of my thesis.

I would like to thank Dr. Jachim Hamacher, for supporting the development of the electron microscopy studies, and for sharing with me his valuable skills and knowledge.

I wish to thank, Prof. Dr. Léon for his support and for evaluating this thesis.

I thank to all the members of INRES-Phytomedizin for their continuous collaboration and also to my colleagues for their important support.

I would like to thank as well, the managers and technicians of the Colombian rose plantations who allowed the collection of samples to obtain the isolates of *Peronospora sparsa* for the study.

My heartfelt gratitude to my mother, who despite the distance, always supported me. Her immense love helped me achieve my goal every day. I am also grateful with all my family, because they were always with me at the distance and they showed me the value of love and the importance of sharing dreams.

Finally, I extend my gratitude to the Universidad Nacional de Colombia for institutional support in the development of my doctoral studies in Germany and to the German Academic Exchange Service (DAAD) for the financial support granted within the framework of the ALECOL agreement.